VTT PUBLICATIONS 334

Duration of load effect on curved glulam beams

Part 2. Long term load tests and analysis

Shankare Gowda, Markku Kortesmaa &
Alpo Ranta-Maunus

VTT Building Technology

TECHNICAL RESEARCH CENTRE OF FINLAND
ESPOO 1998

ISBN 951–38–5212–1 (soft back ed.)
ISSN 1235–0621 (soft back ed.)

ISBN 951–38–5218–0 (URL: http://www.inf.vtt.fi/pdf/)
ISSN 1455–0849 (URL: http://www.inf.vtt.fi/pdf/)

JULKAISIJA – UTGIVARE – PUBLISHER

Valtion teknillinen tutkimuskeskus (VTT), Vuorimiehentie 5, PL 42, 02151 ESPOO
puh. vaihde (90) 4561, telekopio 456 4374, teleksi 125 175 vttin sf

Statens tekniska forskningscentral (VTT), Bergsmansvägen 5, PB 42, 02151 ESBO
tel. växel (90) 4561, telefax 456 4374, telex 125 175 vttin sf

Technical Research Centre of Finland (VTT), Vuorimiehentie 5, P.O.Box 42, FIN–02151 ESPOO, Finland
phone internat. + 358 0 4561, telefax + 358 0 456 4374, telex 125 175 vttin sf

VTT Rakennustekniikka, Rakennusmateriaalit ja -tuotteet sekä puutekniikka,
Puumiehenkuja 2 A, PL 1806, 02044 VTT
puh. vaihde (09) 4561, faksi (09) 456 7027

VTT Byggnaadssteknik, Byggnaaddsmaterial ock -produkter, träteknik,
Träkarlsgränden 2 A, PB 1806, 02044 VTT
tel. växel (09) 4561, fax (09) 456 7027

VTT Building Technology, Building Materials and Products, Wood Technology,
Puumiehenkuja 2 A, P.O.Box 1806, FIN–02044 VTT, Finland
phone internat. + 358 9 4561, fax + 358 9 456 7027

Technical editing Leena Ukskoski

VTT OFFSETPAINO, ESPOO 1998

Gowda, Shankare, Kortesmaa, Markku & Ranta-Maunus, Alpo. Duration of load effect on curved glulam beams. Part 2. Long term load tests and analysis [Kaarevien liimapuupalkkien pitkäaikaislujuus. Osa 2. Pitkäaikaiset kuormitusluokat]. Espoo 1998, Technical Research Centre of Finland, VTT Publications 334. 76 p. + app. 28 p.

UDC 69.011.1:624.011.1:539.4
Keywords wooden structures, structural timber, glulam beams, loads (forces), life (durability), humidity

ABSTRACT

This research related to the duration of load effect on curved glulam is a part of an EC-AIR project carried out at VTT in co-operation with four other EU member countries.

The project includes the long term loading of 32 curved beams, as well as equivalent short term reference tests of 32 beams. The long term loading was made under both constant and cyclically varying humidity conditions. Failure is caused by tensile stress perpendicular to grain.

A calculation procedure is presented to consider the effect of moisture variation as an additional loading. Both calculation and experiments reveal that a period of higher humidity can double the effective loading, depending on the duration of humid period.

Experimental and calculated results are given for duration of load effect of curved glulam for two thicknesses (90 and 140 mm) under constant (85%) and cyclically changing humidity.

Gowda, Shankare, Kortesmaa, Markku & Ranta-Maunus, Alpo. Duration of load effect on curved glulam beams. Part 2. Long term load tests and analysis [Kaarevien liimapuupalkkien pitkäaikaislujuus. Osa 2. Pitkäaikaiset kuormitusluokat]. Espoo 1998, Valtion teknillinen tutkimuskeskus, VTT Publications 334. 76 s. + liitt. 28 s.

UDK 69.011.1:624.011.1:539.4

Avainsanat wooden structures, structural timber, glulam beams, loads (forces), life (durability), humidity

TIIVISTELMÄ

Osana EU:n AIR-ohjelman projektia, jossa tutkittiin eri kokoisten puukannatteiden pitkäaikaislujuutta viidessä maassa, VTT suoritti kaarevien liimapuupalkkien koesarjan ja siihen liittyvän teoreettisen mallinnuksen.

Kaarevan liimapuun kokeet tehtiin sen selvittämiseksi, miten palkin koko, kuormitusaika ja kosteusvaihtelu vaikuttavat lujuuteen vedossa syysuuntaa vastaan kohtisuorassa suunnassa. Pitkäaikaiskokeita tehtiin yhteensä 32 palkilla ja lisäksi sama määrä lyhytaikaiskokeita. Kosteusvaihtelun vaikutusten selittämiseksi kehitettiin myös laskentamenetelmä, johon yhdistettiin kokovaikutus. Tämä julkaisu sisältää pitkäaikaiskokeiden ja teoreettisten laskelmien tulokset.

Koetuloksista päätellään, että kaarevat palkit murtuvat kahdessa viikossa 20 % alemmalla kuormalla kuin lyhytaikaisessa kuormituksessa (5 min), kun kosteus ei vaihtele. Tulosten ekstrapolointi pidemmille kuormitusajoille antaa 25 % aleneman puolessa vuodessa ja 30 % aleneman neljässä vuodessa vakiokuorman alaisena vakiokosteudessa. Käytännön rakenteissa sekä kuorma että kosteus muuttuvat. Kosteuden vaihdellessa lujuuden alenema riippuu ensisijaisesti kosteusvaihtelun laajuudesta ja kostean jakson pituudesta. Kokeissa saatiin 30 - 40 % alempia pitkäaikaislujuuden arvoja kuin arvioitu lyhytaikaislujuus. Kosteuden vaihtelua vastaan palkit voi suojata pintakäsittelyllä.

PREFACE

A large research project (Number AIR2-CT941057) concerning the duration of load effect on different sized timber beams was initiated in 1994 as an EC-AIR project (European Community Agriculture and Fisheries, including agro-industry, food-technology, forestry, acquaculture and rural development) with a joint co-operation of five EC countries. The five countries involved in the project are Finland, Sweden, France, Denmark and Germany. The contact persons and the corresponding participating laboratories from these countries are respectively:

Prof. P. Morlier, Project Co-ordinator
Laboratoire de Rheologie du Bois de Bordeaux (LRBB), France.

Prof. Alpo Ranta-Maunus
Technical Research Centre of Finland (VTT), Finland.

Dr. Preben Hoffmeyer
Technical University of Denmark, Denmark.

Dr. Simon Aicher
Forschungs´ und Materialprüfungsanstalt Baden-Württemberg, Germany.

Dr. Per Johan Gustafsson
Lund Institute of Technology, Sweden.

Dr. J. F. Quillacq
Centre expériméntal de Recherches et d'Etudes du Batiment et des Travaux Publics (CEBTP), France.

The main objective of the project was to investigate the behaviour of different sized wooden beams under short term and long term loading conditions under normal and cyclic relative humidity and moisture content environment.

This report includes the long term test results of curved glulam beams (Task C2), and related theoretical analysis.

CONTENTS

1 INTRODUCTION

A large research program on the duration of load effect on different sized timber beams was initiated in 1994 as a joint EC-AIR project with the co-operation of five EC member countries. The main aim was to investigate both short term and long term load effects on glulam beams and as well as Kerto-LVL beams. In case of long term loading, the specimens were subjected to varying humidity conditions and stepwise increasing loads of four weeks duration. The research objective was to gather information on the factors which affect the long term strength behaviour of timber structures and establish a new scientific basis for the development and modification of Eurocode 5.

Before starting the long term tests, short term tests were carried out on similar beams to know the magnitude of their ultimate load levels. The short term test results were used as a basis for selecting the load levels for long term tests. The testing and analysis of short term tests on both curved glulam beams (Gowda and Ranta-Maunus, 1996) and Kerto-LVL specimens (Fonselius and Ranta-Maunus, 1996) have been completed. The long term tests results on LVL specimens will be published as a separate report.

In this part of the research, assessment of factors which affect the long term behaviour of curved glulam beams are studied under different loading and environmental conditions. An interesting part of this AIR research project is the new loading procedure that is followed in loading of the beams during long term testing. Normally, in case of long term loading the beams are loaded at a certain required load level and kept constant until specimen failure occurs. However, in the present investigation, the loading method consist of applying the loads in stages rather than keeping it constant for many months. Four weeks after the first load step duration, the second load increment was applied in a systematic way. The humidity of the testing environment was also varied cyclically from 55% to 90% during a period of 28 days for the required test series. For some series, the humidity was kept constant at 85%.

This report includes long term test results of 32 glulam beams tested under stepwise loading method and 8 glulam beams tested under short term loading with high constant moisture content. These extra eight beams are in addition to 24 beams reported earlier (Gowda and Ranta-Maunus, 1996).

2 EXPERIMENTAL PROGRAMME

2. 1 Details of material and specimens

The wood material used in the preparation of glulam is Spruce (*Picea abies*) and was supplied by the company Södra Timber of Sweden. The lamellae were strength graded according to coming European strength class C35. Curved glulam beams were manufactured by Late-Rakenteet Oy, Finland. More details about the wood material is given in the short term test report (Gowda and Ranta-Maunus, 1996).

In the long term experiments, a total of four series of tests (C2,2: LT-C2-S2; C2,4: LT-C2-S4; C2,6: LT-C2-S6 and C2,8: LT-C2-S8), having eight specimens in each, were carried out under incremental load and cyclic/constant relative humidity conditions. One additional test series (C2,5: ST-C2-S5b) having eight specimens was tested at a high moisture content level under short term loading.

The specimens in the first series (C2,2) had dimensions of 90 x 600 x 5 300 mm, while the second C2,4 had 90 x 600 x 7 300 mm. The rest of the series had dimensions of 140 x 600 x 7 300 mm. The specimens in all series had 18 laminae and each lamina was 33.3 mm thick. The beams had a mean radius of curvature of 5 700 mm. The details of specimens for all the series are given in Table 1. The numbering of specimens used in this long term testing is as follows:

C*2, X* stands for Curved Beams in Task C2 of project and Specimen Series *X*
LT stands for Long Term loading
ST stands for Short Term loading
S*X* stands for Test Group S and Specimen series *X*
S*X*-*x* stands for Test Group S, Specimen Series *X* and Specimen Number *x* .

Table 1. Summary of all test series with curved beams.

Project Task Test series	Specimens dimensions (mm)	Type of test	Conditions of specimens	Note
C 2,1 ST-C2-S1	90 x 600 x 5 300	Short term	65% RH	Reported in Gowda et al 1996
C 2,2 LT - C2 - S2	90 x 600 x 5 300	Long term	Cyclic	
C 2,3 ST - C2 - S3	90 x 600 x 7 300	Short term	65% RH	Reported in Gowda et al 1996
C 2,4 LT - C2 - S4	90 x 600 x 7 300	Long term	85% RH	
C 2,5a ST - C2 - S5a	140 x 600 x 7 300	Short term	65% RH	Reported in Gowda et al 1996
C 2,5 b ST - C2 - S5b	140 x 600 x 7 300	Short term	Cyclic / 85%RH	
C 2,6 LT - C2 - S6	140 x 600 x 7 300	Long term	Cyclic	
C 2,8 LT - C2 - S8	140 x 600 x 7 300	Long term	85% RH	Surface sealed

2.2 Details of loading and measurements

To carry out the long term tests on curved glulam beams, special test frames were designed and built according to the loading requirements. The experiments were carried out as four point bending tests. For the first series (LT-C2-S2), which had a volume of 0.31 m^3, the distance between the two load positions in the central section of the beam was 2 000 mm apart; for other series their volume were 4 000 mm. The schematic of loading and supporting positions for the series is shown in Figure 1.

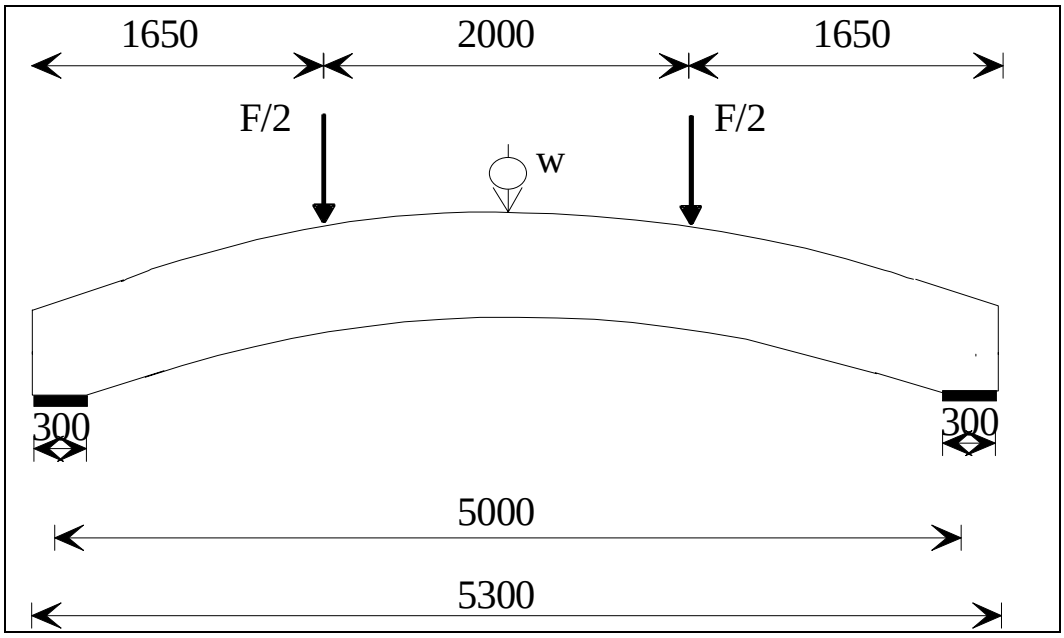

Figure 1. Schematic of loading and supporting positions for LT-C2-S2 series.

The beams were loaded with a heavy-duty spring system and the load was applied through hydraulic jacks at two load positions. Since it was decided to apply the load increments in several stages, the first load level was selected very low, such that no specimens would fail during the first incremental load. The magnitude of the first load increment induced an initial stress level of about 0.2 MPa in perpendicular to grain direction. This low load level was selected such that no specimens will fail under this.

Table 2 shows the load steps followed during the experimental process for the four series. Figure 2 shows the variation of relative humidity cycle used for specimen series LT-C2-S2 and LT-C2-S6, while Figure 3 shows the constant humidity level maintained through out the test period for series LT-C2-S4 and LT-C2-S8.

Table 2. Used step-wise load levels used for long term test series.

Load step	F/2 (kN)			
	LT-C2-S2	LT-C2-S4	LT-C2-S6	LT-C2-S8
1	28	42	43.0	64.5
2	42	56	64.5	86.0
3	56	70	86.0	107.5
4	70	84	107.5	129.0
5	84			

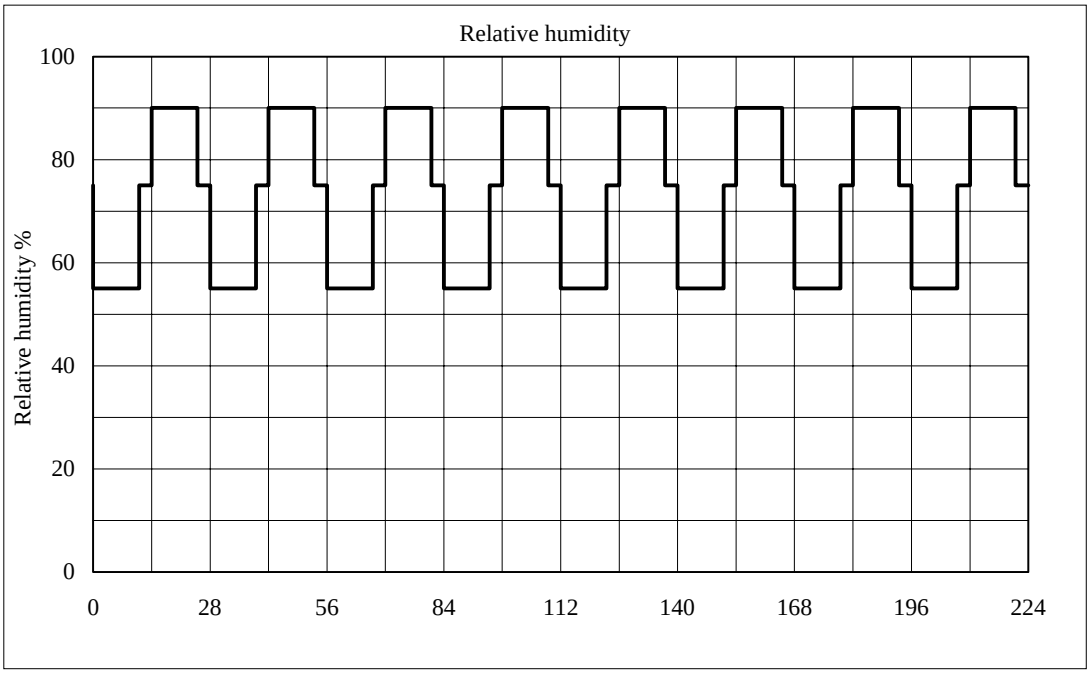

Figure 2. Used moisture cycle for series LT-C2-S2 and LT-C2-S6.

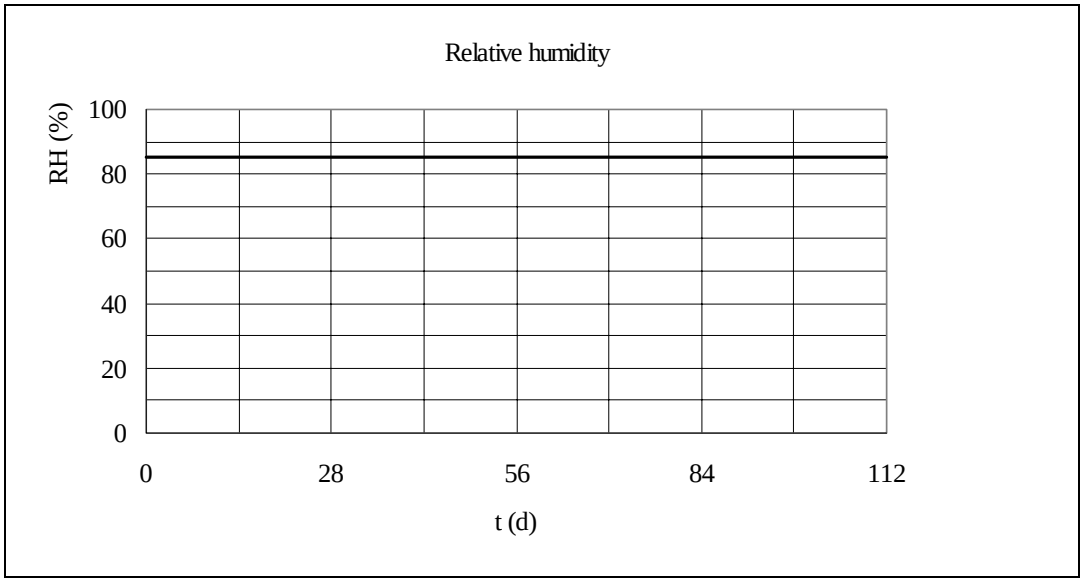

Figure 3. Constant relative humidity used for test series: LT-C2-S4 and S8.

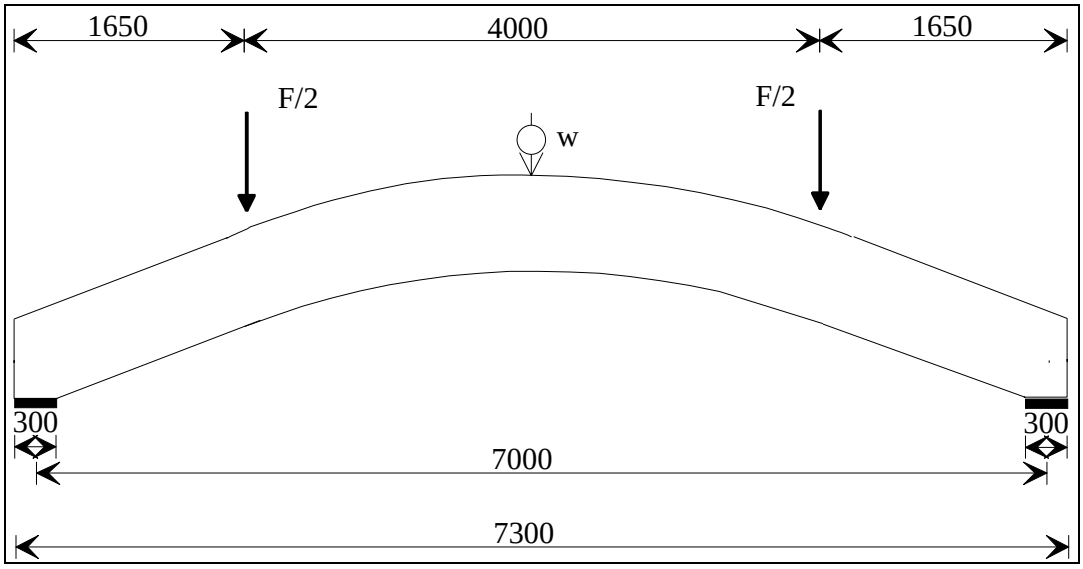

Figure 4. Schematic of loading and supporting positions for specimens having a length of 7.3 m.

Figure 5. Photograph of specimens and loading springs for long term testing.

For specimens with larger dimensions having a volume of 0.65 m^3, the distance between the two load points in the center was kept at 4 000 mm. Figure 4 shows the schematic loading and supporting positions, while Figure 5 shows the photograph of specimens under load in climatic room loaded with springs.

The creep deformation of beams at the crown in the centre was measured using one dial gauge. To avoid lateral deformations during experiment, special steel bars were used. Figures 6 and 7 shows photographs of specimens under loading, the position of dial gauge at the crown and the lateral supports of the beams.

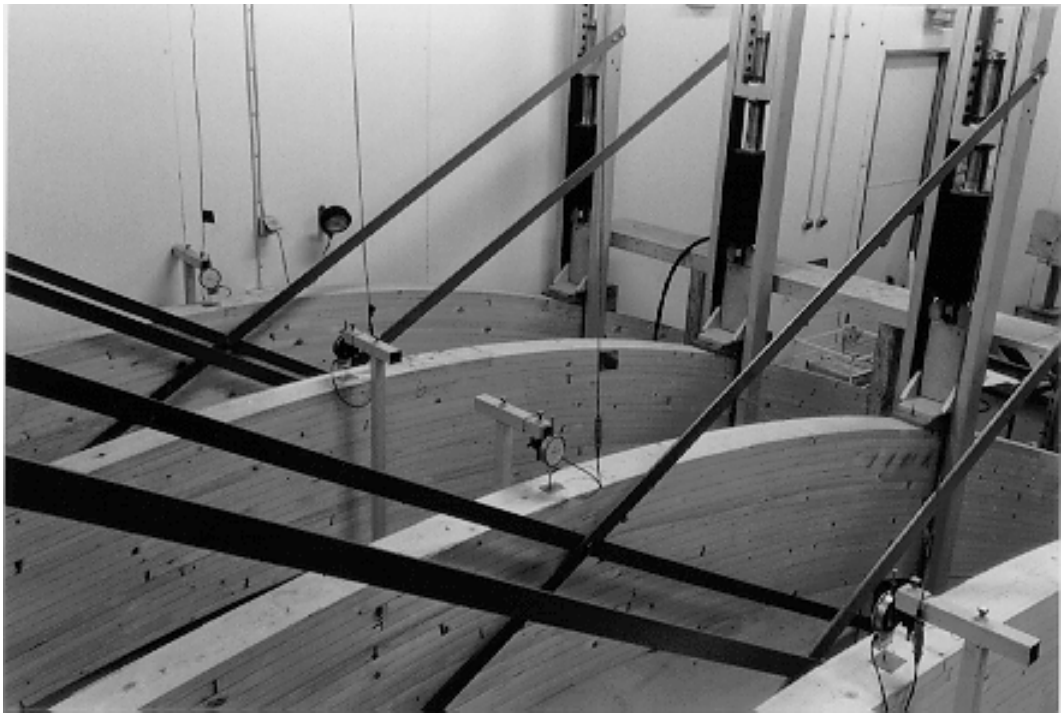

Figure 6. Photograph of specimens with dial gauge and lateral supports.

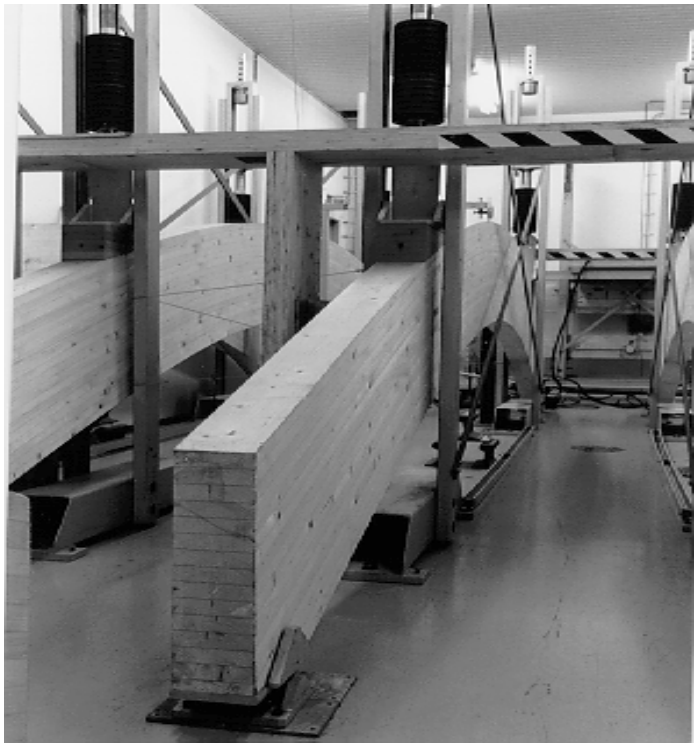

Figure 7. Photograph of specimens with end supports.

2.3 Details of short term tests

These short term test specimens were remaining beams from the earlier tests, which were reported in Part 1 Short term reference tests series (Gowda and Ranta-Maunus, 1996). The beams were kept in high moisture conditions before the tests were made. Four beams were kept in the cyclic climate of long-term experiments, and tested at the time of maximum humidity. The other four beams were conditioned at 85% RH. During the tests, the deformations were measured at the crown and mid-central section of the beams. The schematic of loading and displacement measurement positions are shown in Figure 8. the photograph of test set up, lateral supports and loading frame are shown in Figure 9.

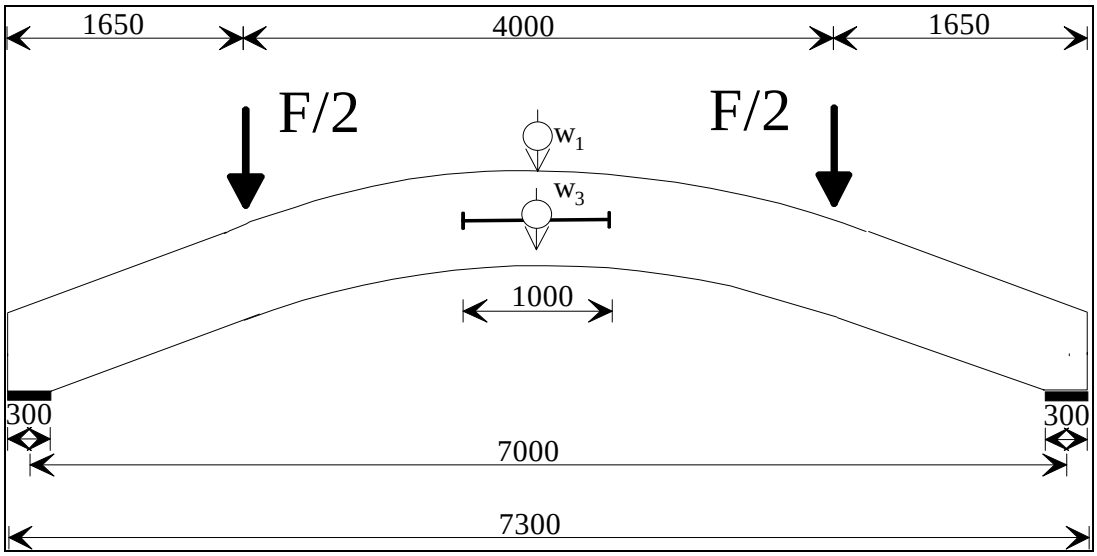

Figure 8. Schematic of loading and measurement positions for series ST-C2-S5b.

Figure 9. Photograph of test set up for short term tests: series ST-C2-S5b.

To see the difference in the curvature of the beams, vertical heights were measured at five locations at 1 000 mm apart as shown in Figure 10. The measurements indicate some difference in heights on either side of the beam from the centre. The values of heights and other beam parameters are given in Table 3.

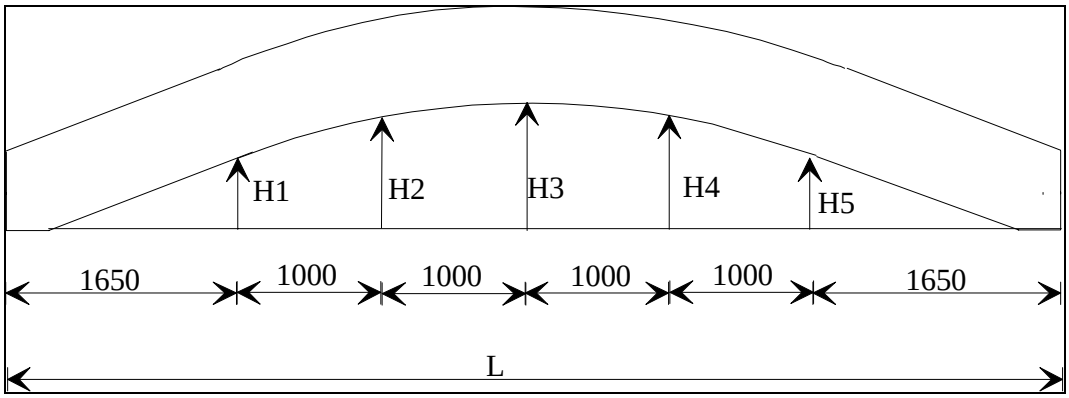

Figure 10. Bottom surface measurements for short term tests: series ST-C2-S5b

Table 3. Details of specimen parameters for short term test series ST-C2-S5b.

Specimens parameters								
Specimen designation	Heights of bottom surface of beam (mm)					Width mm	Depth mm	Weight kg
	H1	H2	H3	H4	H5			
ST-C2-S5b-1	490	764	869	788	529	141.1	605	322
ST-C2-S5b-2	494	779	880	795	533	141.9	609	317
ST-C2-S5b-3	498	770	871	792	532	140.9	605	320
ST-C2-S5b-4	495	770	876	793	530	140.1	605	327

3 EXPERIMENTAL RESULTS

3.1 Density

To determine the density of specimens, small samples were cut from the large glulam beams after their tests were completed. Several samples were taken from each beam. Table 4 give details of samples, their density and moisture content values. In some cases, the samples were cut at the centre, top and bottom of the laminae where failure crack appeared. The mean values of density (before oven drying) and moisture content for each series is given in Table 4. The details of samples, the laminates where the samples are taken and the laminae numbers, density and moisture content values for all series is given in Appendix A.

Table 4. Mean values of density and M. C. for all series of tests.

Specimen numbers	Density (D1) before ovendry (kg/m3)	Moisture Content %	Specimen numbers	Density (D1) before ovendry (kg/m3)	Moisture Content %
LT-C2-S2-2	484	13.07	LT-C2-S8-1	427	13.2
LT-C2-S2-5	488	13.19	LT-C2-S8-2	478	13.9
LT-C2-S2-4	491	13.52	LT-C2-S8-3	493	13.3
LT-C2-S2-3	504	13.70	LT-C2-S8-4	489	13.7
LT-C2-S2-1	513	13.37	LT-C2-S8-5	499	14.4
LT-C2-S2-8	520	13.71	LT-C2-S8-6	438	13.7
LT-C2-S2-6	532	13.31	LT-C2-S8-7	507	13.7
LT-C2-S2-7	535	13.47	LT-C2-S8-8	491	13.3
Mean	**508**	**13.4**	**Mean**	**478**	**13.7**
LT-C2-S4-1	514	11.64	ST-C2-S5b-1	472	13.1
LT-C2-S4-2	525	11.25	ST-C2-S5b-2	477	13.7
LT-C2-S4-3	486	11.35	ST-C2-S5b-3	478	13.4
LT-C2-S4-4	511	11.33	ST-C2-S5b-4	505	12.8
LT-C2-S4-5	481	10.68	ST-C2-S5b-5	487	14.3
LT-C2-S4-6	436	11.60	ST-C2-S5b-6	513	15.5
LT-C2-S4-7	499	10.85	ST-C2-S5b-7	481	14.8
LT-C2-S4-8	454	10.47	ST-C2-S5b-8	490	15.1
Mean	**488**	**11.15**	**Mean**	**488**	**14.1**
LT-C2-S6-1	425	12.11			
LT-C2-S6-2	486	12.67			
LT-C2-S6-3	487	12.71			
LT-C2-S6-4	487	12.48			
LT-C2-S6-5	462	12.85			
LT-C2-S6-6	486	12.73			
LT-C2-S6-7	451	12.09			
LT-C2-S6-8	518	12.51			
Mean	**475**	**12.5**			

The density values for all series tested in this program (LT-C2-S2, LT-C2-S4, LT-C2-S6, LT-C2-S8 and ST-C2-S5b), ranged from a minimum of 475 kg/m^3 to a maximum of 508 kg/m^3, while the moisture content from a minimum of 11.5 to a maximum of 14.1%. It should be observed that, these moisture content values are in most cases different from the moisture content during failure of beams, and can be considered only as reference for density values.

Using the density and moisture content data, graphical plots of density versus specimen numbers were obtained. The respective graphs are shown in Figures 11 through 15.

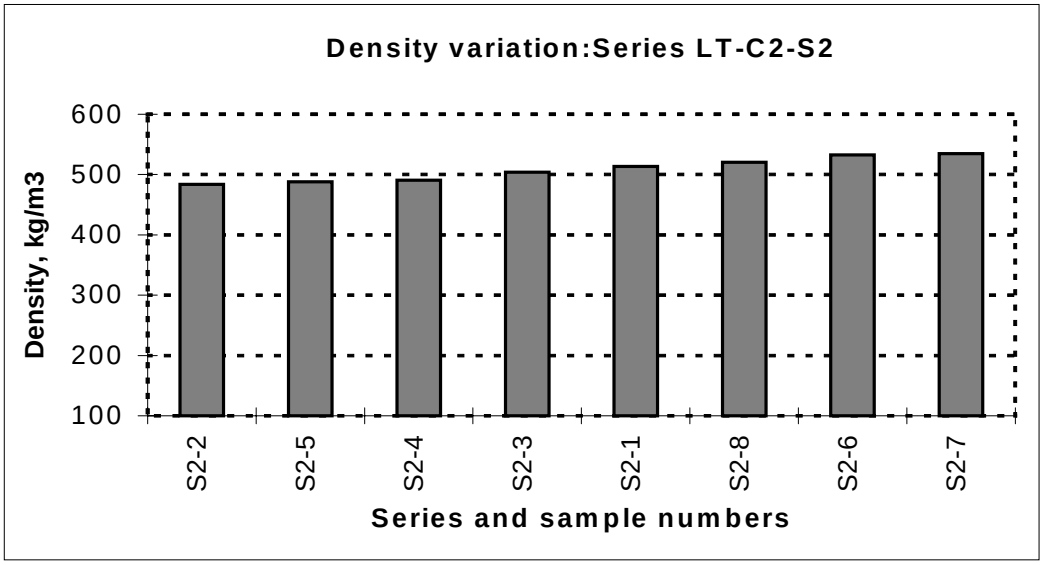

Figure 11. Variation of density (before ovendry) for specimen series LT-C2-S2.

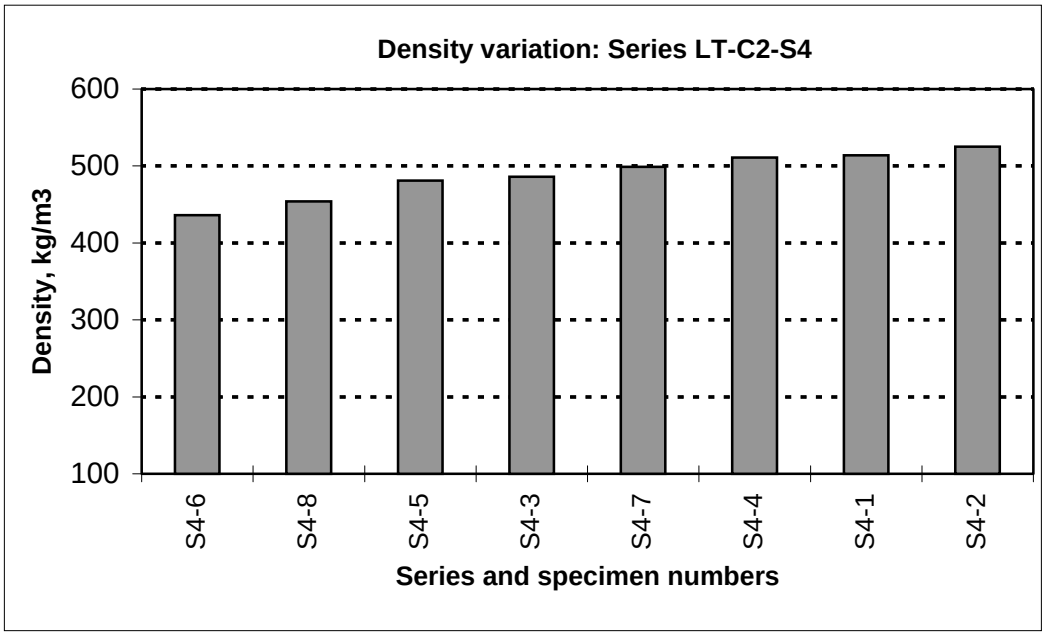

Figure 12. Variation of density (before ovendry) for specimen series LT-C2-S4.

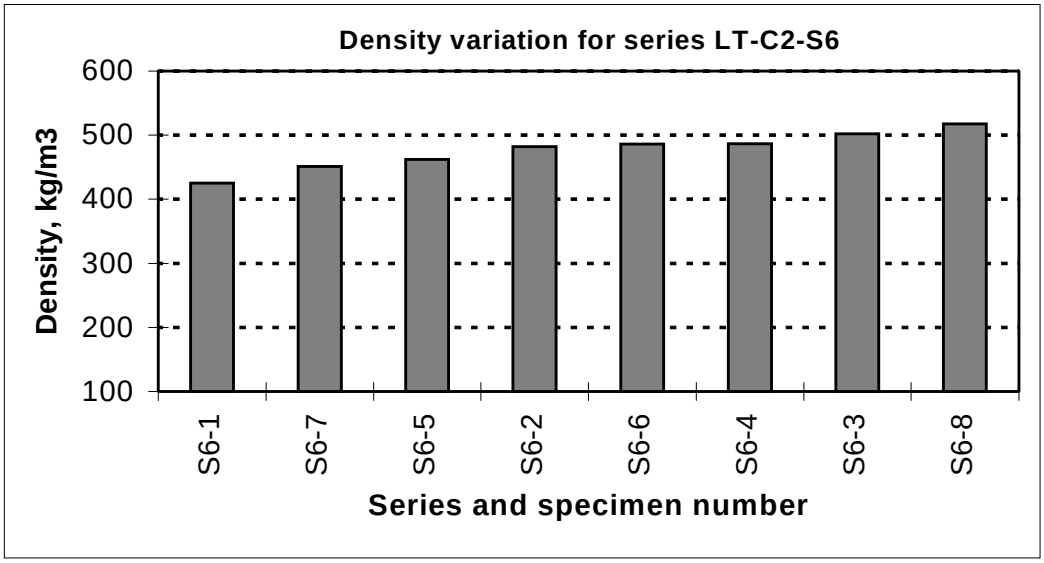

Figure 13. Variation of density (before oven dry) for specimen series LT-C2-S6.

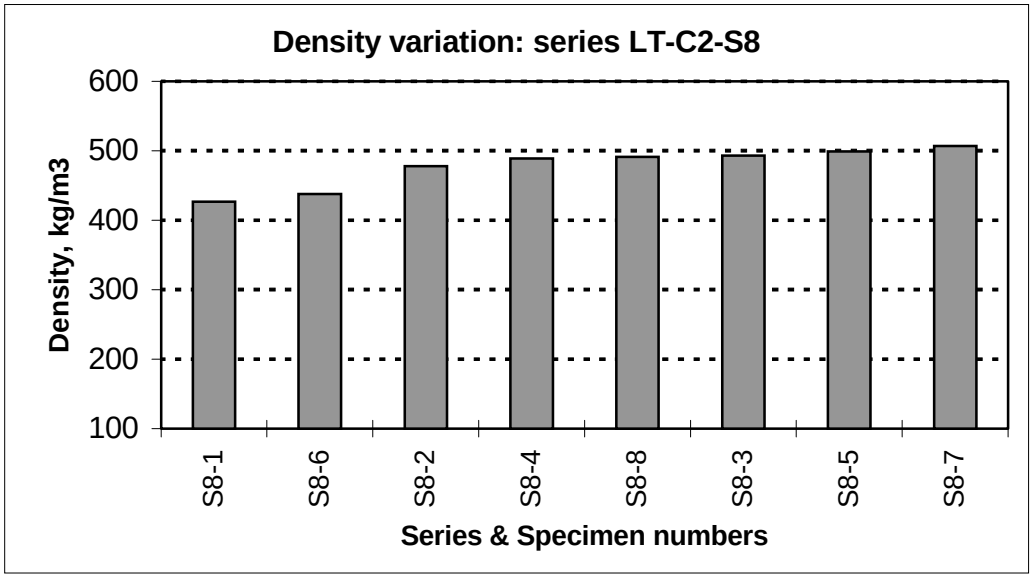

Figure 14. Variation of density (before ovendry) for specimen series LT-C2-S8.

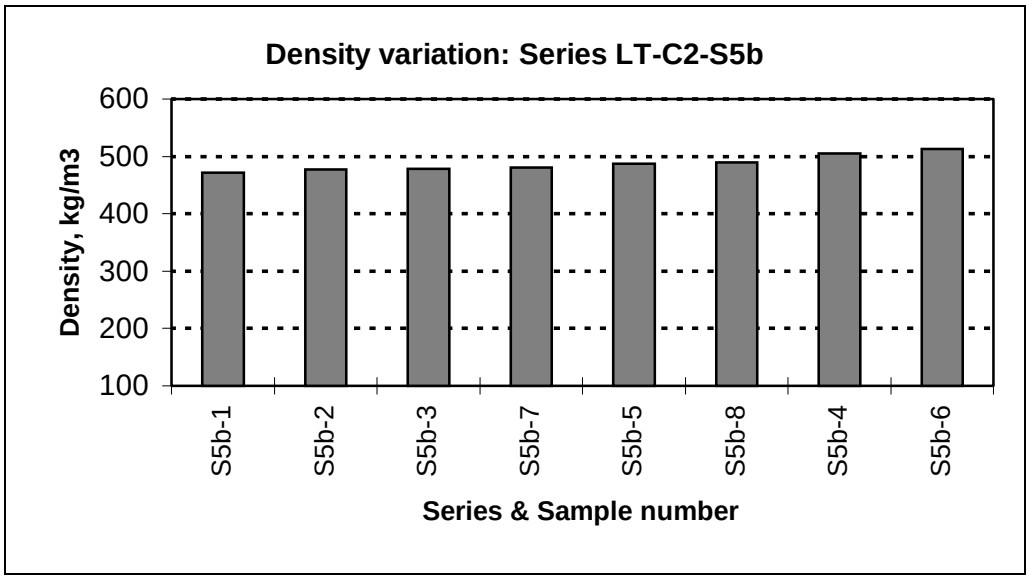

Figure 15. Variation of density (before oven dry) for specimen series LT-C2-S5b.

In series S2 the samples for density and moisture content measurements were taken from all the 18 lamellae, while in remaining series, two or three test samples were taken. The location where the crack appeared in the laminae is given in chapter 4 of this report.

3.2 Moisture in long term experiments

The relative humidity (RH) and temperature of the room where the specimens were stored were measured on a regular basis and the data recorded. This procedure was followed for all the series. As an example, the variation of RH and temperature of the room is shown in Figure 16 for series S6.

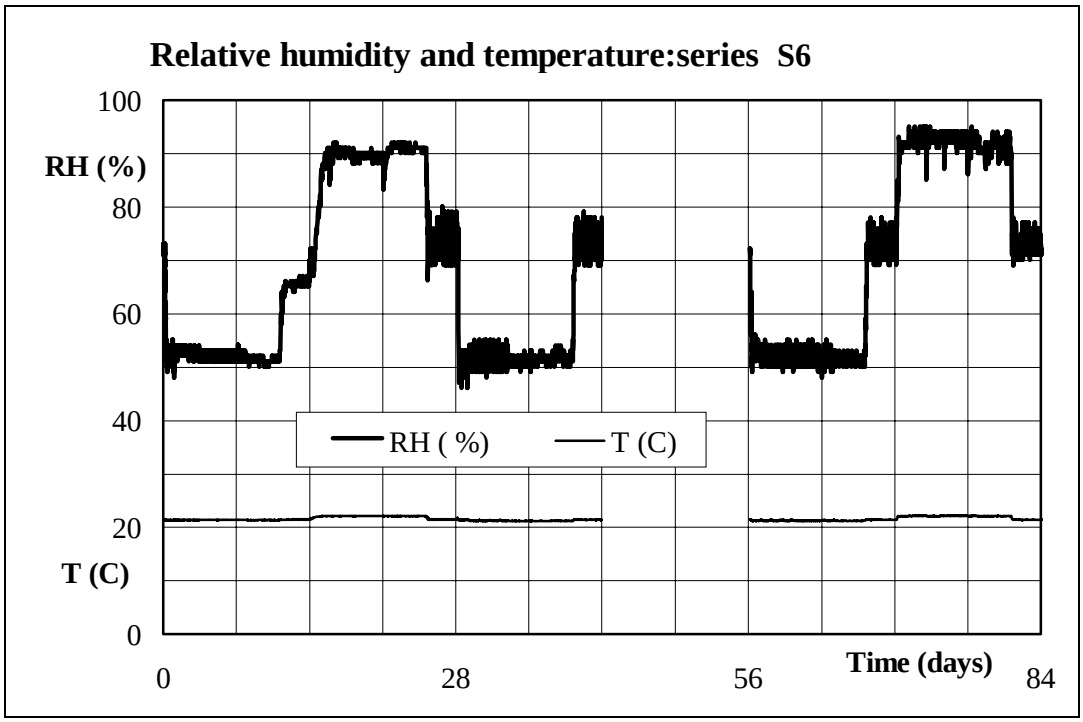

Figure 16. Variation of relative humidity and temperature for series S6.

To monitor the variation of moisture content in series S2 during testing, small glulam samples were used. These samples of glulam were weighed regularly during a cycle of variation as illustrated in Figures 17 (a) and 17(b). With these samples, the effect of moisture variation with different end surface conditions can also be observed.

The symbols in Figures 17 a and b indicate the location, depth and thickness of samples taken from the end of glulam beams. For example, in LB100 and LB50, L represents glulam beam, B represents the location of sample taken, while 50 and 100 represent the thickness of samples in mm. Similarly, in LD60 the letter D shows the location of sample taken at the end (quarter of cross section) of glulam beam and the numbers indicate the thickness of samples in mm. Sealing of specimen surfaces is indicated in Figure 17 by lines drawn along the sides of samples. Since the values are very close to each other, the symbols of different samples are in the same positions. More details about end conditions of samples, their locations and other explanations are given in Appendix A.

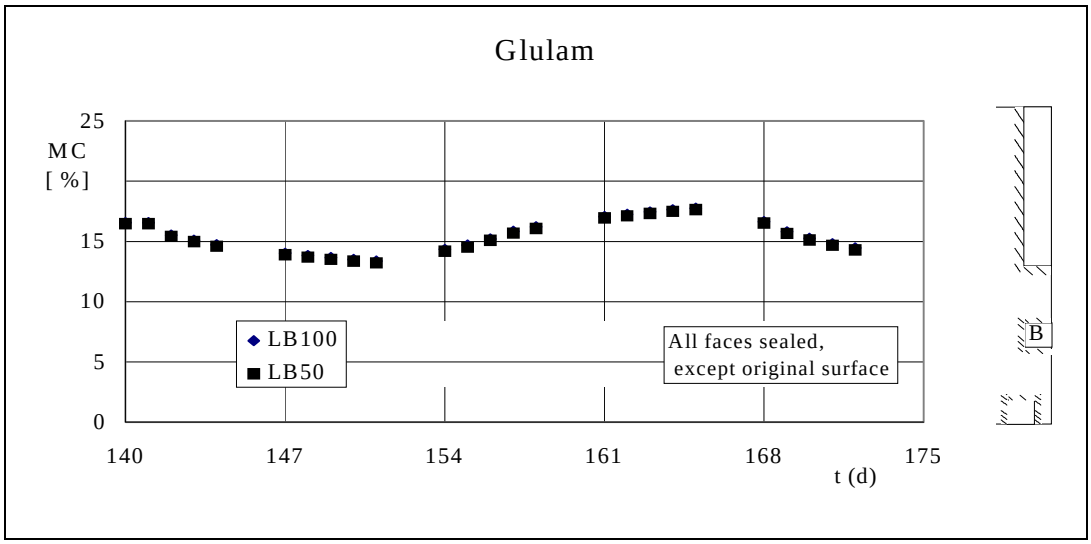

Figure 17(a). Average moisture content variation during humidity cycle. Simulating 90 mm thick glulam beams.

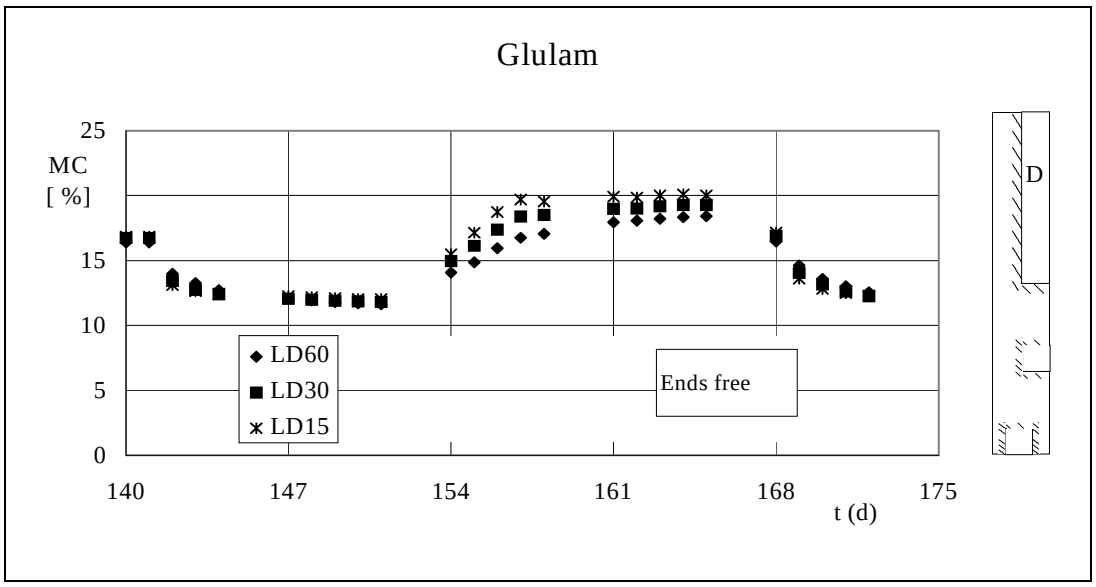

Figure 17(b). Average moisture content variation during humidity cycle. Simulating near surface locations.

To observe the moisture content in glulam beams at constant 85% RH, measurement of moisture content was made using electrical moisture meter (FMD moisture meter). The measurements were made in November 1996, while the beams were tested during May 1997. The procedure laid out in the European Drying Group (EDG) recommendation (Welling, 1994) was followed to measure the M.C. in the specimens. The measurements were taken at depths of 1/6, 1/3 and 1/2 of the beam. In addition, moisture measurements at the 4th lamella from the top, the middle lamella and the 4th lamella from the bottom of the beams were also made. The measured data are given in Table 5.

Table 5. Moisture content in glulam beam series S4 (November 1996).

	Moisture content (MC) measured by electrical moisture meter (FMD-moisture meter)				
		Measurements on top & bottom faces of beam			
Beam	Place of measurement	MC (1/3 of the thickness)	MC (1/6 of the thickness)	MC (1/2 of the thickness)	MC on top (1/5 of beam width)
1	Top lamella	18.5	18.5	18.5	
	Bottom lamella	19.7	19.7	19.7	
	4th lamella from the top				18.9
	Middle lamella				19.7
	4th lamella from bottom				18.7
2	Top lamella	19.0	19.0	19.0	
	Bottom lamella	19.0	19.0	21.0	
	4th lamella from the top				18.2
	Middle lamella				19.3
	4th lamella from bottom				19.3
3	Top lamella	18.1	18.1	18.1	
	Bottom lamella	19.8	19.8	19.8	
	4th lamella from the top				19.6
	Middle lamella				19.3
	4th lamella from bottom				20.0
4	Top lamella	19.2	19.2	19.2	
	Bottom lamella	19.7	19.7	19.7	
	4th lamella from the top				19.7
	Middle lamella				19.6
	4th lamella from bottom				19.8
5	Top lamella	18.0	18.0	18.0	
	Bottom lamella	19.3	19.3	19.3	
	4th lamella from the top				19.3
	Middle lamella				19.4
	4th lamella from bottom				19.1
6	Top lamella	19.4	19.4	19.4	
	Bottom lamella	19.8	19.6	19.6	
	4th lamella from the top				19.3
	Middle lamella				20.2
	4th lamella from bottom				19.3
7	Top lamella	17.8	17.8	17.8	
	Bottom lamella	19.9	19.9	19.9	
	4th lamella from the top				19.0
	Middle lamella				19.8
	4th lamella from bottom				19.7
8	Top lamella	18.6	18.6	18.6	
	Bottom lamella	19.6	19.6	19.6	
	4th lamella from the top				19.5
	Middle lamella				18.8
	4th lamella from bottom				19.4
Mean	**All**	**19.1**	**19.1**	**19.2**	**19.4**
	Top	**18.6**	**18.6**	**18.6**	
	Bottom	**19.6**	**19.6**	**19.8**	
	4th from top				**19.2**
	Middle				**19.5**
	4th from bottom				**19.4**

Using the above M.C. data, graphical plots were made to see the possible moisture variation. These graphs are shown in Figures *18(a)* and 18(b). The variation shows no significant change among the laminates. However, a slight variation can be observed among the three places where the measurements were made. The mean moisture content of all the three measurements is 19.4%.

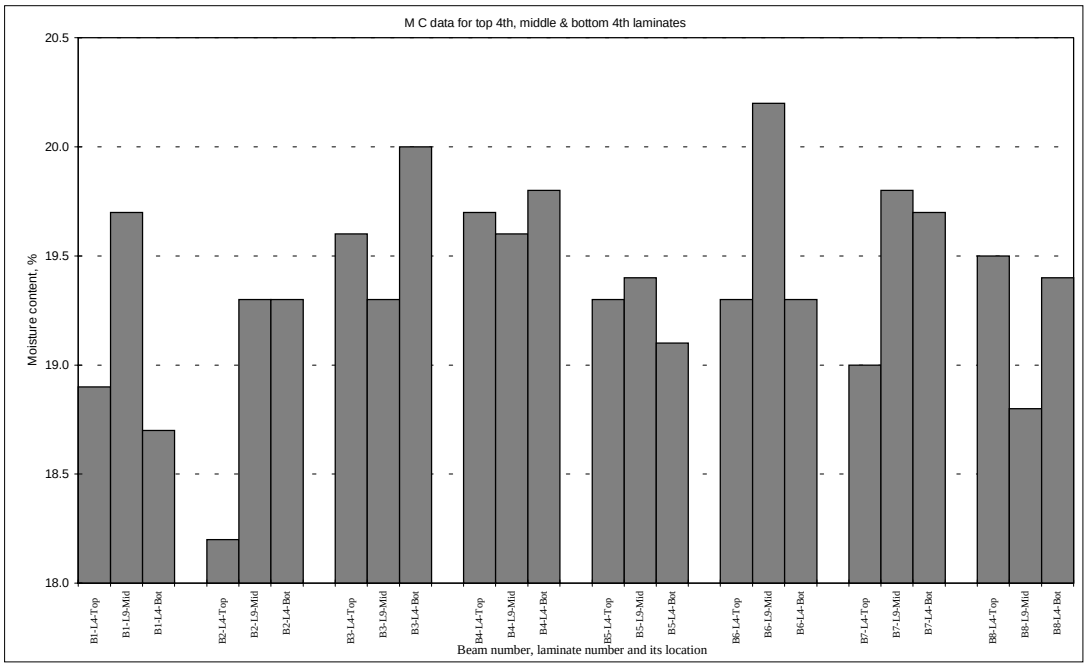

Figure 18(a). M.C. at different levels of glulam beam specimens.

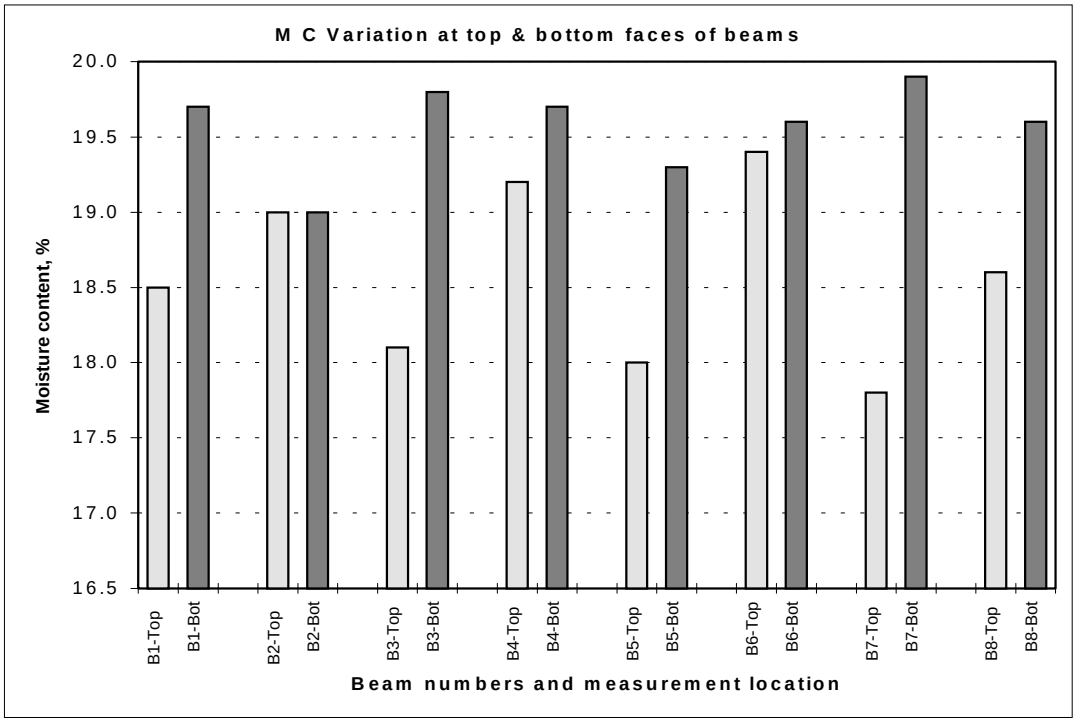

Figure 18(b). M.C. at top and bottom lamellae of glulam beam specimens.

Figure 18 (a) shows no consistent variation of M.C. among the eight beams. However, Figure 18(b), shows a variation in M.C. between top and bottom surfaces of beams with lower values on top surfaces. The mean value of M.C. on top surface is 18.6% and on bottom surface is 19.6%. The mean of all values is about 19.3%.

3.3 Monitoring of load levels in long term experiments

After the application of required loads for the beams, the magnitude of the load was measured regularly to ensure that there is no decrease in the levels. Since the beams were loaded by springs and the beams were creeping due to stress, there was time dependent variation in the load levels. To balance this effect, the loads were set to target values once a week, after first load increase the correction was often made after 1 - 2 days.

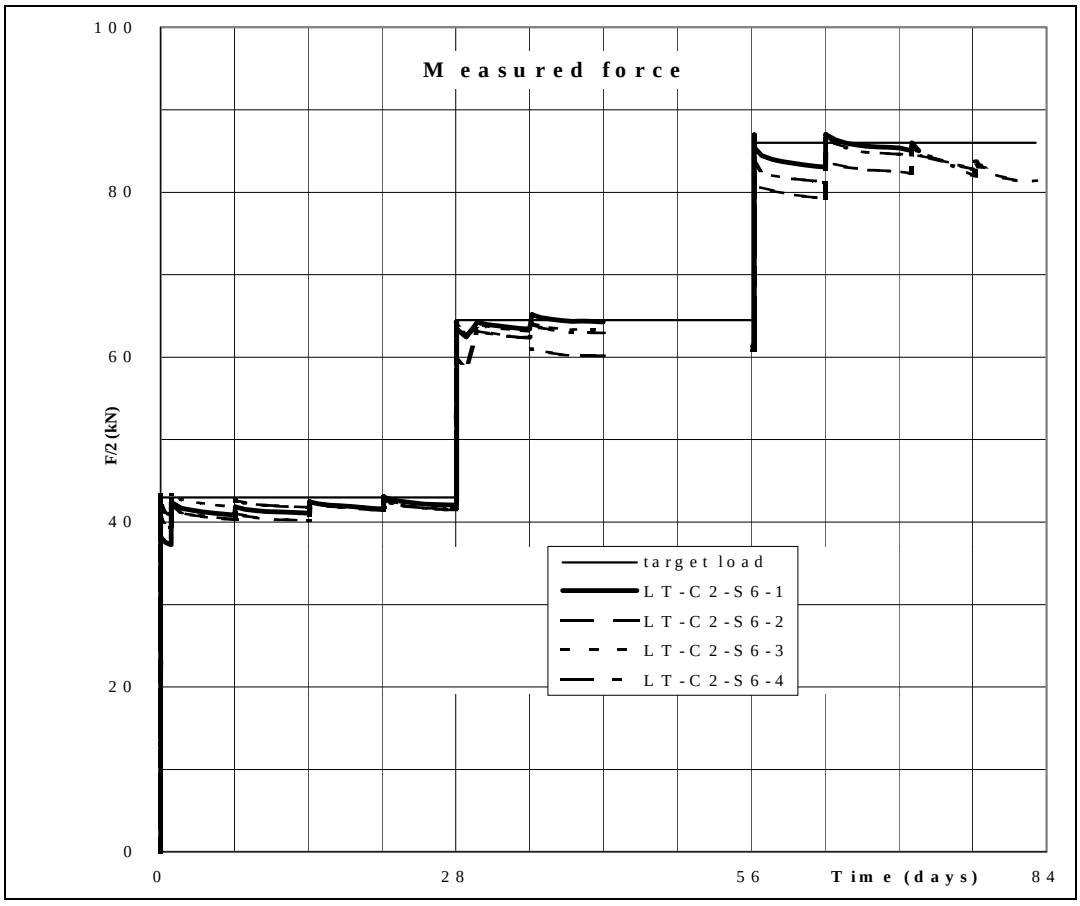

Figure 19(a). Support reaction measurements of four beams.

In addition, an independent check of load history was done by measuring one support reaction of four beams continuously. The measured support forces is

shown in Figure 19(a). In the graph, two weeks data is missing because of failure of a PC hard disk during that period. As can be seen in the graph, the magnitude of the force level decreased during the end of the two weeks period was normally found to be less than 5% of applied load. However, in calculations, the target values of loads have been used. The plots of individual measurements of support reaction forces for individual beams are given in Appendix C.

3.4 Measurement of deformations during long term experiments

To monitor the changes in creep deformation of specimens during long term experiments, one dial gauge was used for each beam at the crown in the centre. Figure 19(b) shows the deformation versus time for the beams in series S6. The plots of measurements for individual specimens for all the three series are given in Appendix D.

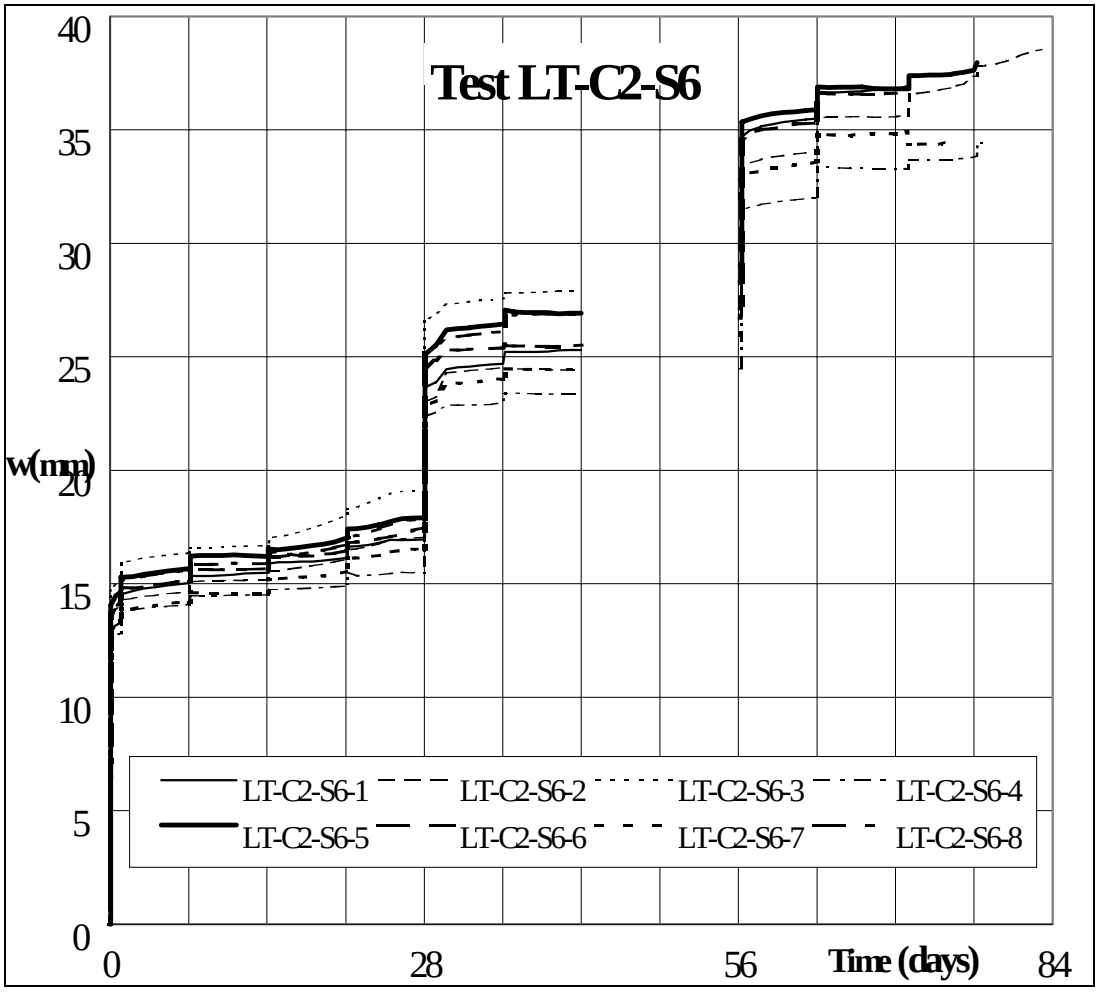

Figure 19(b). Deflection measurements of beams for S6 series.

3.5 Load duration and ultimate stress

Eight specimens at a time were tested in each series and tests on the first series (LT-C2-S2) were carried our during early 1995. The tests on the second series (LT-C2-S6) were carried out from Fall 1995 to Spring 1996. The third series (LT-C2-S4) in late 1996. The fourth series (LT-C2-S8) were tested in 1997. The creep deformation of the specimens and the relative humidity changes in the test hall were measured with a computer controlled measuring system through out the experiments. The details of the test results for each series is discussed separately in the following sections.

3.5.1 Extra short term tests: series ST-C2-S5b

A set of specimens belonging to ST-C2-S5b series were stored as follows: First half of series (specimens 1 to 4) was stored in the cyclic climate of experiment of series S2 and these beams were removed for testing when the moisture content was maximum (1995). The second half of series (specimens 5 to 8) was stored at a constant high relative humidity room (85%) for a year before testing under short term loading (1997). The aim was to study the strength effect of beams due to high constant humidity (85%). The beams were loaded gradually and the loading rate was controlled in such a way that the total time to failure of beams was about 5 ± 2 minutes. The deflection during loading was measured at two locations.

Table 6. Beam parameters, moments and displacements: ST-C2-S5b series.

Specimens	Width w	Height h	Rmean	Pmax	Moment, Mmax	Maximum deformation (mm)	
	mm	mm	mm	kN	kNm	at Crown	at Centre
ST-C2-S5b-1	141	605	5700	246.8	185.0	36.31	0.673
ST-C2-S5b-2	142	609	5700	215.0	161.3	33.04	0.595
ST-C2-S5b-3	141	605	5700	288.8	216.6	48.57	0.906
ST-C2-S5b-4	140	605	5700	245.8	184.4	40.29	0.763
ST-C2-S5b-5	141	607	5700	265.7	199.3	44.47	0.917
ST-C2-S5b-6	141	610	5700	312.0	216.0	52.06	0.967
ST-C2-S5b-7	141	611	5700	279.4	209.6	47.79	0.809
ST-C2-S5b-8	142	609	5700	284.2	213.2	49.77	0.894
Mean	**141**	**608**	**5700**	**267**	**198.16**	**44.04**	**0.816**

The load-deflection data recorded during loading was used to plot the load versus deformation graphs for the eight beams. The beam parameters, maximum loads and maximum deflections at crown and mid-central section of the beams are given in Table 6. The load versus mid-central section deflection for the beams is given below in Figures 20 and 21 respectively.

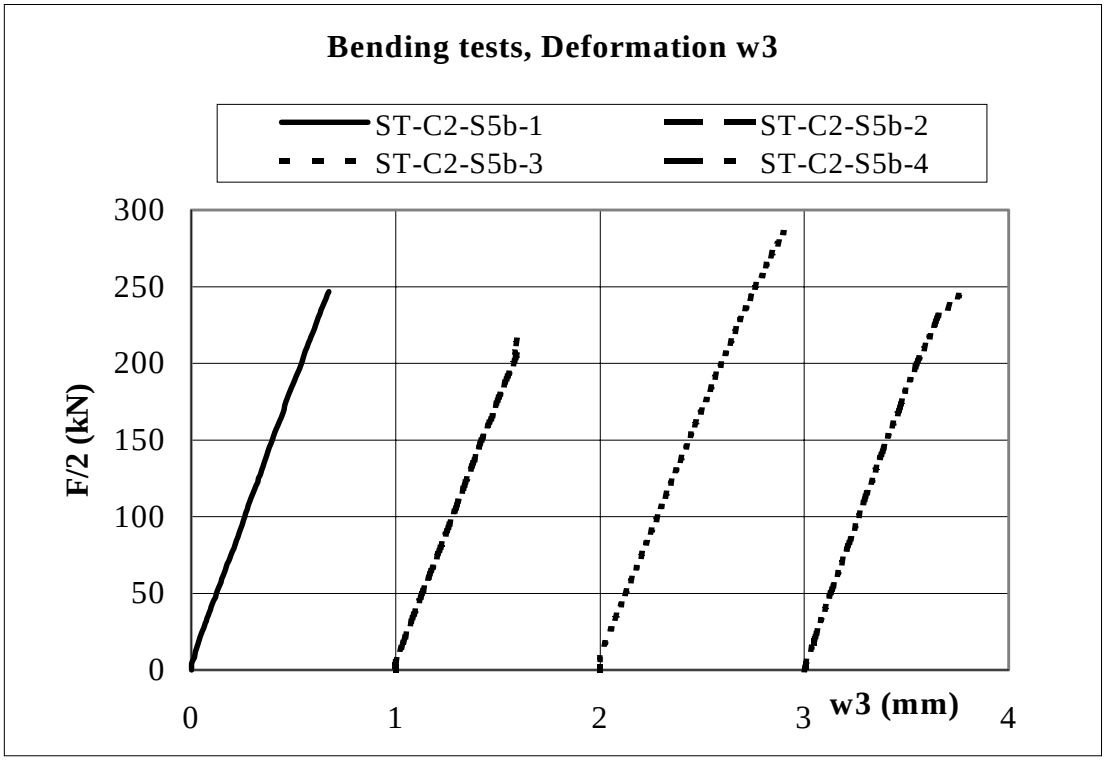

Figure 20. Load versus mid-central deflection (w3) for ST-C2-S5b series.

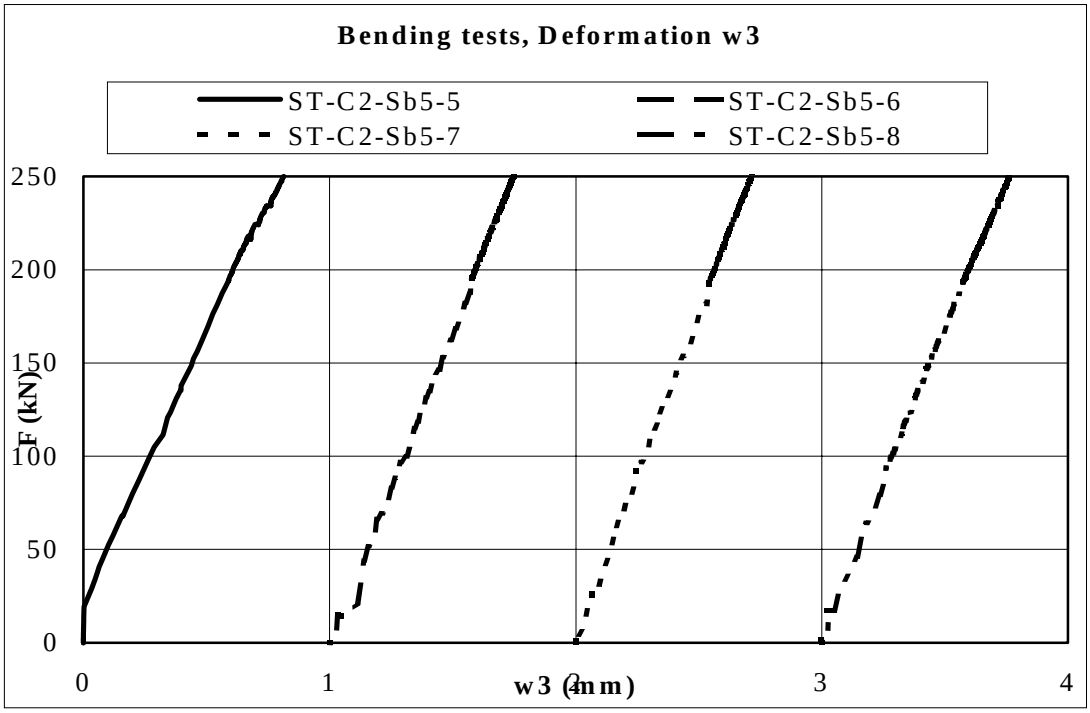

Figure 21. Load versus mid-central deflection (w3) for ST-C2-S5b series.

The load versus crown deformations of are given in Figures 22 and 23 respectively.

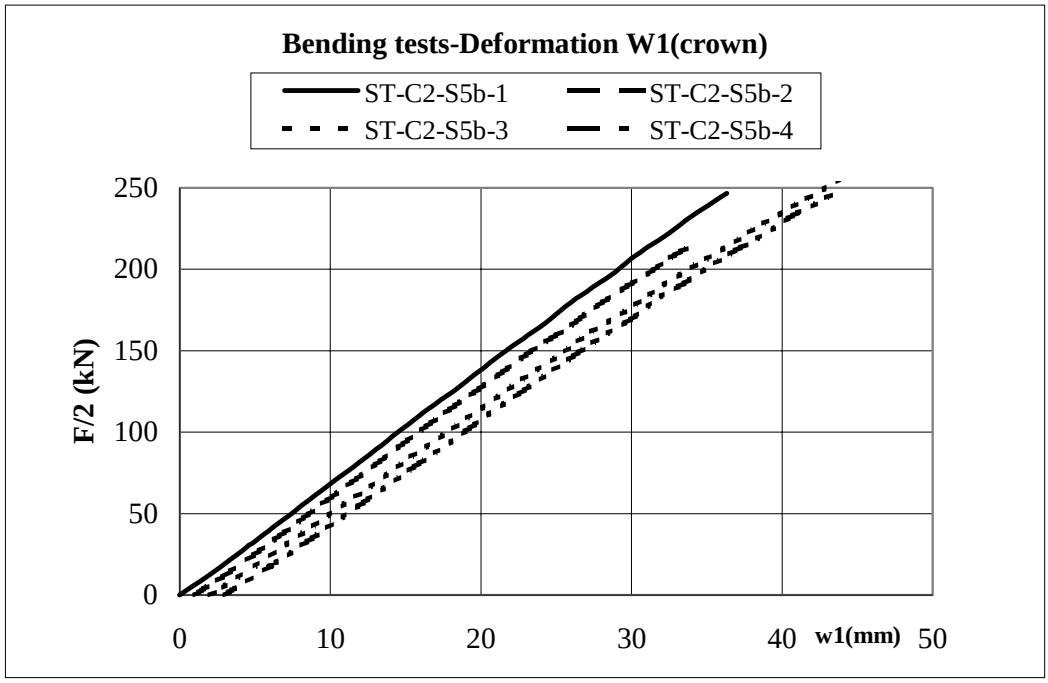

Figure 22. Load versus crown deflection(w1) curves for ST-C2-S5b series.

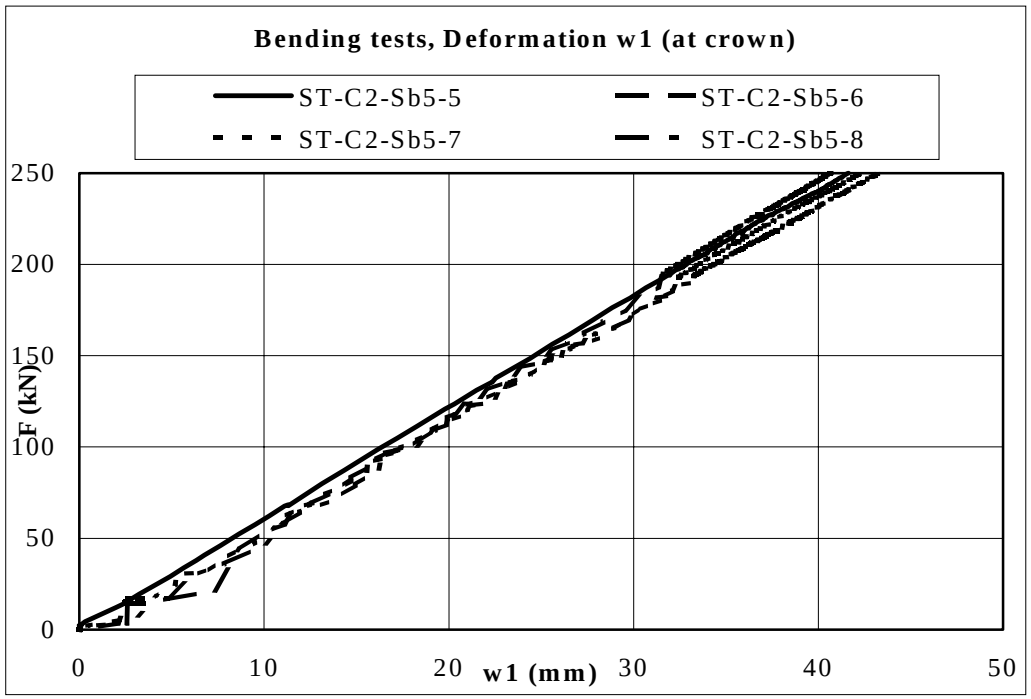

Figure 23. Load versus crown deflection(w1) curves for ST-C2-S5b series.

Table 7 a. Ultimate loads, tensile and bending stresses for the four beams in series ST-C2-S5b after cyclic humidity.

Specimen designation	Ultimate load	Maximum Tensile stress N/mm2	Maximum Bending stress N/mm2
	kN	$\sigma_{t,90}$	σ_b
ST-C2-S5b-1	246.8	0.571	22.45
ST-C2-S5b-2	215.0	0.491	19.19
ST-C2-S5b-3	288.8	0.669	26.29
ST-C2-S5b-4	245.8	0.572	22.54
Mean	**249.1**	**0.576**	**22.62**

Table 7 b. Ultimate loads, tensile and bending stresses for the remaining four beams in series ST-C2-S5b at 85% RH.

Specimen designation	Ultimate load	Maximum Tensile stress N/mm2	Maximum Bending stress N/mm2
	kN	$\sigma_{t,90}$	σ_b
ST-C2-S5b-5	265.7	0.613	24.03
ST-C2-S5b-6	312.0	0.716	25.80
ST-C2-S5b-7	279.4	0.640	24.95
ST-C2-S5b-8	284.2	0.649	25.36
Mean	**285.3**	**0.654**	**25.04**

The test data of short term specimens are given in Tables 7a and 7b respectively for each set of four specimens in series S5b. The data indicate that, the mean values of maximum ultimate load, tensile strength perpendicular to grain and bending strength for the second set of beams are higher than the first set of beams. The first set of four specimens S5b-1 to S5b-4 which were stored in a cyclic climate exhibit weaker strength than the second set of specimens S5b-5 to S5b-8 which were stored at constant humidity of 85%.

The first half of the beams (at cyclic humidity) had the same average strength as series S5a at 65% RH. The previous knowledge is that the tensile strength at 85% RH should be lower than at 65%, but we got conflicting results in experiments. Hence, we conclude that tensile strength is practically independent from moisture content within this range. Accordingly, all results in test series S5a and S5b will be combined in the analysis to follow.

3.5.2 Long term tests: Series LT-C2-S2

The eight beams in this series were first conditioned at 75% RH, and then subjected to a changing relative humidity for 56 days (8 weeks) without any load on them. During this time, the 28 days cyclic relative humidity in the test hall was varied from 55➢75➢90➢75➢55 as shown in Figure 25, and the same cyclic variation was continued when the specimens were under the load application.

The first load level was applied in such a way that it induced about 0.2 MPa mean tension stress perpendicular to grain in the beams. This intensity was kept nominally constant for 28 days. The subsequent load increment of 4 weeks duration was applied as planned and the variation of relative humidity continued until the failure of all specimens occurred. Between second and third load level, there was interruption in loading for 21 days (Fig. 24), because some repair work needed to be made for test rigs.

Deflection measurements from start to end of testing are shown in Appendix D. Since the force was applied by springs, a gradual decrease in load due to creep deformation was noticed. To rectify this, the load levels were corrected manually once a week on average, which can be seen in deflection curves. During high humidity (90%) the electrical deflection measurement was not reliable. To check these measurements, manual measurements were also made for comparison. The manual measurements are shown with dot symbols on the graphs given in Appendix D (creep deformation of specimens).

Table 8 shows the magnitude of the ultimate failure stress perpendicular to grain and the time duration of each beam for specimen series LT-C2-S2. The total number of days each beam was subjected to loading during the final cyclic RH range are also shown in the same table. The failure stress and number of days the beams sustained the failure load level is shown in Figure 24, while the cyclic variation of relative humidity for the complete duration of testing is shown in Figure 25.

Table 8. Tension stress perpendicular to grain and failure time for specimen series LT-C2-S2.

Specimens	Tension stress perpendicular to grain ($\sigma_{t,90}$)* (MPa)	Failure time during final load & RH cycle	Total load duration of specimens (**t**-56) ** ; (days)	RH during failure, %
LT-C2-S2-2	0.41	10 min.	140-77=63	75
LT-C2-S2-3	0.41	24 d	165-77=88	75
LT-C2-S2-4	0.51	21 d	189-77=112	90
LT-C2-S2-1	0.61	5 sec	196-77=119	75
LT-C2-S2-5	0.61	5 sec	196-77=119	75
LT-C2-S2-8	0.61	4 d	200-77=123	55
LT-C2-S2-7	0.61	16 d	212-77=135	90
LT-C2-S2-6	0.61	18 d	214-77=137	90

***** Stress level during final load & RH cycle;****** Beams in cyclic RH for 56+21 days without load.

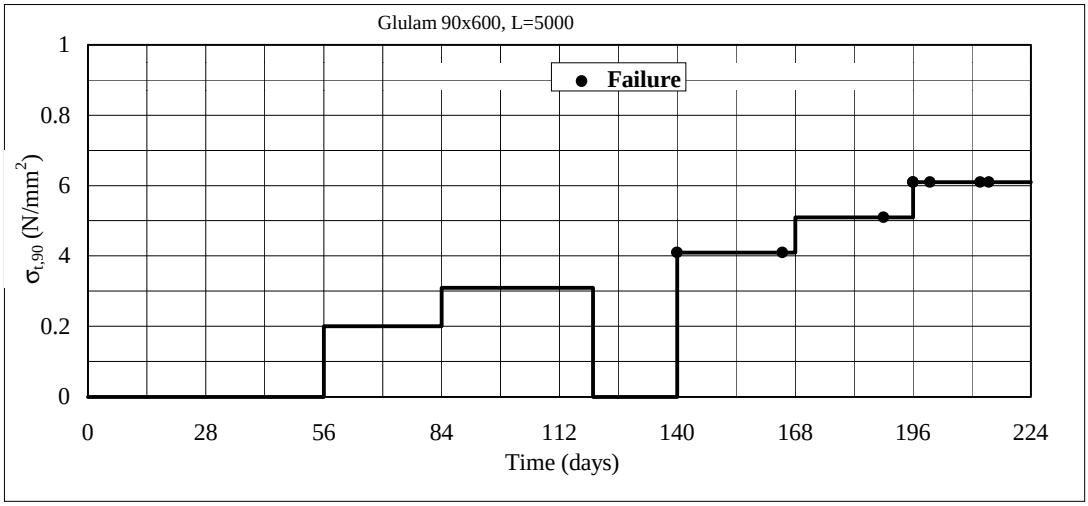

Figure 24. Tension stress versus time to failure for specimen series LT-C2-S2.

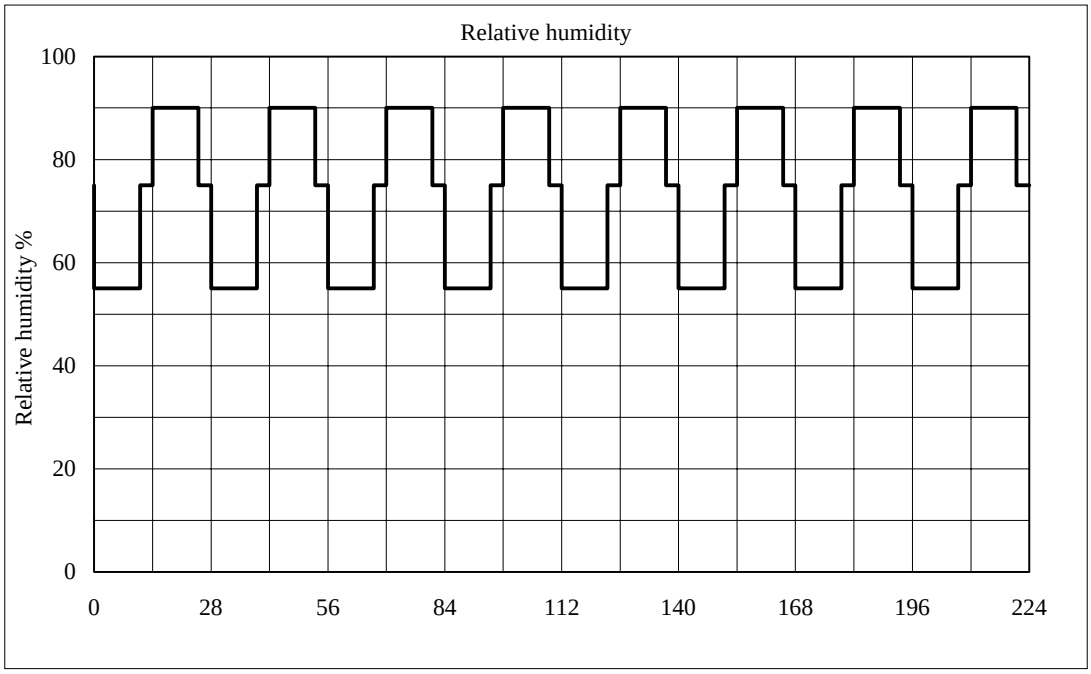

Figure 25. Relative humidity versus time for specimen series LT-C2-S2.

The load duration of specimens for series LT-C2-S2 is shown graphically in Figure 26. Figure 27 shows specimens along with specimen number and ultimate load versus stress perpendicular to grain.

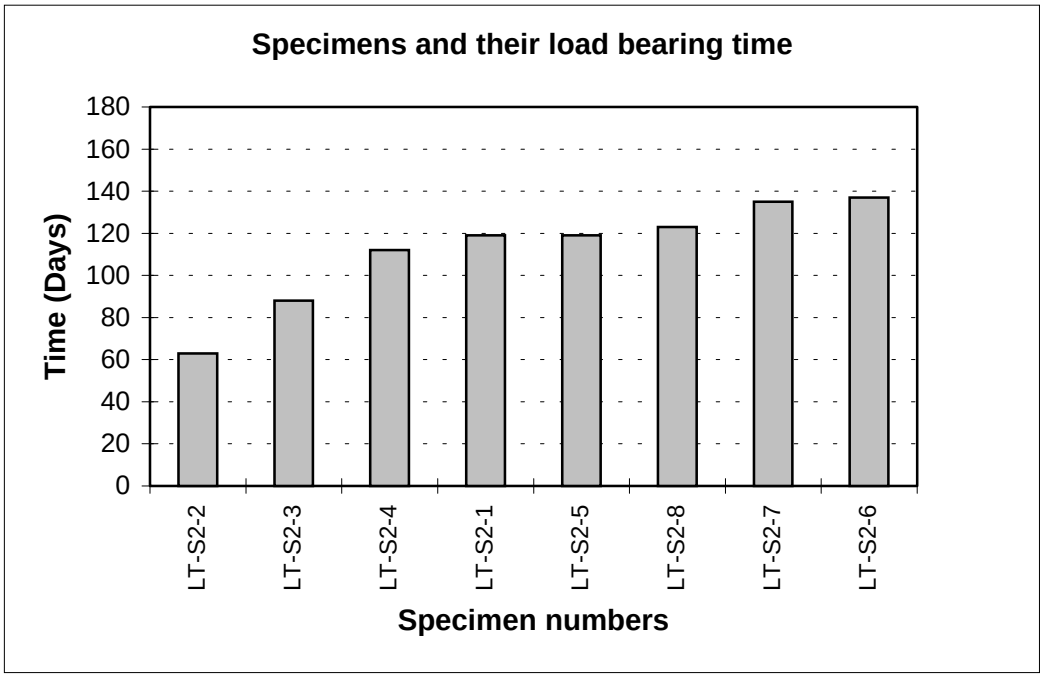

Figure 26. Variation of load-duration for specimens in series LT-C2-S2.

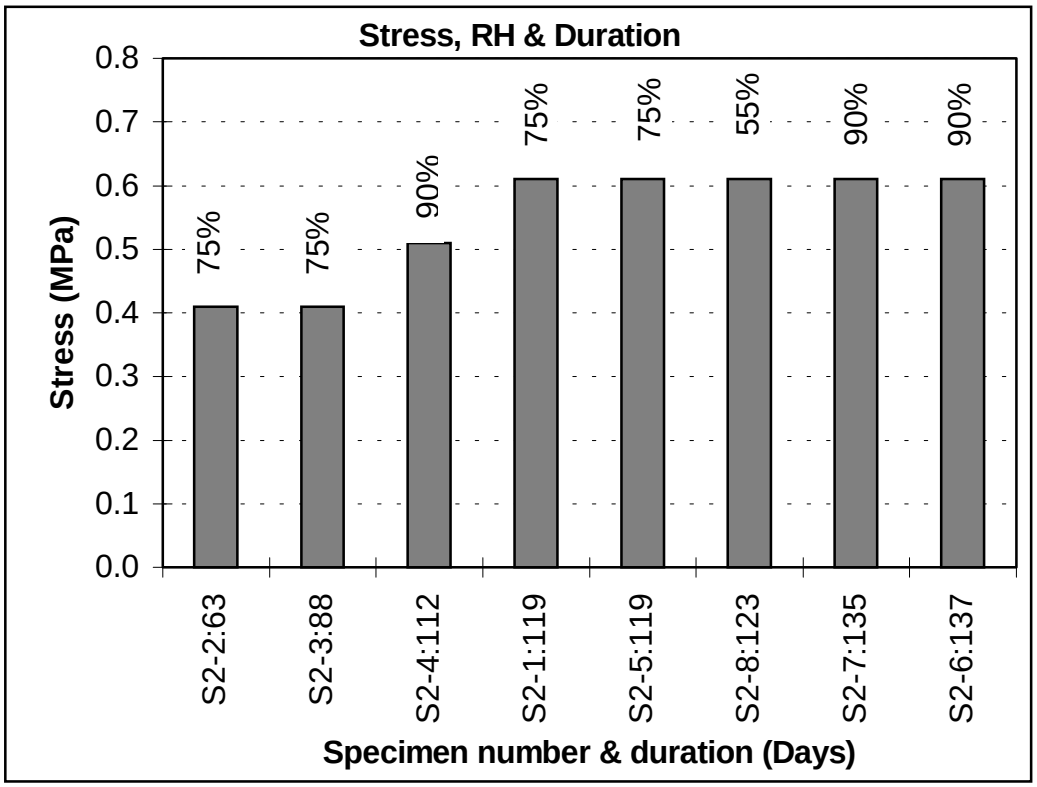

Figure 27. Stress perpendicular to grain vs. load-duration for series LT-C2-S2.

As can be seen in the graphs, beam 2(S2-2) failed first at a stress level of 0.41 MPa after 63 days (10 minutes after load increase), while beam 3 failed after 88 days (24 days after load increase) under same stress level. Beam 4 failed after 112 days at 0.51 MPa, while beam 6 failed last after 137 days at 0.61 MPa.

Figure 27 shows the stress level and relative humidity at the time of failure for specimen series LT-C2-S2. The specimen numbers and their corresponding number of days of load duration (e.g. ***S2-2*:63**) are given on the ***x***-axis. Only one specimen failed when the relative humidity level was 55%, while the rest of the specimens have failed when the cyclic relative humidity level was 75% or more.

3.5.3 Series LT-C2-S4

This series of long term tests (LT-C2-S4), included eight specimens and tests were carried out similar to the first series, except constant moisture conditions. The curved glulam beams in this series were conditioned at 85% RH, and had dimensions of 90 x 600 x 7300 mm. The tension stress perpendicular to grain during failure, the number of days the specimens sustained the load during the last incremental load and the number of days the beams survived the incremental load are shown in Table 9.

The incremental stress induced on the beams during the testing period is shown in Figure 28, while relative humidity is shown in Figure 29. As can be seen in Figure 28, the first and second load increments on the beams induced stress levels of 0.31 MPa and 0.41 MPa respectively. During this 56 days, no specimens failed. When the third load increment was applied, it created a stress of 0.51 MPa causing failure of beam S4-3 after 57 days. As the same load continued, another beam S4-4 failed after 70 days. When the final load increment was made after 84 days, with a stress level of 0.61 MPa, the rest of the beams failed except specimen S4-6. After about 112 days the test was terminated.

Figure 30 shows load duration versus beams failed in ascending order. The beam S4-6 did not fail when other beams failed and the test was terminated after 112 days. However, for comparison, this specimen is included in graphs. Figure 31 shows duration versus tension stress perpendicular to grain, while Figure 32 shows stress versus specimens and their corresponding load duration days.

Table 9. Tension stress perpendicular to grain and failure time for specimen series LT-C2-S4.

Specimen numbers	$\sigma_{t,90}$ (MPa)	Time from start of cycle	Total loading time (days)
LT-C2-S4-3	0.51	1 d	57 d
LT-C2-S4-4	0.51	14 d	70 d
LT-C2-S4-1	0.61	3 d	87 d
LT-C2-S4-8	0.61	4 d	88 d
LT-C2-S4-5	0.61	9 d	93 d
LT-C2-S4-7	0.61	14 d	98 d
LT-C2-S4-2	0.61	21 d	105 d
LT-C2-S4-6	0.61		no failure

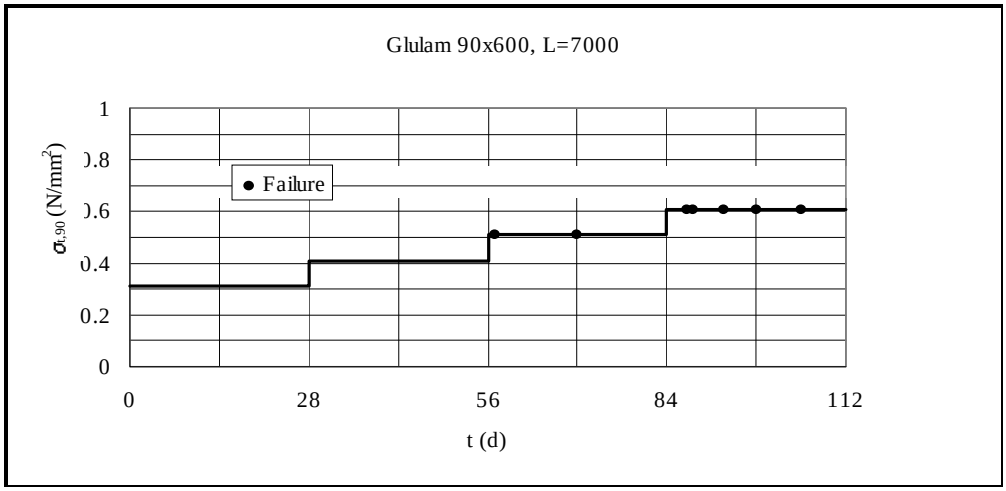

Figure 28. Tension stress versus time to failure for specimen series LT-C2-S4.

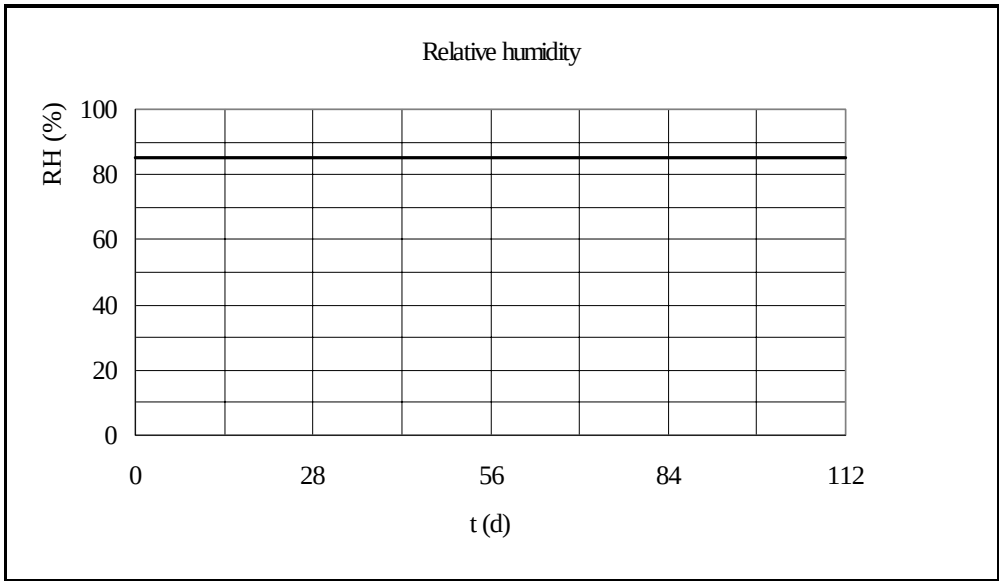

Figure 29. Constant relative humidity level used for specimen series LT-C2-S4.

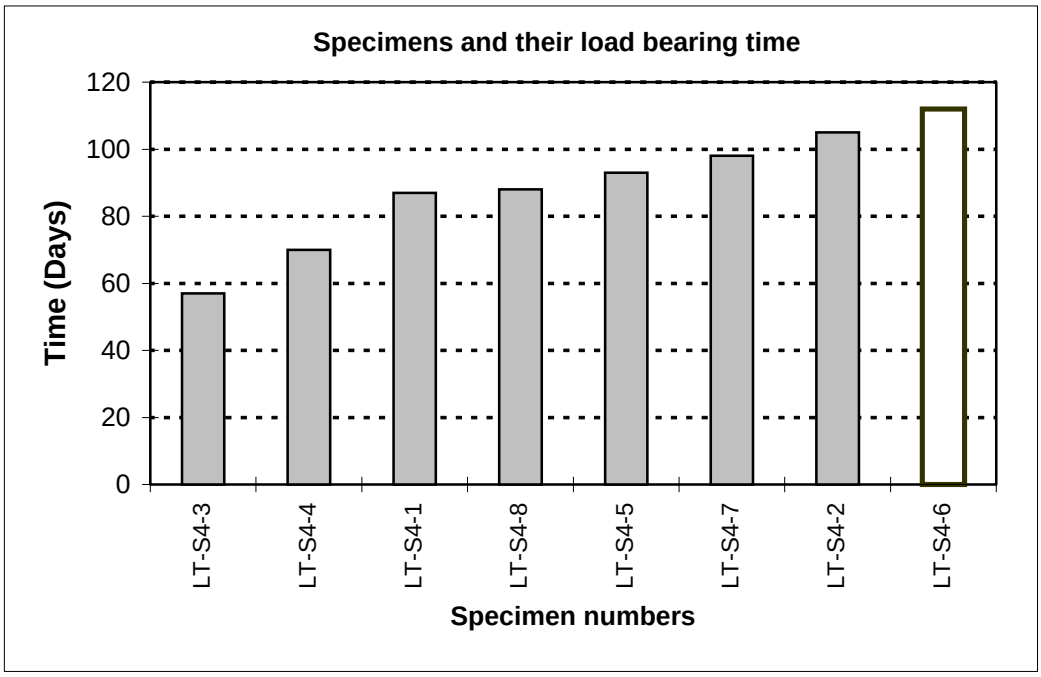

Figure 30. Variation of load duration for specimen series LT-C2-S4 (specimen S4-6 did not fail before termination of experiment).

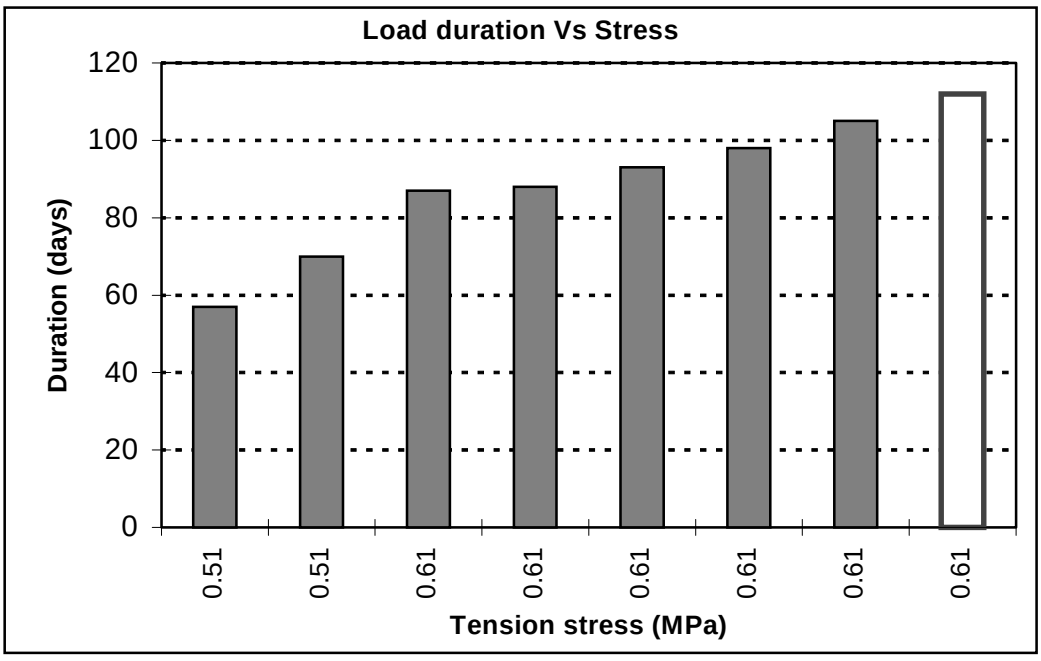

Figure 31. Load duration versus stress perpendicular to grain for LT-C2-S4 (specimen S4-6 did not fail before termination of experiment).

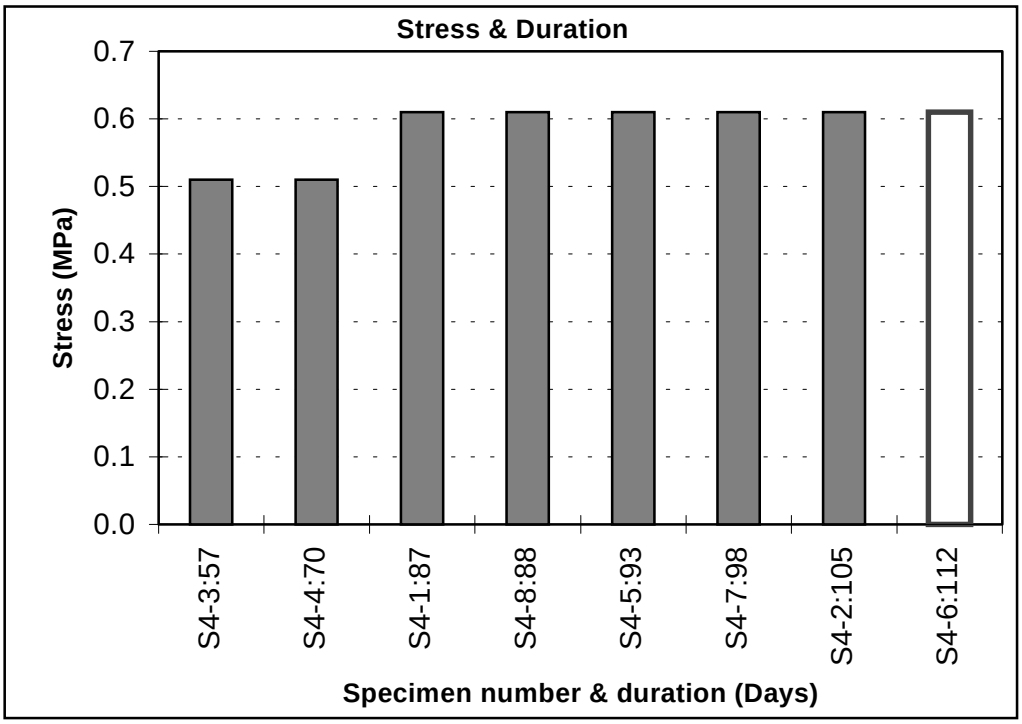

Figure 32. Stress perpendicular to grain vs. load duration for LT-C2-S4 series (specimen S4-6 did not fail before termination of experiment).

3.5.4 Series LT-C2-S6

In this series (LT-C2-S6) of long term tests, eight specimens were tested under identical conditions similar to the first series. The curved glulam beams had dimensions of 140 x 600 x 7 300 mm. The loading and supporting system for the specimens in this series is shown in Figure 4. The tension stress perpendicular to grain during failure, the number of days the specimens sustained the load during the last incremental load and the cyclic relative humidity level are shown in Table 10.

As can be seen in Table 10 and Figure 33, two beams, S6-3 and S6-8 failed after 55 days and 56 days respectively at a stress level of 0.30 MPa, while failure in all other specimens occurred when the stress level was 0.40 MPa. Only beam number 2 (S6-2) had a stress level of 0.51 for about one hour duration. Failure of all the beams in this series has occurred when the relative humidity level was 75% or 90%.

Figure 35 and Figure 36 show magnitude of failure stress perpendicular to grain and the load duration for series LT-C2-S6, while Figure 34 shows the cyclic variation of relative humidity during the entire test period (55➢75➢90➢75➢55).

Table 10. Tension stress, load duration and failure time for series LT-C2-S6 (b x h =140 x 600, L=7000).

Specimen number	Tension stress* $\sigma_{t,90}$ (MPa)	Failure time from start of final cycle	Total load duration (days)	RH during failure (%)
LT-C2-S6-3	0.30	27 d	55	75
LT-C2-S6-8	0.30	28 d	56	75
LT-C2-S6-6	0.40	14 d	70	75
LT-C2-S6-1	0.40	15 d	71	75
LT-C2-S6-7	0.40	19 d	75	90
LT-C2-S6-5	0.40	21 d	77	90
LT-C2-S6-4	0.40	22 d	78	90
LT-C2-S6-2	0.51	1 h	84	75

***** Tension stress perpendicular to grain during final incremental load.

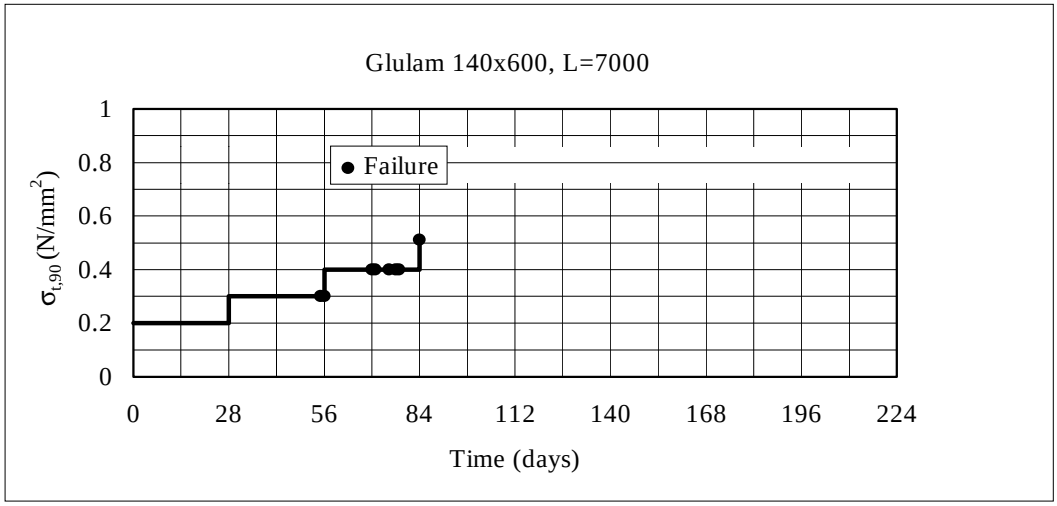

Figure 33. Tension stress versus time to failure for specimen series LT-C2-S6.

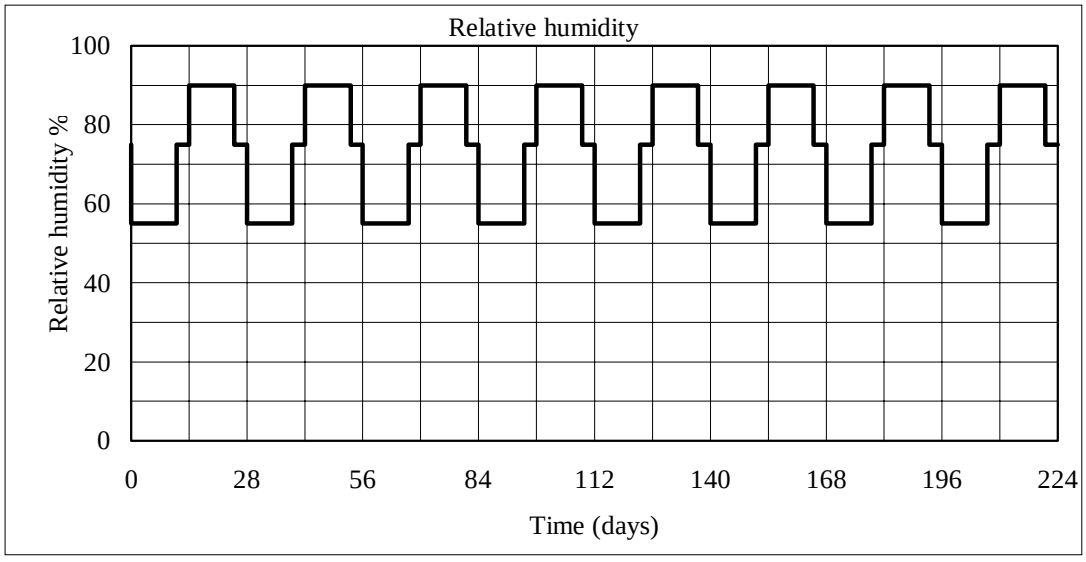

Figure 34. Relative humidity versus time for specimen series LT-C2-S6.

All the specimens in this series have failed at a lower stress level and shorter number of days when compared to the rest of the series. The specimens in this series had larger thickness and the reason for early failure life of these specimens may be attributed to the so called *"thickness effect"*, as in the case of short term strength (Ranta-Maunus, 1996).

Figure 35 shows a plot of tension stress perpendicular to grain and the number of days the specimens were able to resist the applied load until failure. The ***x***-axis shows the specimen number in series LT-C2-S6 and the number of days it sustained the load. The level of relative humidity at the time of failure of specimen is also given in the graph. In this series, the failure of all the beams have occurred when the relative humidity was between 75% and 90%.

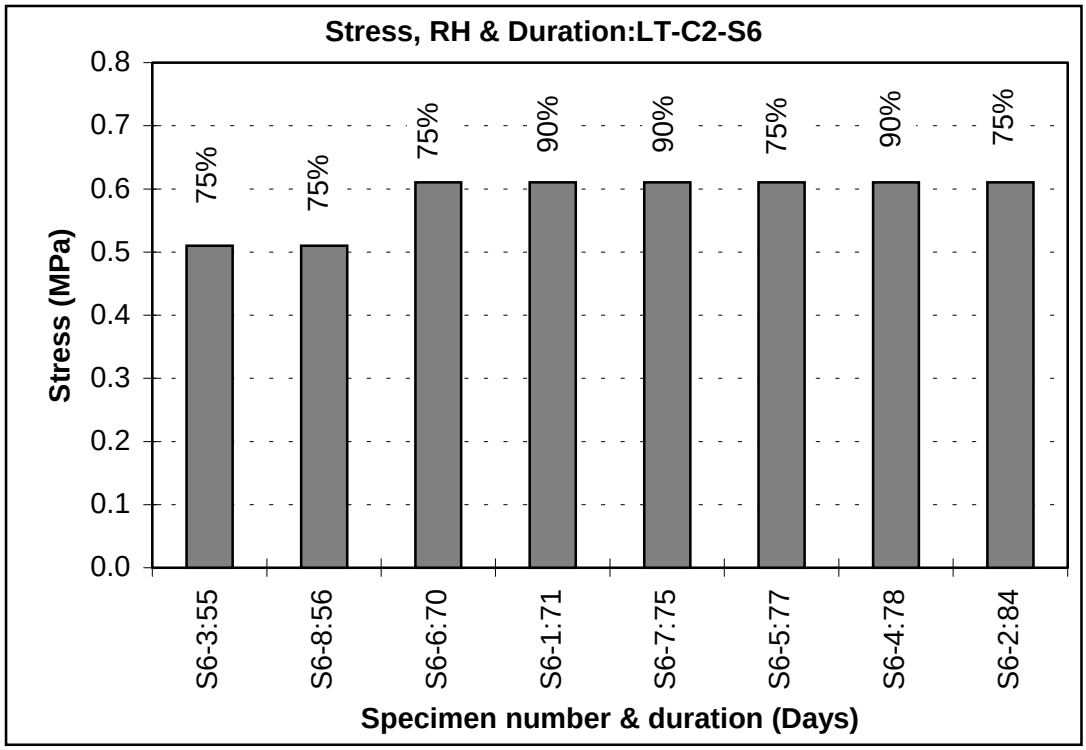

Figure 35. Stress perpendicular to grain VS. load duration for LT-C2-S6 series.

A profile of the load duration behaviour of specimens in the series LT-C2-S6 is shown in Figure 36, where the time duration of the beams versus the specimen numbers was plotted graphically in an ascending order. Specimen 3 had the lowest number of days (55), while specimen 2 had the highest number of days (84) during the loaded period.

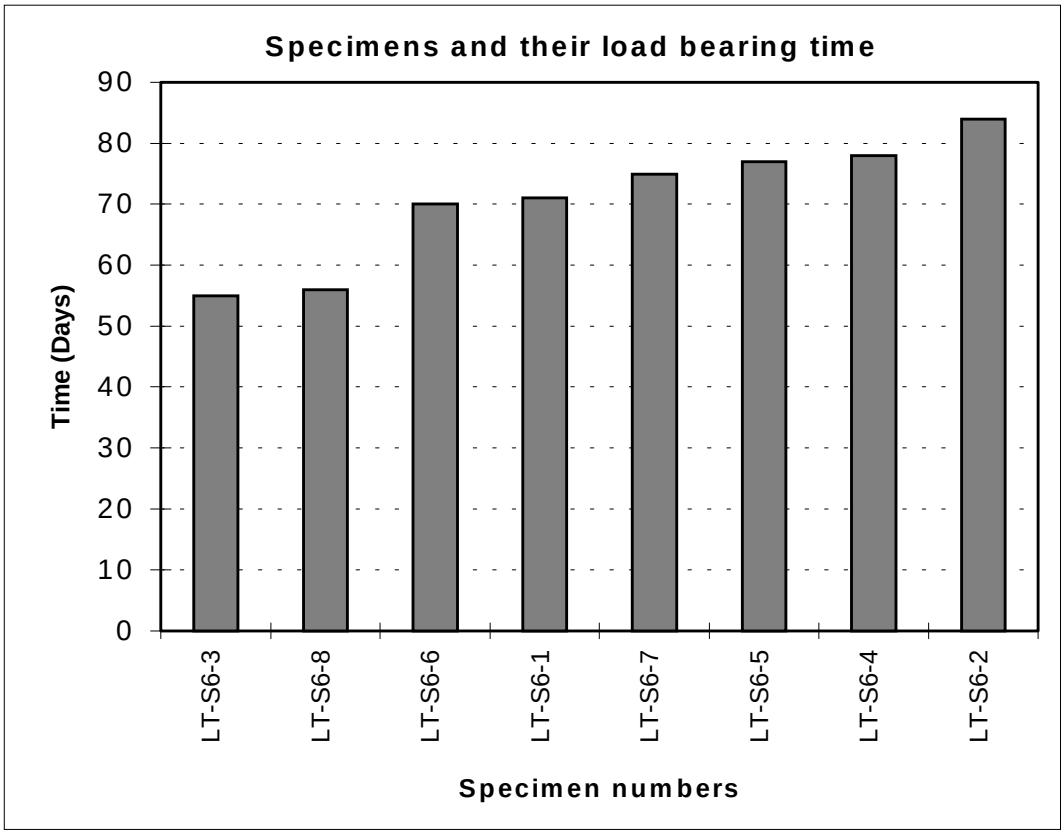

Figure 36. Load duration versus failure for specimen series LT-C2-S6.

3.5.5 Series LT-C2-S8

In this series (LT-C2-S8), eight specimens were tested under constant relative humidity conditions during the entire test period. The curved glulam beams had dimensions of 140 x 600 x 7 300 mm. The beams were painted with a vapour barrier to ensure the constant moisture content. Only four beams failed under long term loading, while the other four beams did not fail before the termination of test. The tension stress perpendicular to grain during failure, the number of days the specimens sustained the load during the last incremental load are shown in Table 11.

The four beams (S8-1, S8-3, S8-4 and S8-6) in this series which did not fail under long term testing were tested again in ramp loading. The short term strengths of these beams are also given in the Table 11. Figure 37 shows record of tensile stress versus time to failure, while Figure 38 shows the constant humidity maintained during the experiment.

Table 11. Tension stress, load duration and failure time for series LT-C2-S8.

Specimen number	$\sigma_{t,90}$ (MPa)	Time from start of cycle	Total loading time	Failure load in short term, kN	$\sigma_{t,90}$ (MPa)
LT-C2-S8-1+		No failure	Survived	257.6	0.60+
LT-C2-S8-2	0.40	26 d	75 d		
LT-C2-S8-3+		No failure	Survived	275.7	0.63+
LT-C2-S8-4+		No failure	Survived	240.6	0.55+
LT-C2-S8-5	0.46 *	7 d	83 d		
LT-C2-S8-6+		No failure	Survived	252.5	0.58+
LT-C2-S8-7	0.46	1 d	78 d		
LT-C2-S8-8	0.46	14 d	91 d		

* Bending failure at σ_b = 17.3 MPa. + Beams later tested under short term tests.

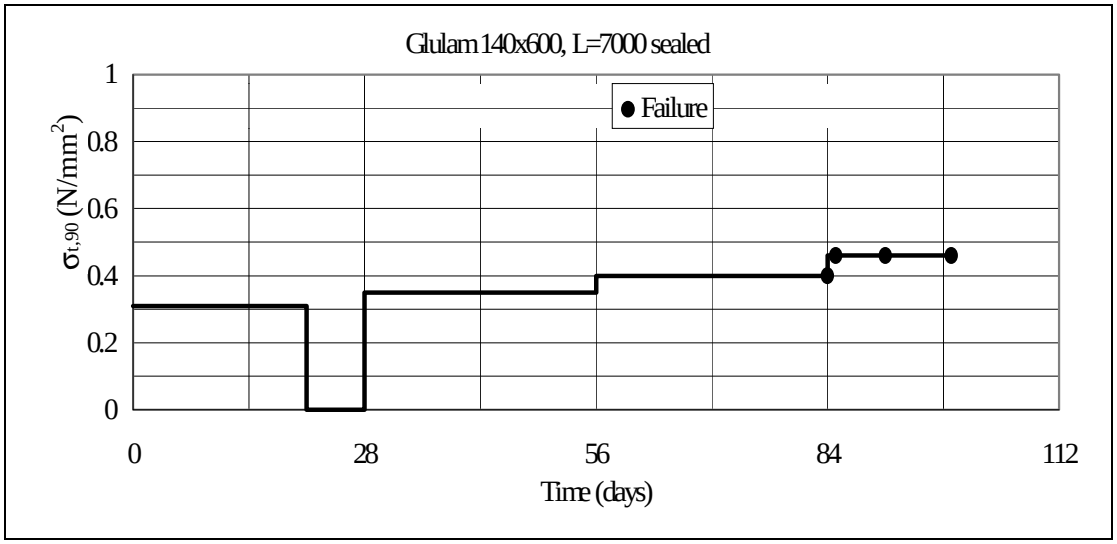

Figure 37. Tension stress versus time to failure for specimen series LT-C2-S8.

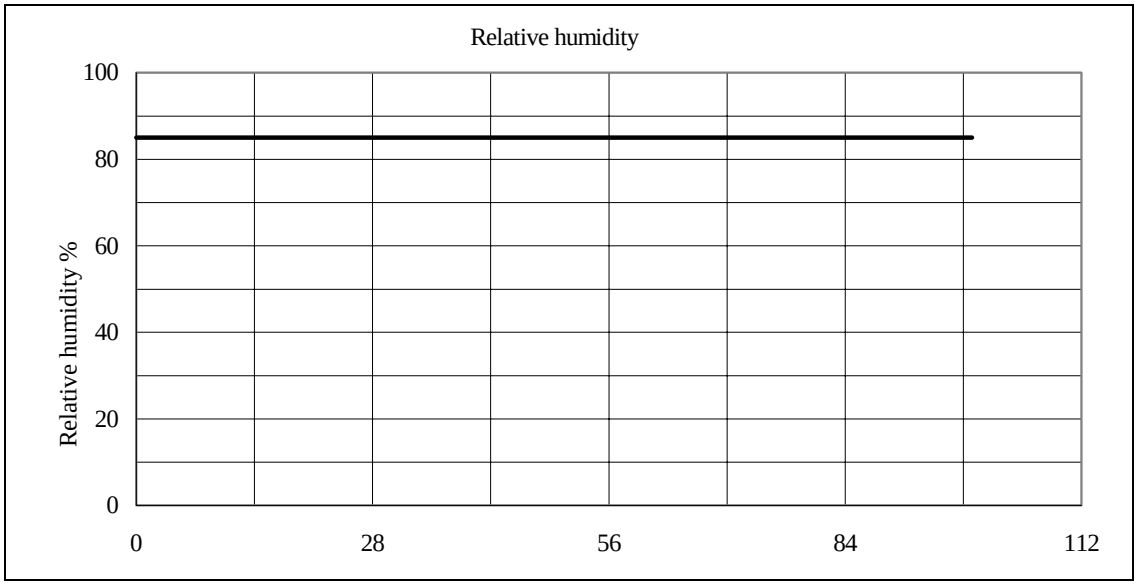

Figure 38. Constant relative humidity level used for specimen series LT-C2-S8.

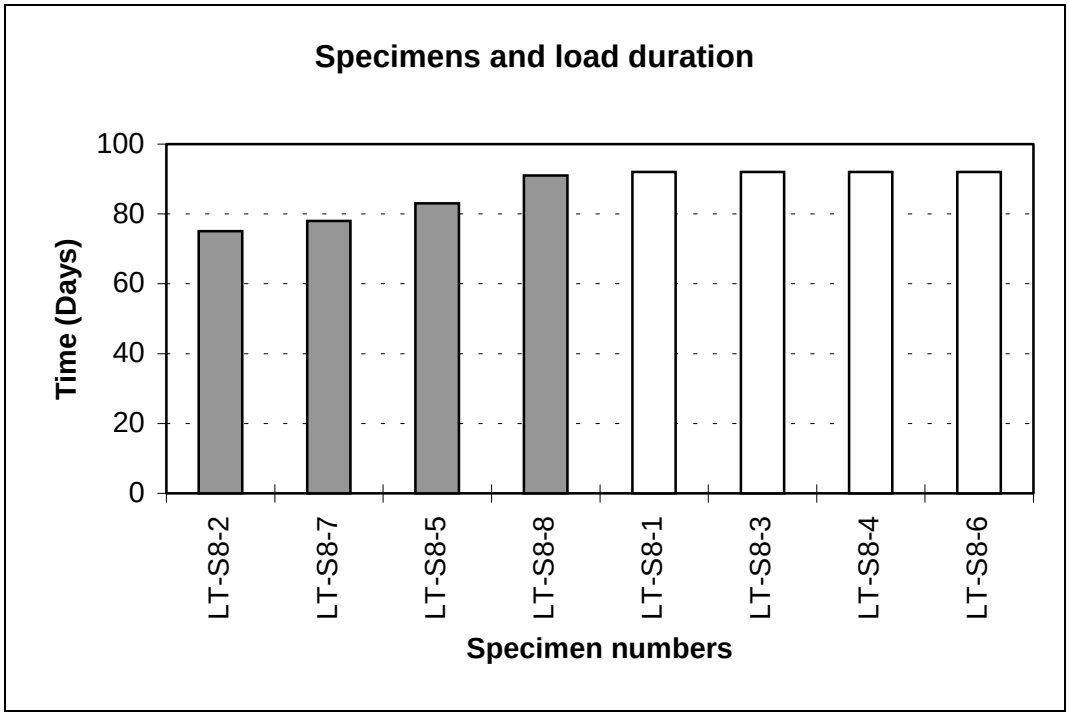

Figure 39. Load duration versus specimen failure for series LT-C2-S8 (specimens S8-1, S8-3, S8-4 & S8-6 did not fail before termination of experiment).

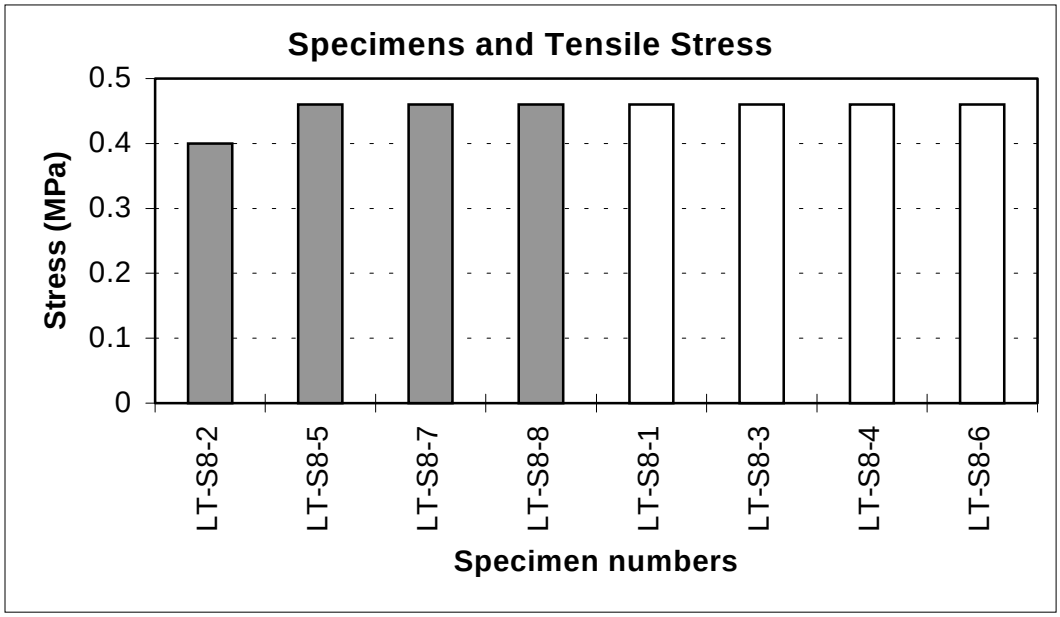

Figure 40. Stress perpendicular to grain vs. specimens for series LT-C2-S8 (specimens S8-1, S8-3, S8-4 & S8-6 did not fail before termination of experiment).

3.6 Comparison of results

A comparison of results of all the four series: LT-C2-S2, LT-C2-S4, LT-C2-S6 and LT-C2-S8 was made by plotting the load duration of beams versus specimen series and are shown in Figures 41 and 42. In Figure 41, two series of specimens are compared. In both cases, the relative humidity was cyclic and the loading method was same, the difference is the size of specimens. Series S2 had smaller size specimens while S6 had larger size. All beams in series S2 have higher load duration than S6 series.

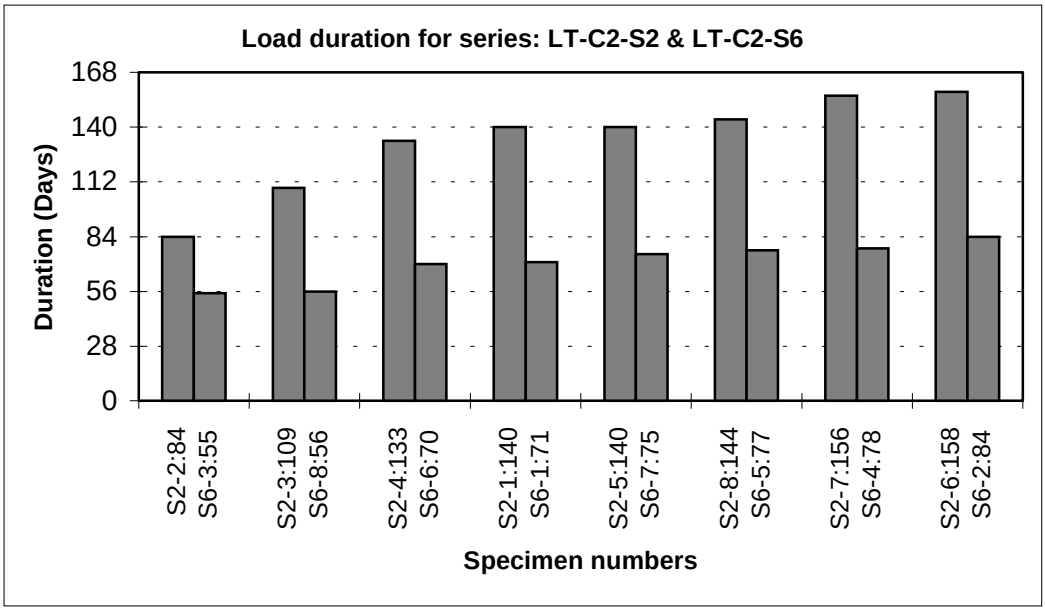

Figure 41. Comparison of load duration between LT-C2-S2 and LT-C2-S6 series.

The summary of tension stress perpendicular to grain and also the load duration time at final load level for all the four series of long term tests is given in Table 12.

Table 12. Summary of tension stress and load duration for all series.

LT-C2-S2		LT-C2-S4		LT-C2-S6		LT-C2-S8	
Stress, MPa	Time (days)	Stress, MPa	Time (days)	Stress, MPa	Time (days)	Stress, MPa	Time (days)
0.41	63	0.51	57	0.3	55	0.40	75
0.41	88	0.51	70	0.3	56	0.46	78
0.51	112	0.61	87	0.4	70	0.46	83
0.61	119	0.61	88	0.4	71	0.46	91
0.61	119	0.61	93	0.4	75	0.60*	S T
0.61	123	0.61	98	0.4	77	0.63*	S T
0.61	135	0.61	105	0.4	78	0.55*	S T
0.61	137	0.61	105	0.51	84	0.58*	S T

***** Specimens tested later in short term (ST) load.

Table 13. Load duration of specimens in all series in days (Load duration calculated from start of tensile stress 0.3 MPa).

Load duration of specimens				
Order of failure	S2 series	S4 series	S6 series	S8 series
1	35	57	27	75
2	60	70	28	78
3	84	87	42	83
4	91	88	43	91
5	91	93	47	91
6	95	98	49	91
7	107	105	50	91
8	109	105	56	91

It is to be noted that, series S4 and S8 were tested with a higher starting stress level of 0.3 MPa and had constant relative humidity, while for series S2 and S6 the starting stress level was 0.2 MPa and had cyclic RH variation. To compare the results in a consistent manner, the number of days the specimens were loaded starting from the stress level of 0.3 MPa and above was taken into consideration. Accordingly, the time during which the specimens were loaded at lower loads is subtracted. The data are given in Table 13 and the same data are used to obtain a comparison graph of load duration for the four series and is shown in Figure 42.

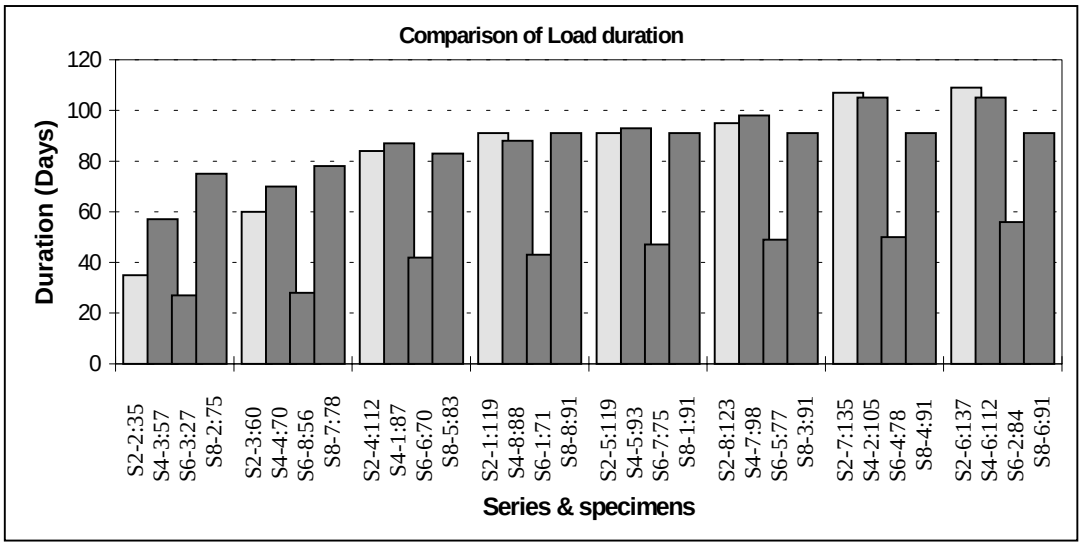

Figure 42. Comparison of load duration among all the long term test series. Load duration calculated from starting at 0.3 MPa.

In Figure 42, it can be noted that the thicker beams of series S6 show least load duration in comparison to other series. This significant change in load duration behaviour may be due to size effect.

Table 14. Summary of both old and new test results.

Serial number	Specimens	Apex Volume, m^3	Mean stress, MPa
1	FMPA tensile	0.01	0.883
2	Old tests	0.039	1.200
3	ST-C2-S1	0.109	0.850
4	LT-C2-S2	0.310	0.548
5	ST-C2-S3	0.22	0.695
6	LT-C2-S4	0.420	0.585
7	ST-C2-S5	0.343	0.587
8	LT-C2-S6	0.343	0.389
9	LT-C2-S8	0.343	0.445

Table 14 summarises the collection of tensile test results both old and new tests on glulam beams along with their apex volume. In addition, the test data of tensile experiments carried out by FMPA laboratory (Aicher and Dill-Langer, 1995), are included for comparison. The material used by FMPA for tensile test specimens was glulam with spruce lamination having 33.3 mm thick with 90 mm width.

Figure 43 shows a comparison of volume versus tensile strength of specimens. Even if we ignore the tensile strength data of FMPA, the effect of volume on the tensile strength of glulam beams seems significant. The long term beams in S6 series and S8 series had the highest volume but lowest tensile strength, while old glulam beams (90 x 400 x 4 300 mm, Gowda and Ranta-Maunus, 1993) with an apex volume of 0.039 m^3 show the highest tensile strength. The graph shows specimen series with increasing volume in ascending order.

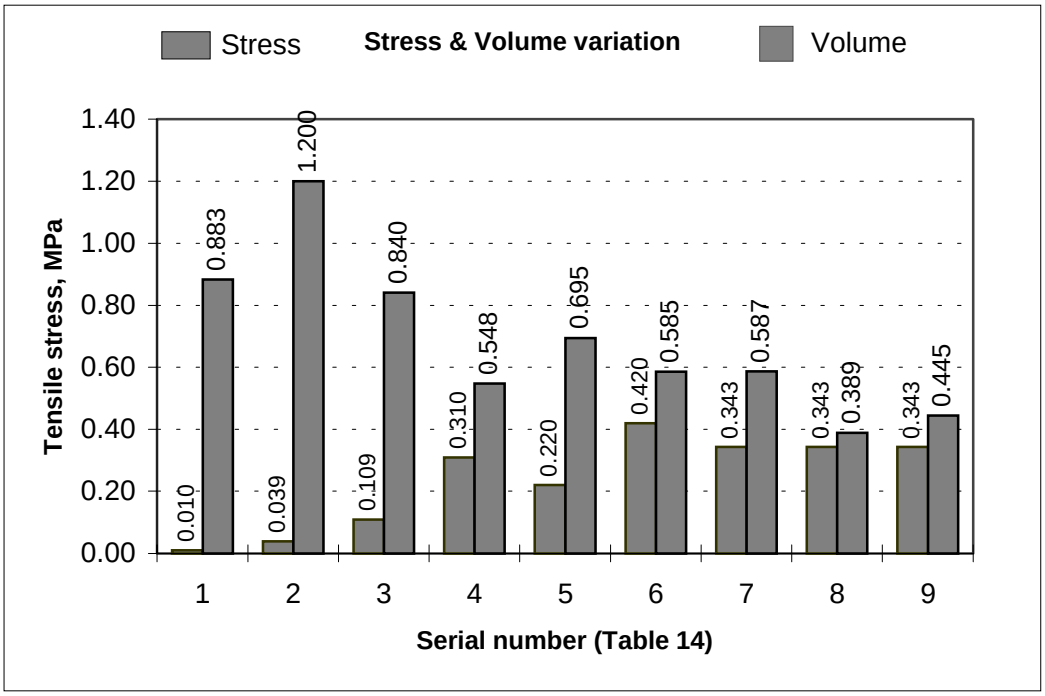

Figure 43. Volumetric (apex volume, m^3) and stress comparison of specimens- both old and new test data.

4 FAILURE BEHAVIOUR OF SPECIMENS

In all cases the failure of beams took place with the appearance of a single major crack at the central section of the beams. After testing was completed photographs of failed specimens were taken and are included in Appendix E for all series. However, for each individual series the appearance of failure crack and the growth of annual rings is given below.

4.1 Series LT-C2-S2

After the completion of tests, separate samples were taken from each beam by cutting through all the laminates at the central section. The dimensions of the samples (W x T x L) in this series is 88 x 20 x 600 mm. From these samples, it is easy to see the appearance of failure cracks and the layout of laminates along with their growth rings. The photograph of all the eight beams in this group is shown in Figure 44.

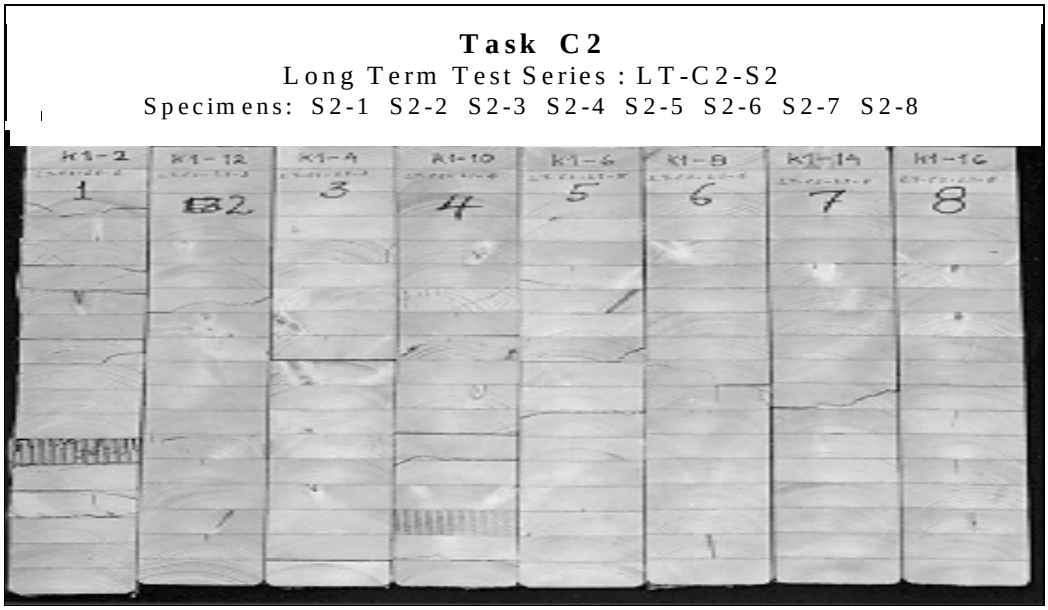

Figure 44. Samples from LT-C2-S2 series with yearly growth rings and failure cracks.

The analysis of failure patterns of specimens in series LT-C2-S2 indicate how the failure cracks appeared during failure. The failure range of all beams in this series is 63 days to a maximum of 137 days (Table 8). Specimen S2-2 failed within 10 minutes when the stress was increased from 0.30 MPa to 0.41 MPa. Specimens S2-1 and S2-5 were failed within few seconds when the stress level was increased from 0.51 MPa to 0.61 MPa.

In specimens S2-2, S2-3, S2-6, S2-7 and S2-8, only one major crack formation was found after failure, while in specimens S2-1, S2-4 and S2-5 multiple cracks appeared in few locations. The sixth laminate from bottom in specimen S2-1 was a finger joint location and this laminate had many local multiple cracks within the laminate. The brittle failure cracks can be seen in Figure 44.

4.2 Series LT-C2-S4

In this case also normal samples were taken to determine the density and moisture content of each beams. The failure cracks and the growth rings are shown in Figure 45 for all the eight specimens. In this series, three specimens had single major failure cracks while the rest of the beams failed with multiple cracks. The minimum failure tension stress perpendicular to grain was 0.51 MPa, while the maximum was 0.61 MPa. Beam LT-C2-S4-3 had a load duration of 57 days while beam LT-C2-S4-2 had 105 days. Specimen LT-C2-S4-6 did not fail for almost 112 days, after which the load was terminated.

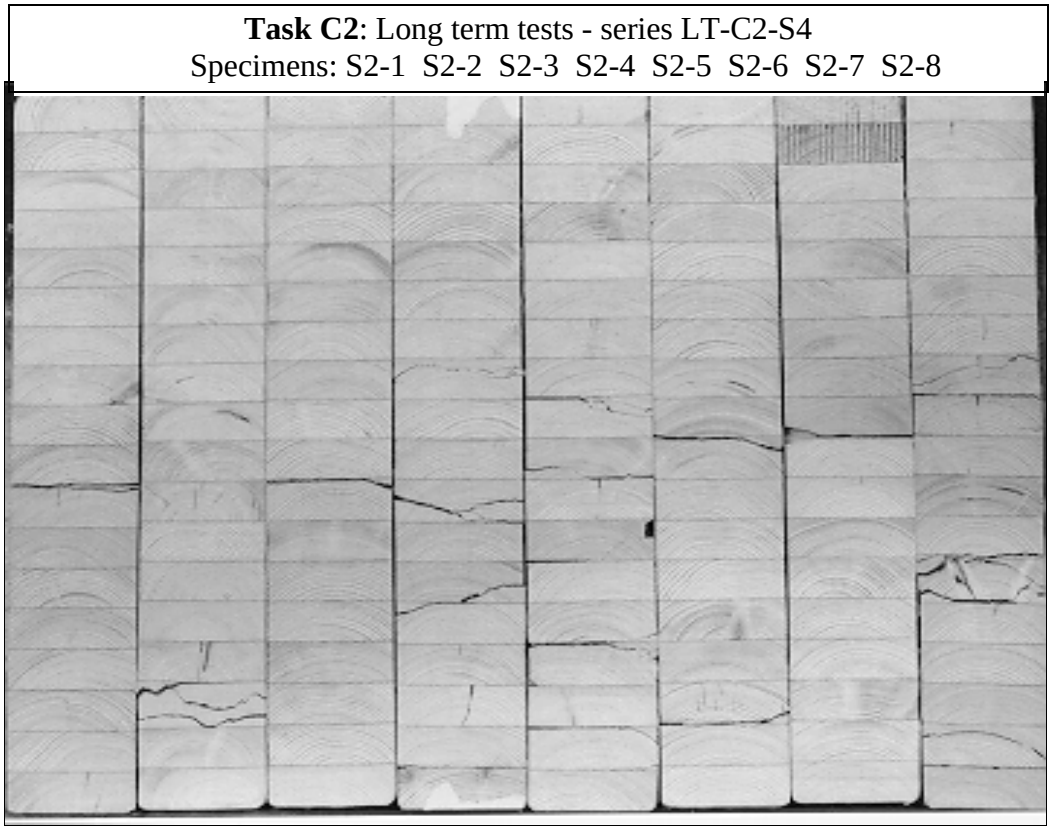

Figure 45. Samples from LT-C2-S4 series with failure cracks and yearly growth rings.

4.3 Series LT-C2-S6

In this series also separate samples were taken from each beam by cutting through all the laminates at the central section. The dimensions of the samples (W x T x L) were 140 x 20 x 600 mm. The photograph of all the samples together is shown in Figure 46. The appearance of failure cracks, the layout of laminates and their yearly growth of rings can be seen.

Task C2
Long Term Test Series: LT-C2-S6
Specimens: S6-1 S6-2 S6-3 S6-4 S6-5 S6-7 S6-8

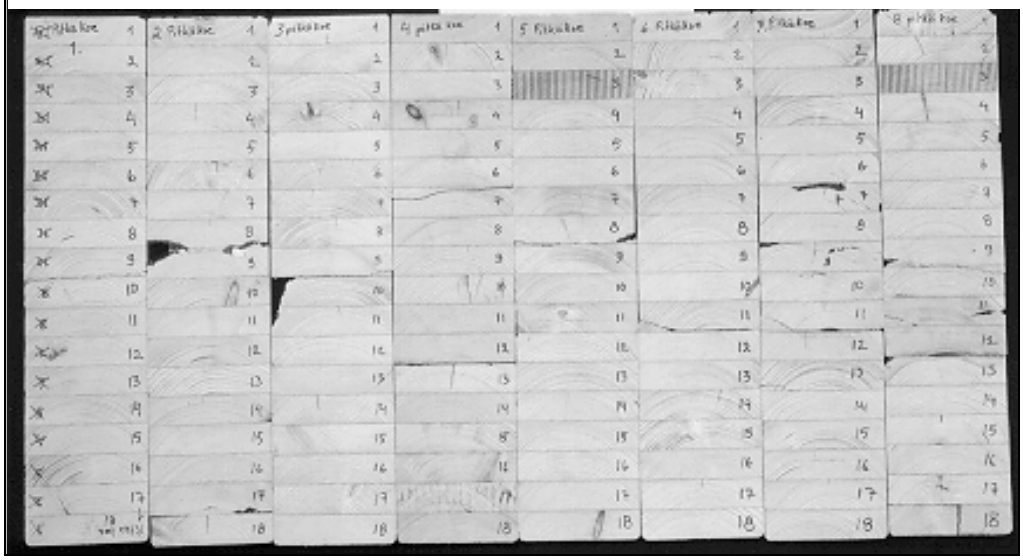

Figure 46. Samples from LT-C2-S6 series showing failure cracks and yearly growth rings.

In this S6 series, the samples are wider than the S2 series. The first failure of beam S6-3 occurred 55 days after loading and beam S6-2 sustained load for a maximum number of 84 days (Table 10).

Specimens S6-2, S6-3, S6-5 and S6-6 had only one major failure crack and specimens S6-1 and S6-4 had two major cracks, while specimens S6-7 and S6-8 had multiple cracks. The failure crack appearances can be seen in Figure 46.

4.4 Series LT-C2-S8

Moisture samples and failure crack patterns for series LT-C2-S8 is shown in Figure 47. In this case also some sample had multiple cracks during failure.

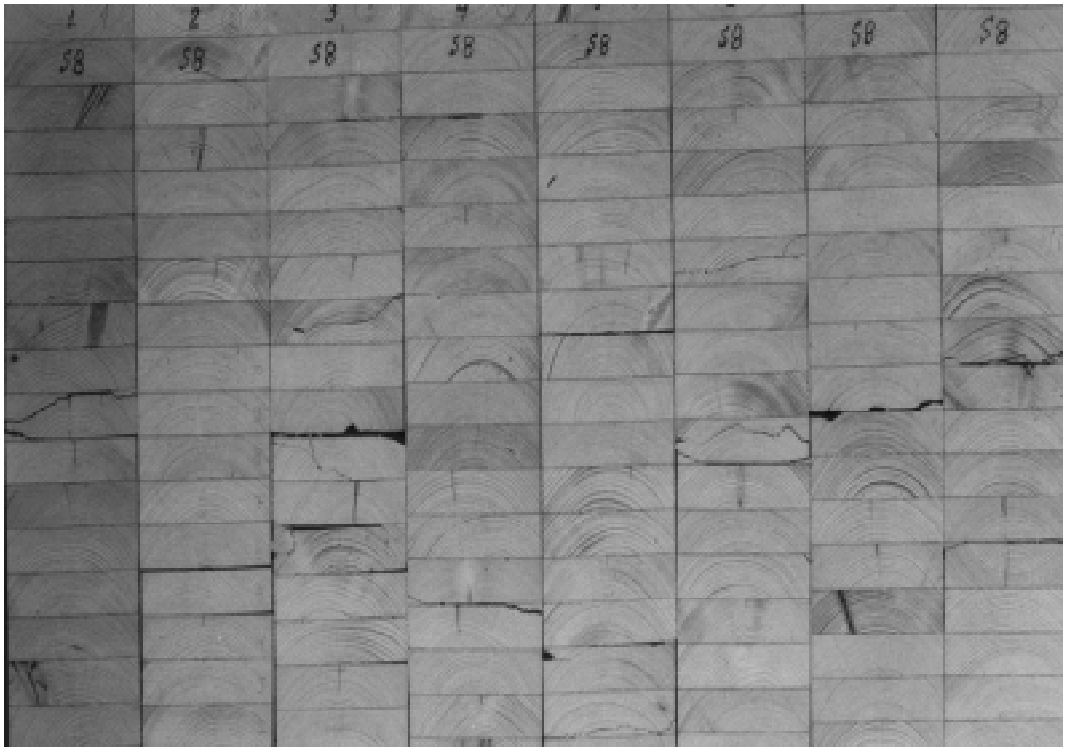

Figure 47. Samples from LT-C2-S8 series showing failure cracks and yearly growth rings.

5 DISCUSSION OF EXPERIMENTAL RESULTS

5.1 Short term experiments

Short term experiments of curved beams have been reported by Gowda and Ranta-Maunus (1996). Here a summary of the results is given including the new results from series ST-C2-S5b (high moisture content). The new strength results indicate no dependence on moisture content, instead the values are somewhat higher than the earlier ones with lower moisture content. Therefore, the results in test series 5a and 5b have been combined. The cumulative distributions of short term strength are illustrated in Figure 48. The fitted normal, lognormal and Weibull distributions give characteristic values as given in the Table 15.

Table 15. Characteristic values for tensile strength perpendicular to grain (N/mm^2), obtained by fitting 2-parameter Weibull, normal and lognormal distributions to the curved beams results.

	S1			S3			S5		
	Normal	Log-normal	Weibull	Normal	Log-normal	Weibull	Normal	Log-normal	Weibull
50 %	0.838	0.835	0.848	0.719	0.717	0.706	0.600	0.595	0.611
5 %	0.731	0.736	0.716	0.632	0.635	0.596	0.472	0.481	0.464

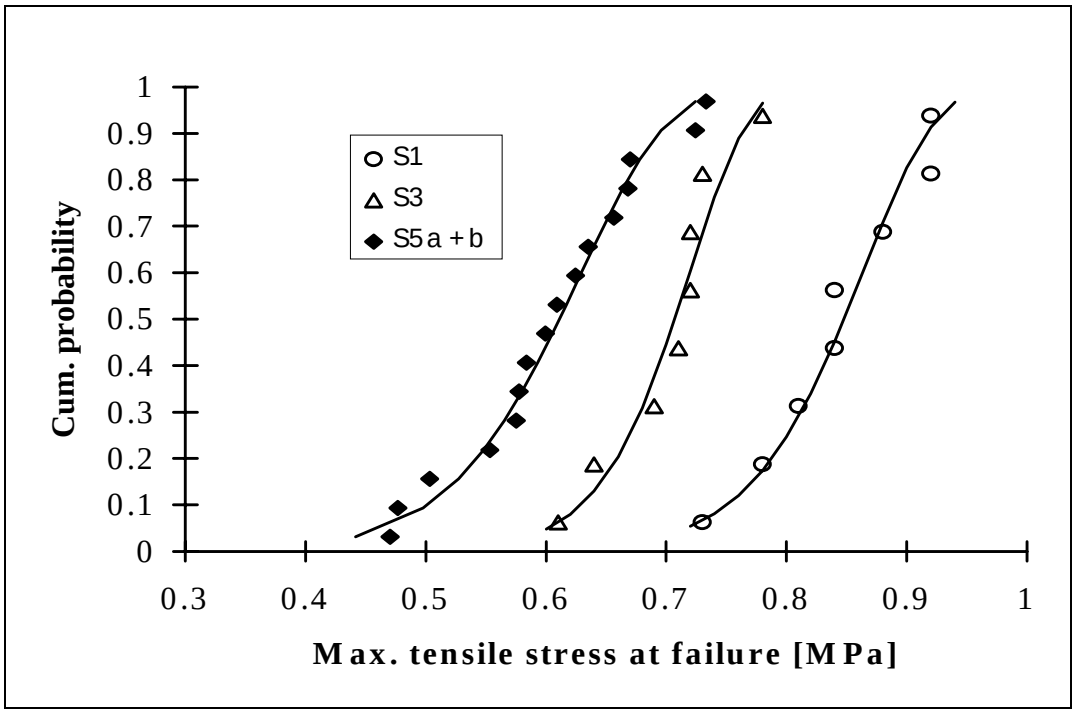

Figure 48. Cumulative distributions of all short term strength values with curved glulam: observations and Weibul fitting.

5.2 Long term experiments

Failure stresses of all specimens are collected in the form of cumulative probability plot and are shown in Figure 49. For reference, the fitted curves of short term strength are also shown as in Figure 48. In series S8 half of the specimens did not fail at the final long term loading stress level and the residual strength was tested by ramp loading.

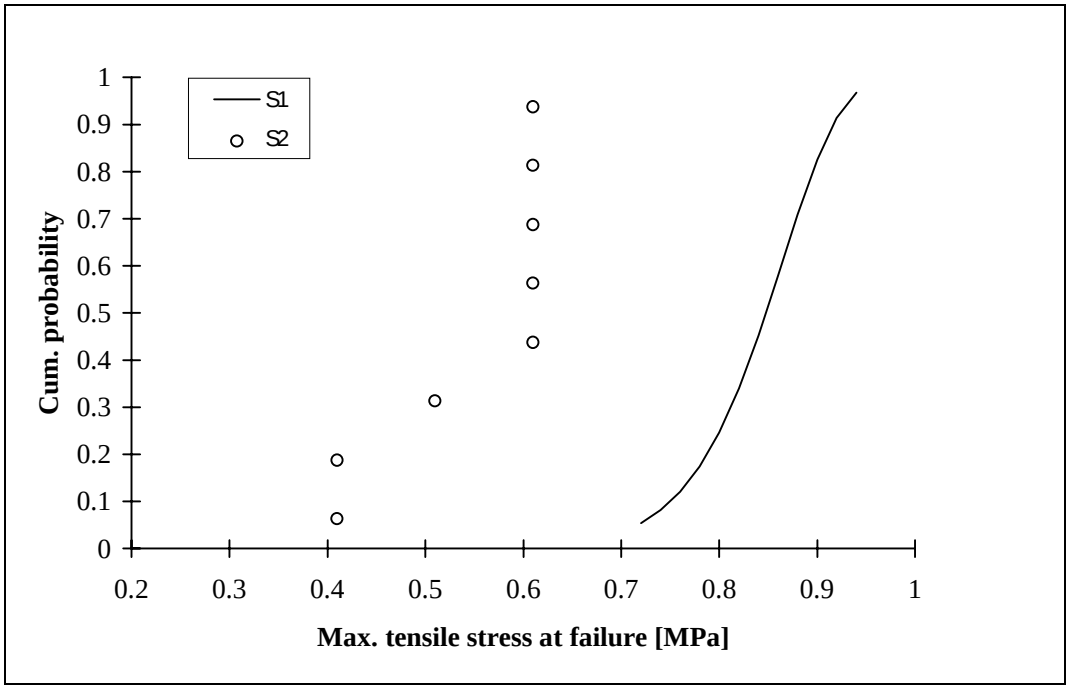

Figure 49. Cumulative plot of long term strength results (points) with short term strength reference curve (S1 is reference curve for S2).

The cumulative plot of long term strength results (points) along with short term strength reference curves for other series are given in Figures 50 and 51 respectively. The S1 series curve is the reference curve for S2 (same size), S3 is for S4 and S5 is reference curve for both S6 and S8 series.

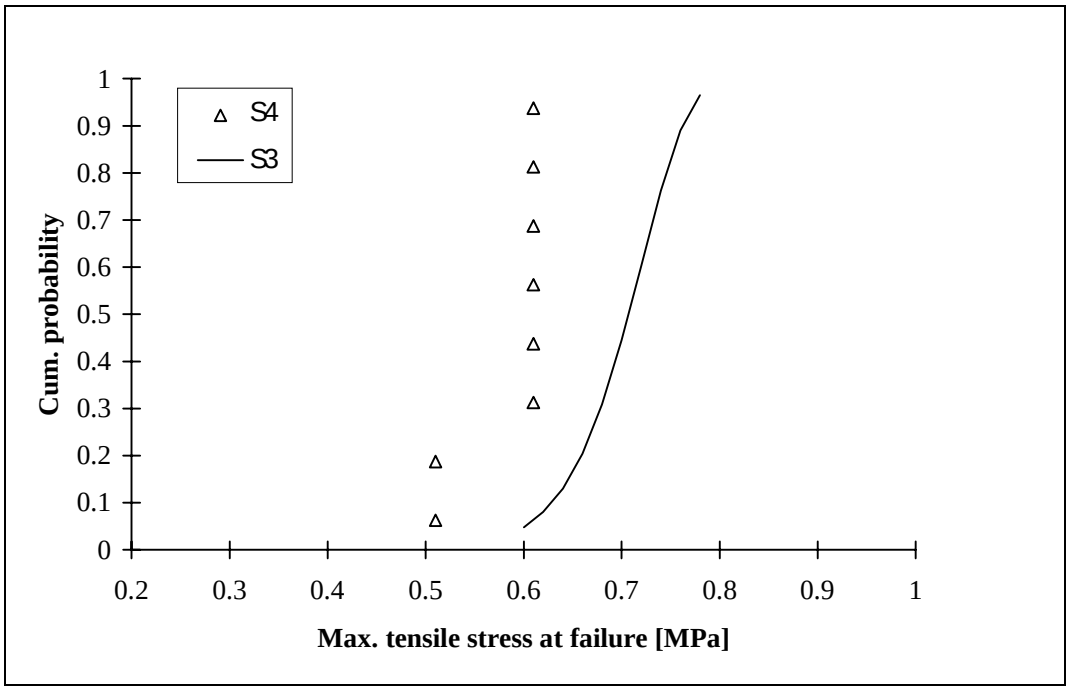

Figure 50. Cumulative plot of long term strength results (points) with short term strength reference curve (S3 is reference curve for S4).

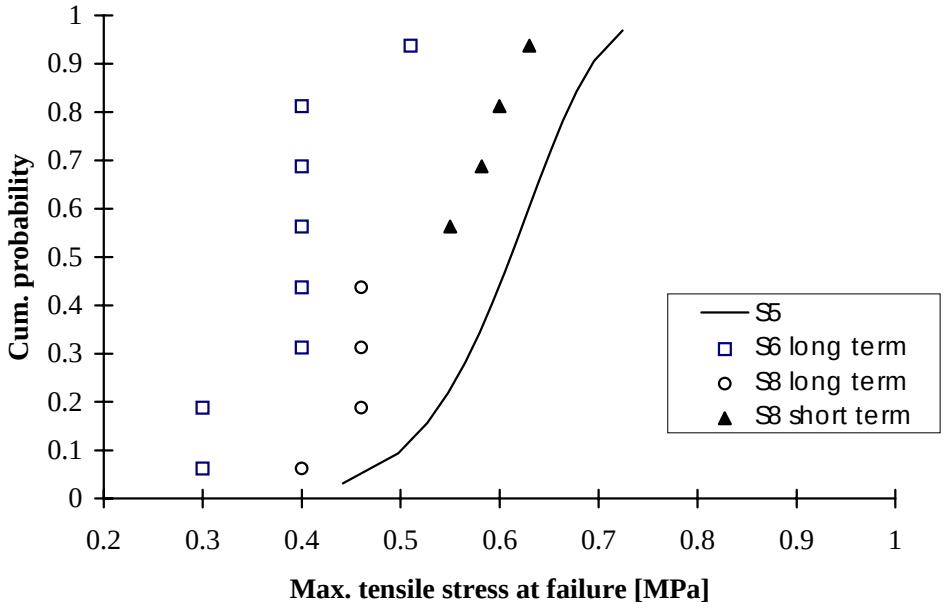

Figure 51. Cumulative plot of long term strength results (points) with short term strength reference curve (S5 is reference curve for S6 & S8).

The long-term test results are summarized in Table 16, by giving the time to failure at final stress level and the nominal stress of an "average" beam, which is here the 4th weakest beam of the 8 beams in each series. For comparison, also the estimated short term strength of the 4th weakest beam based on results shown in Figure 48 is given.

Table 16. Summary of long term test results. Time to failure and tensile stress perpendicular to grain of the "average" beam.

	S2	S4	S6	S8
Size (width x height x constant moment span) *mm*	90x 600 x2000	90x600x 4000	140x600x 4000	140 x 600 x 4000
Climate	Cyclic	85% RH	Cyclic	85%RH
Time-to-failure *days*	28 [1)]	4	15	14
Stress N/mm^2	0.51	0.61	0.40	0.46
Ref. short term strength N/mm^2	0.84	0.70	0.60	0.60
k_{DOL}	0.61	0.87	0.67	0.77

[1)] Failed immediately after the load was raised to next higher level.

The reasons why the strength under long duration loading is lower than in short term testing at constant moisture content can be explained as follows:

- material is getting weaker due to accumulating damage or creep due to a constant high stress level. The factor to take this reduction into account is denoted by k_t.
- stress distribution: load bearing capacity of the member is getting lower because of changed stress distribution caused by creep and hygroexpansion. The factor to take this reduction into account is denoted by k_σ.
- moisture content level: short term strength of material is different under actual loading conditions because of raised moisture content or temperature. The factor to take this reduction into account is denoted by k_{MC}.

The total effect of load duration combined with moisture effects is calculated by

$$k_{DoL} = k_{MC} k_\sigma k_t \,. \qquad (1)$$

Firstly, k_{MC} should be determined by short term experiments at different moisture contents (here $k_{MC} = 1$), secondly k_t will be calculated based on experiments made under constant humidity conditions, and finally k_σ can be determined from cyclic humidity tests.

5.3 The effect of loading time

Two long term test series were made at constant relative humidity of 85%. These results will be directly used to calculate k_t. Only the time to failure at final load level of the "average" beam closest to 50 percentile level is used in the analysis and in the calculation of relative stress level the short term strength at the same fractile level is used. This approach was proposed by Preben Hoffmeyer (1996). The test results shown in Figures 50 and 51 are given in Table 17(a).

More than 10% difference k_{DOL} in S4 and S8 tests with two thicknesses 90 and 140 mm is observed. This difference is believed to be of statistical nature, because k_{DOL}-factors are expected to be the same for different thicknesses under constant moisture content. The following differences in the test arrangements will be pointed out:

- S4 and S8 experiments had constant moisture content and spring loading exposing the maximum nominal load only for a short time followed by stress relaxation.

- earlier experiments were loaded by dead loads being constant during the experiment under slightly varying moisture conditions. Accordingly, this experiment is more severe than true constant humidity experiment. Structural analysis gives an indication that the true k_t -factor in old experiment would be 0.80...0.83.

Table 17(a) Calculation of k_t factor directly from experiments for "average" beam.

	Old experiments (Test 2)*	S4	S8
Time to failure (days)	13	4	14
Failure stress (MPa)	0.90	0.61	0.46
Reference strength (MPa) at 65% RH	1.18	0.70	0.60
k_t at time of failure	0.76	0.87	0.77
k_t at time of 6 months	0.70	0.81	0.71
Notes	Force control Painted beams in cyclic humidity	Spring loading Constant 85% RH	Spring loading Constant 85% RH

***** Long term test report (Ranta-Maunus & Gowda 1994).

Figure 52 shows the stress level versus log time to failure curves for curved beams at constant moisture content and the new test results are compared with old test data.

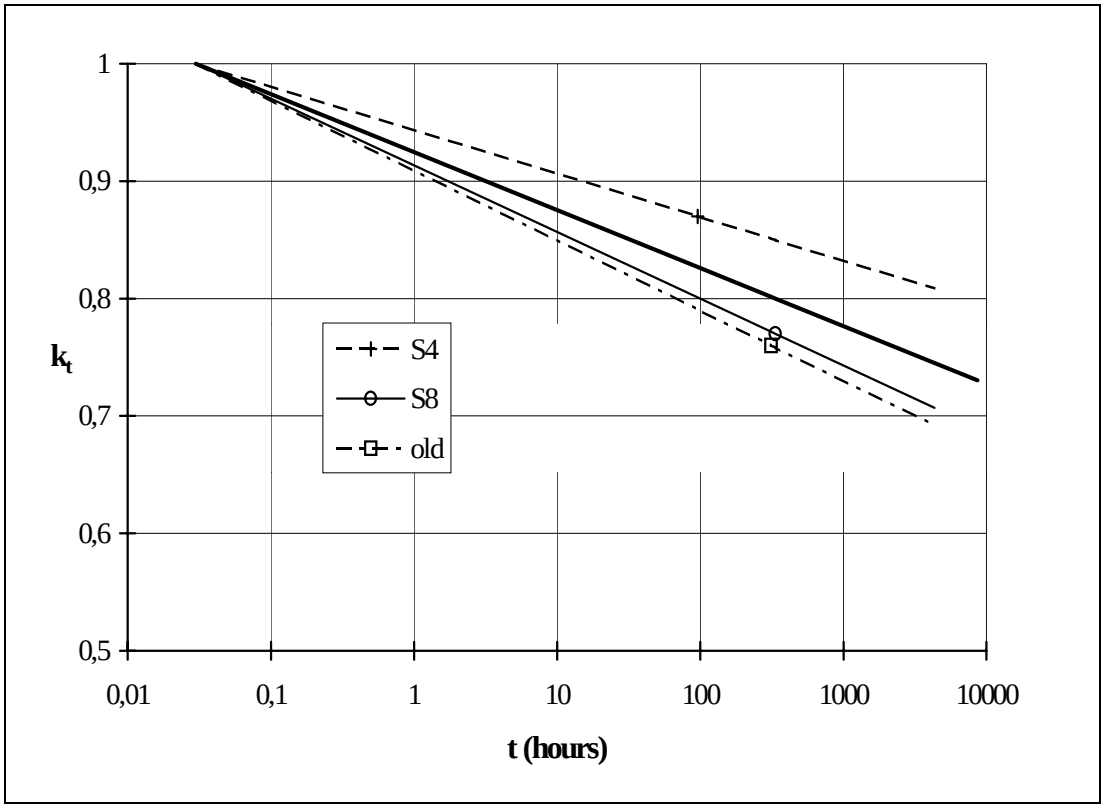

Figure 52. Stress level vs. log time to failure curves for curved beams at constant moisture content. The observation points show when the "average" beam closest to 50 percentile failed. S4 and S8 were made at constant 85% RH and loaded by spring system, whereas "old"(earlier experiments) had painted beams under force controlled load and cyclic humidity conditions (40<->85%). The thick line indicates the best estimate adopted.

5.4 Effect of stress redistribution

The effect of stress redistribution during loading to the load bearing capacity of curved beams caused by moisture gradients and mechano sorptive creep will be estimated based on comparison of results obtained under constant and cyclic moisture conditions.

k_σ will be calculated as follows:

$$k_\sigma = \frac{k_{DoL}}{k_t}. \qquad (2)$$

The calculation and results are shown in Table 17(b). Estimated k_t is based on the average behaviour of S4 and S8 tests corresponding to a line passing through points $k_t = 0.8$ at 14 days and $k_t = 1$ at 0.03 hours. The 4th and 5th beams in series S2 broke immediately after the load was raised from 0.51 MPa to 0.61 MPa. This indicates that the damage had been developed on the earlier stress level 0.51 MPa. For this analysis we used the information as the 4th beam would have been failed at 28 days before increasing the load. As a result we obtained $k_\sigma = 0.82$ in the moisture cycle at S6 tests, in which beam width was 140 mm, and 0.76 at S2 test with beam width 90 mm.

Table 17(b). Calculation of k_σ factor directly from experiments for "average" beam.

	Old experiments (Test 2)*	S2	S6
Time to failure (days)	20	28	17
Estimated k_t	0.79	0.79	0.80
Observed k_{DoL}	0.55	0.60	0.66
$k_\sigma = \frac{k_{DoL}}{k_t}$	0.70	0.76	0.82

***** Long term test report (Ranta-Maunus & Gowda 1994).

6 STRESS ANALYSIS

In this chapter an effort is made to calculate the stress distribution in glulam beams in order to explain the size and DoL-effects observed. In this analysis the distribution of stress perpendicular to grain through thickness is of interest. The mean value of stress in the middle of the beam is calculated as in Eurocode 5.

The following calculation is based on a combined moisture transport and structural analysis of a beam cross-section. The software developed for simulation of wood drying (Hukka, 1996) has been modified and used in the analysis. This method is one dimensional in thickness direction of the beam. For comparison, also 2-D FEA has been applied as described by Hanhijärvi (1995) and Hanhijärvi & Ranta-Maunus (1996). Here, only the 1-D analysis is reported.

In moisture and heat transfer analysis the control-volume method is used (Hukka 1996). As boundary conditions, temperature and relative humidity of air are given at different times.

6.1 Stress calculation method

In stress calculation a horizontal cross-section of the beam is analysed as illustrated in Figure 53. The stiffness of the material in loading direction depends on the orientation of annual rings in the cross-section. It is assumed (Dinwoodie, 1981) that

$$\frac{1}{E_\alpha} = \frac{\sin^2\alpha\cos^2\alpha}{G_{RT}} + \frac{\sin^4\alpha}{E_T} + \frac{\cos^2\alpha(\cos^2\alpha - \sin^2\alpha)}{E_R}. \qquad (3)$$

where E_α is the apparent modulus of elasticity in the direction of the stress and α is the angle between radial direction and loading direction. The values of elastic moduli used in the analysis are: E_R = 1000 MPa, E_T = 500 MPa and G_{RT}= 40 MPa. All material data are given in Appendix B.

Shrinkage and swelling in different positions has been calculated as a function of the angle α:

$$s_\alpha = \sin^2\alpha\ s_T + \cos^2\alpha\ s_R\ . \qquad (4)$$

where s_T and s_R are hygroexpansion in tangential and radial directions respectively, depending linearly on moisture content change. An example of the stress distribution obtained by this elastic analysis is shown in Figure 54 illustrating the sensitivity of stress distribution on pith location.

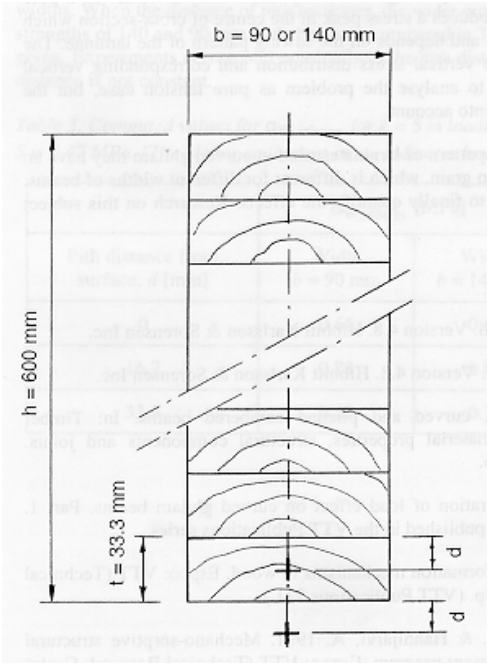

Figure 53. Cross-sectional dimensions of the tested beams: height h = 600 mm, width b = 90 mm or 140 mm. d indicates the assumed distance of the pith location from the lower surface of the lamina.

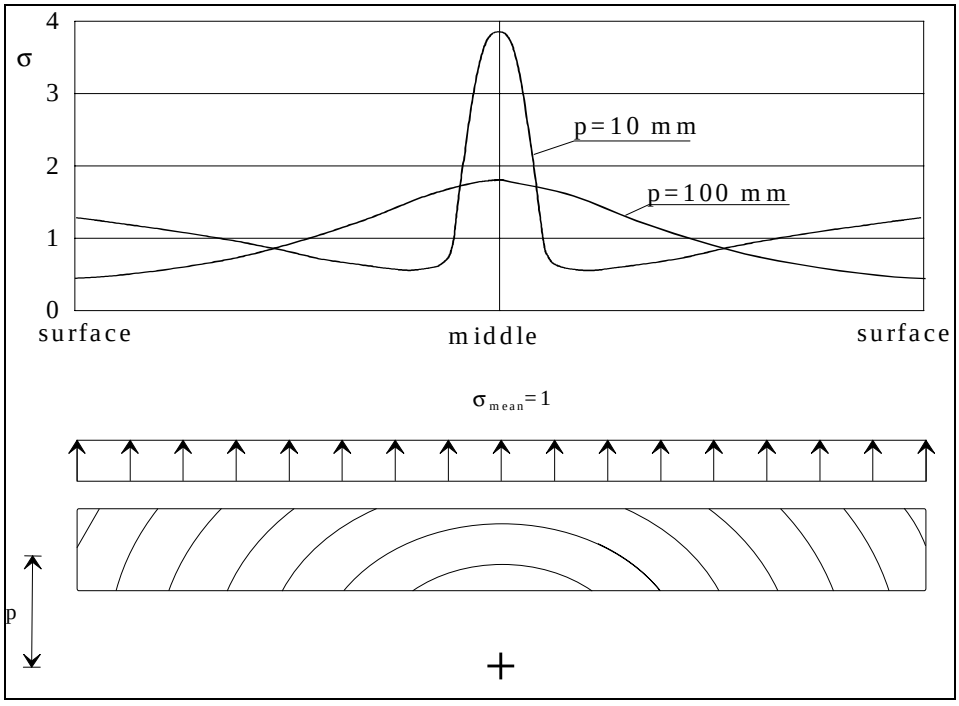

Figure 54. Stress distribution in 90 mm wide beams for two pith distances p=d+t/2.

The viscoelastic behaviour has been modelled using the generalised Kelvin material model with seven Kelvin-units in series and the elastic response is included within the viscoelastic effect. Time-moisture content equivalence and a shift factor is used in modelling the dependency of creep rate on moisture content. Mechano-sorptive creep is also modelled using Kelvin four units in series, whose deformation depends on the absolute value of the moisture content change but not time. Modelling of both the viscoelastic behaviour and the mechano-sorptive behaviour resemble the models given by Joyet (1992) (simplified mechano-sorptive model), only with more units in series. The model response in the transverse directions has also been calibrated to correspond roughly to the creep results of Joyet (1992).

Two boundary conditions are applied:

- total force corresponds to the stresses caused by external load applied on the beam:

$$\int \sigma dx = \frac{3M}{2Rh}. \tag{5}$$

where M is the bending moment acting on curved beam, R is the mean radius of curvature and h is height of the beam.

- total strain is constant through the cross-section.

6.2 Strength criterion

The hypothesis used in this analysis is that the Weibull theory can be used to predict the strength when stress distribution is uneven, especially in the direction of through thickness. The effective stress, called Weibull stress is, calculated as

$$\sigma_{t,90,W} = \left(\frac{1}{V_{\text{ref}}} \int_V \sigma_{t,90}^k dV \right)^{1/k} . \tag{6}$$

The following values are used: k = 5, V = volume of the constant moment span in the case of beam tests. The reference volume $V_{ref} = 0.01\ m^3$.

Equivalent stress calculated in eqn.(6) gives the value of a hypothetical constant stress in the reference volume V_{ref} causing the same probability of failure as the actual stress distribution in the actual volume V. It has to be noticed, that the reference stresses are calculated to be compared to each others and have no direct relevance to any measured or calculated values. The analysis can be expanded to

comparison of strength observed in tension experiments and curved beams, when the stress variation in height direction of the beam is taken into account. For such comparison the Weibull stress values given for beams here should be divided by 1.22 (Gowda and Ranta-Maunus 1996).

In elastic analysis the maximum stress is concentrated in a small area in the middle of beam as we can see in Figure 53. As a strength criterion we use equivalent Weibull stress as calculated by eqn. (6). When the effect of moisture gradients is included, high tensile stresses can be obtained also at the surface. In this case the question arise, whether it is correct to use the same Weibull stress value as strength criterion at surface, where the annual ring orientation is different: while vertical stresses are radial in the middle, the direction approaches tangential in extreme cases at the surface.

It is known that the tangential strength is not much more than half the radial strength. What was not known to us was the tensile strength in directions between radial and tangential. Therefore a small series of experiments were made with angles usual in our test beams. The results are given in Appendix B. The conclusion of the experiments is that the same strength can be used in different depths for our test beams. However, one has to keep in mind that when the direction of stress is closer to tangential, lower strength values have to be used. Here, to cover also cases with tangential stresses, $\sigma_{t,90}$ in eqn. (6) is replaced by:

$$\sigma_{t,90,\alpha} = \left\{ \begin{array}{l} \max\{\sigma_{t.90},0\},\ for \quad \alpha < 45^\circ \\ \max\{\sigma_{t,90},0\}\dfrac{\alpha}{45^\circ},\ for \quad \alpha \geq 45^\circ \end{array} \right\} \qquad (7)$$

In other words, stress in tangential direction is multiplied by 2, and the same strength is used in all directions.

6.3 Analysis of short term experiments

By an elastic analysis the distribution of stresses perpendicular to the grain caused by bending moment in a cross-section are calculated corresponding to the situation in short term loading. The main variables in the analysis are the width (90 or 140 mm) and the sawing pattern (position of the pith). Height of beam is 600 mm. In the experiments the sawing patterns followed were as follows:

The lamellae having 33.3 mm thick were sawn nominally with a distance of 16.7 mm from pith (d in Figure 53). In practice the pith distance was varying, being close to the nominal value (15 to 30 mm) in most cases of 90 wide lamellae. For 140 mm wide lamellae the usual value of pith distance was 30 - 50 mm.

First, the elastic stresses in a tensile bar having variable E-modulus in the cross-section are calculated simply by assuming a linear relation between stress and E-modulus, which depends on the orientation of annual rings. The through width stress distributions are given in Figure 54. In all cases we obtain a considerable stress peak in the centre line of the specimen on which the pith is located, depending on the distance of pith from the plane in which stresses are calculated. This calculation is intended to describe the behaviour of tension specimen made of relatively thin lamellae, justify the ignoring of stress variation in thickness direction of lamellae. The results are assumed to be applicable to curved beams also.

Effective Weibull stresses are calculated for beam sizes and failure loads obtained in short term experiments. Results are summarised in Table 18 together with long term test analysis. In all calculations reference volume $V_{ref.}$ is 0.01 m^3 and k = 5 in eqn. (6). Since the pith distance is not being determined prior to fabrication of beams, in calculations two different values have been used such that most of the actual pith distances are between these two values. If the calculated Weibull stress is a good strength criterion and all variables including pith distance known, we should obtain the same value for Weibull stress for different size of beams. Mean values of failure loads are used in the calculation. The obtained Weibull stresses range from 2.1 to 3.2 MPa and depend strongly on pith distance.

By this analysis, we can also see whether this method of analysis may describe the volume effect observed, but we cannot confirm it, because the lamellae were not selected according to pith distance. The distribution of stress for different pith distances is shown in Figure 55.

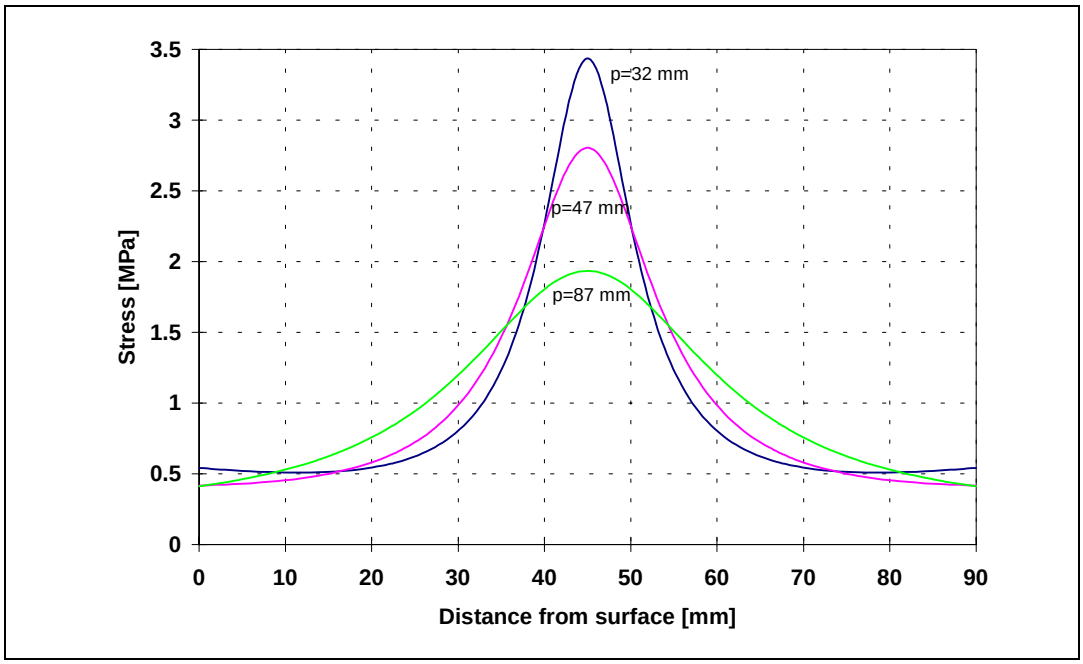

Figure 55. Distribution of stress for pith distances p = 32, 47 and 87 mm. Width of lamella 90 mm and σ_{mean}= 1 MPa (For S4 series).

6.4 Simulation of long term experiments

A combined moisture transport and structural analysis including the effects of hygroexpansion, viscoelastic creep and mechano-sorptive creep, is used to calculate the stress development simulating the experiments as follows:

- 90 mm wide, d=15 and 30 mm
- 140 mm wide, d= 30 and 50 mm.

Section in the middle of 33.3 mm thick lamella is analysed and accordingly the distance of pith from the plane analysed is p = 32, 47, and 67 mm.

6.4.1 Constant moisture content

Figure 56 shows the result of the simulation of test for LT-C2-S4 series, which had 90 mm wide beams at constant RH 85%. Figure shows the stress development at surface and in the middle of the beam when p = 47 mm. Most of the beams failed during the last load step when the applied external load caused a mean stress of 0.61 MPa. This analysis has been made at ideal moisture constant. Weibul stresses given in Table 18 are a little higher because a small increase in moisture content was assumed to correspond more closely to actual test conditions.

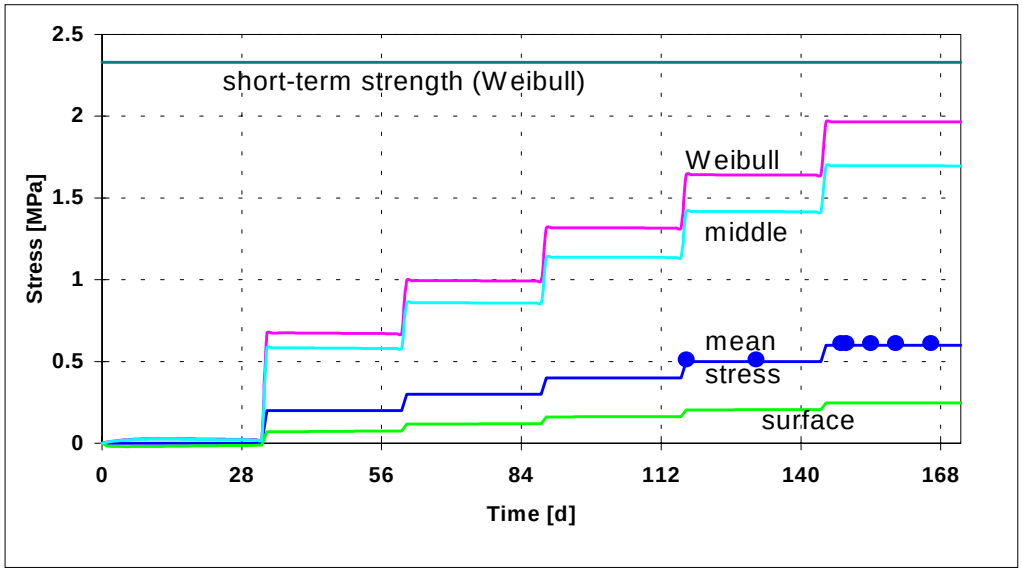

Figure 56. Calculated vertical stresses in the middle and at surface of beam simulating tests in LT-C2-S4 series. Weibull stress σ_W (eqn.(6)) is calculated with V_{ref} = 0.01m^3, V =0.09x0.6x4 m^3 and k = 5, p = d+t/2 = 47 mm. Weibull stress level corresponding to the average short term strength is also given. Dots on mean stress curve denote the time of failures during test.

Experiment LT-C2-S8 was also made at constant humidity. The only difference compared to S4 series was in dimensions of the beams: larger width (140 mm). The Weibull stresses are illustrated in Figure 57, where a sensitivity study is also included with respect to a different initial moisture content from the equilibrium value under long term test. The comparison is made based on 3% difference in conditioning and long term loading moisture contents. We may conclude that during the first couple of months the level of Weibull stresses is strongly influenced by the accuracy of conditioning moisture content. Otherwise if the humidity is changing during the experiment, this has a strong influence on the observed strength value.

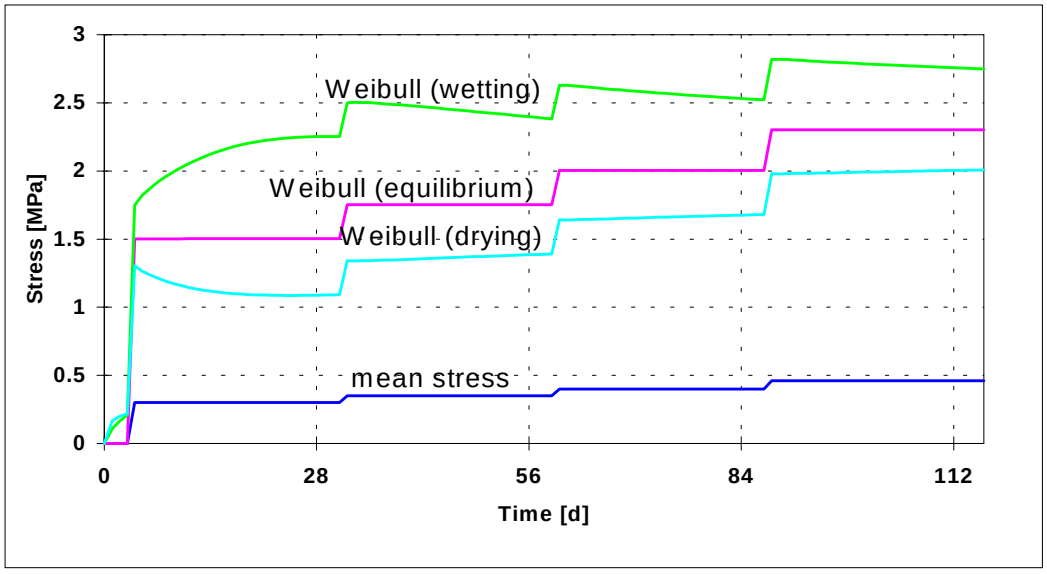

Figure 57. Calculated Weibull stresses in test LT-C2-S4 series (equilibrium). V_{ref} = 0.01m^3, V=0.14x0.6x4m^3, k= 5 and p = 47 mm. Drying and wetting curves refer to the case when the curved beam has been conditioned to 3 % higher or lower moisture content than where it will be loaded 4 days after removal to another constant humidity environment.

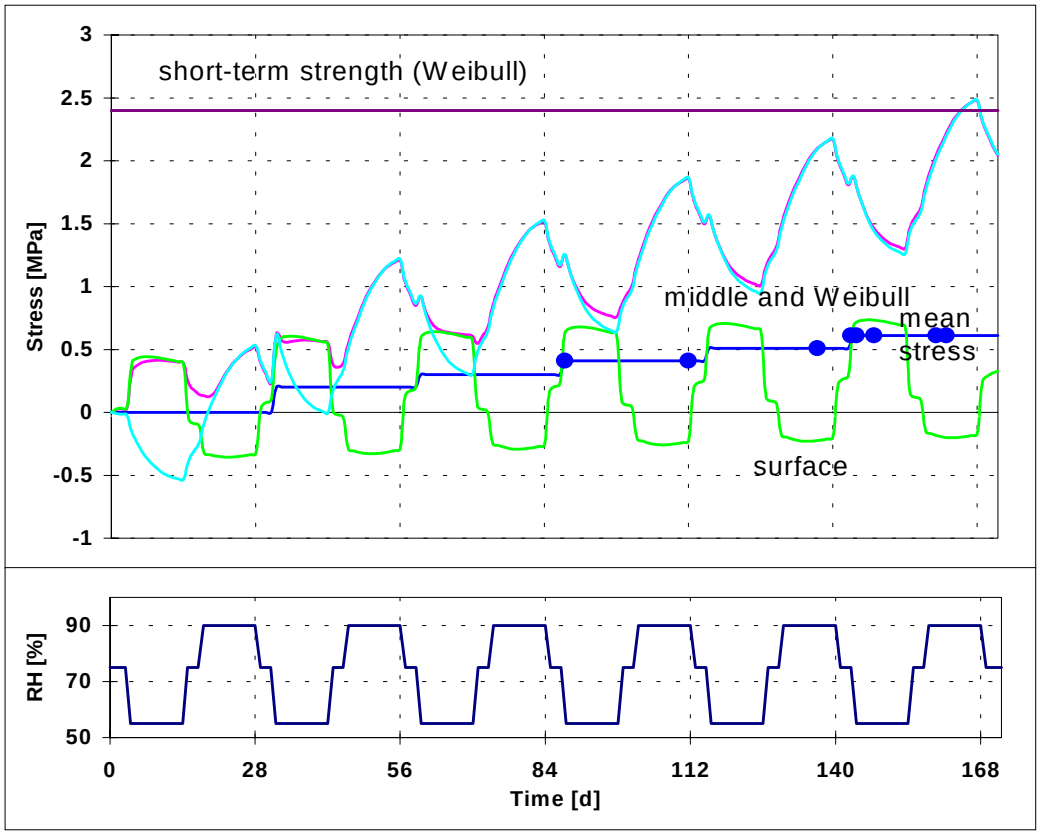

Figure 58. Calculated vertical stresses in the middle and at surface of beam simulating tests in LT-C2-S2 series. Weibull stress σ_W(eqn. (6)) is calculated with V_{ref} = 0.01m^3, V =0.09x0.6x2 m^3 and k = 5, p = d+t/2 = 47 mm. Weibull stress level corresponding to the average short term strength (p = 47 mm) is also given. Dots on mean stress curve denote the time of failures of beams during test.

6.4.2 Cyclic moisture content

Figure 58 shows the calculated stresses simulating tests in LT-C2-S2 series, having 90 mm wide beams in cyclic humidity and the calculated moisture history is given in Figure 61. Moisture content at surface is varying between 11% and 18% and in the middle it remains close to 15%. Effect of one moisture cycle before loading is also shown: σ_W = 0.5 MPa is obtained before loading corresponding to the effect of external load affecting mean stress = 0.2 MPa for this size of beam without moisture changes. In the calculation the value of p = 47 mm.

Weibull stresses are nearly equal to the stresses in the middle of beam. Maximum stresses are obtained at the end of moist period, the value being dependent on the duration of humid season. Weibull stress caused by the average of short term strength (0.85 MPa) is 2.4 which is reached in cyclic climate during the final load level (0.61 MPa). At that time all the beams were broken.

The stress distribution through width of the beam is shown after the dry period (126 days) and after the following wet period (140 days) when the average stress is 0.5 MPa (Figure 59). Calculated Weibull stresses at the same times are 1.01 and 2.17 MPa respectively. Weibull stresses are sensitive to the value of pith distance. To demonstrate the effect, Weibull stresses for two pith distances (32 and 47 mm) are shown in Figure 60.

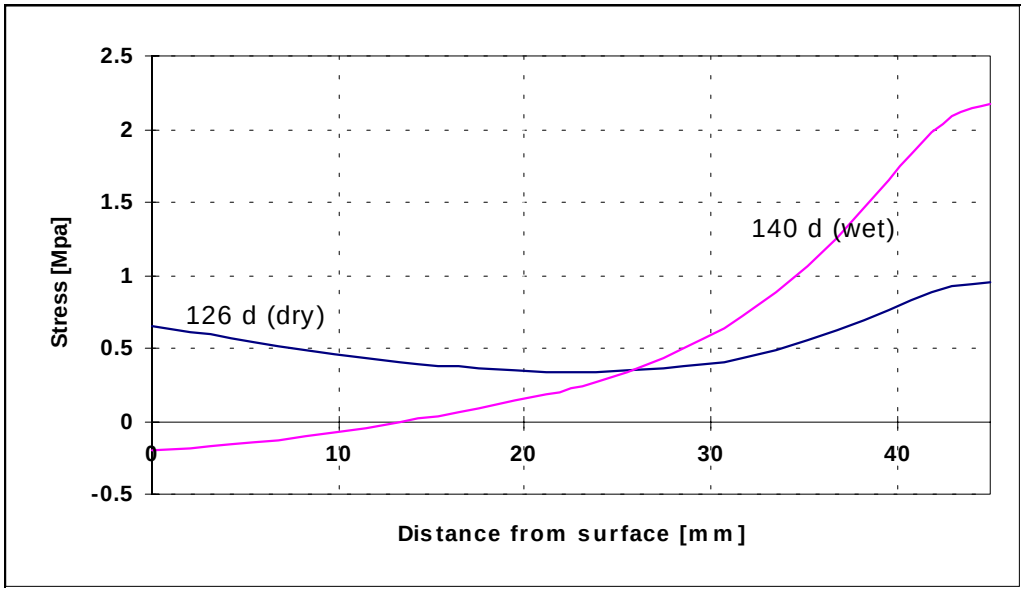

Figure 59. Calculated stress distribution for half thickness of beam in test series LT-C2-S2 after dry period (126 d) and wet period (140d). Same conditions as in Figure 60.

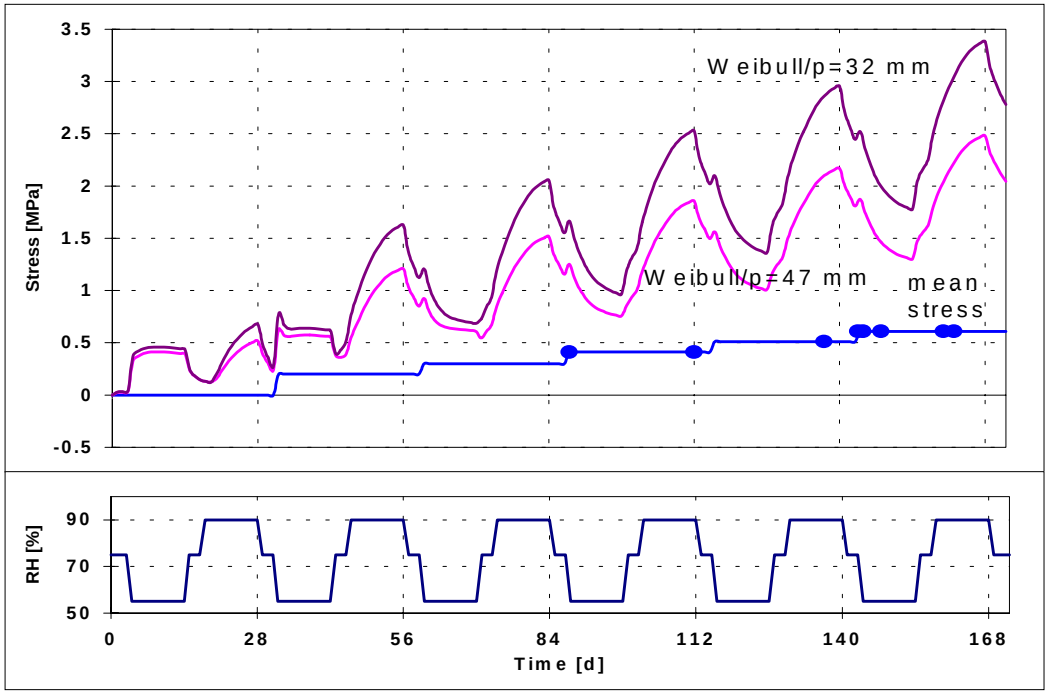

Figure 60. Simulation of test series LT-C2-S2: Weibull stresses for two pith distances. Same conditions as in Figure 58.

Table 18. Computed Weibull stress values and derived DoL-factors on 50-percentile level.

Specimen series	**Old S3**		**Old S2**		**S2**		**S4**		**S6**		**S8**
Humidity	Cyclic		Cyclic (paint)		Cyclic		85%		Cyclic		85%
Volume *lxhxb* (m)	1x0.4 x0.09		1x0.4 x0.09		2x0.6 x0.09		4x0.6 x0.09		4x0.6 x0.14		4x0.6x0.14
Short term ref. strength $f_{t,90,50\%}$ (MPa)	1.21		1.21		0.85		0.71		0.61		0.61
Long term failure load $\sigma_{t,90,50\%}$ (MPa)	0.68		0.92		0.51		0.60		0.40		0.46
DoL-ratio = k_{DoL}	0.56		0.76		0.60		0.85		0.66		0.77
Pith distance p (mm)	47	87	47	87	32	47	32	47	47	67	47
Short term strength f_w	2.75	2.15	2.75	2.15	3.24	2.40	3.14	2.33	3.04	2.25	3.04
Long term strength f_w	2.04	1.74	2.21	1.79	2.95	2.17	2.84	2.05	2.39	1.70	2.30
True DoL-ratio = k_t	0.74	0.81	0.80	0.83	0.91	0.90	0.90	0.88	0.79	0.76	0.76
$k_\sigma = \frac{k_{DoL}}{k_t}$	0.76	0.69	0.95	0.92	0.66	0.67	0.94	0.97	0.83	0.86	1.02

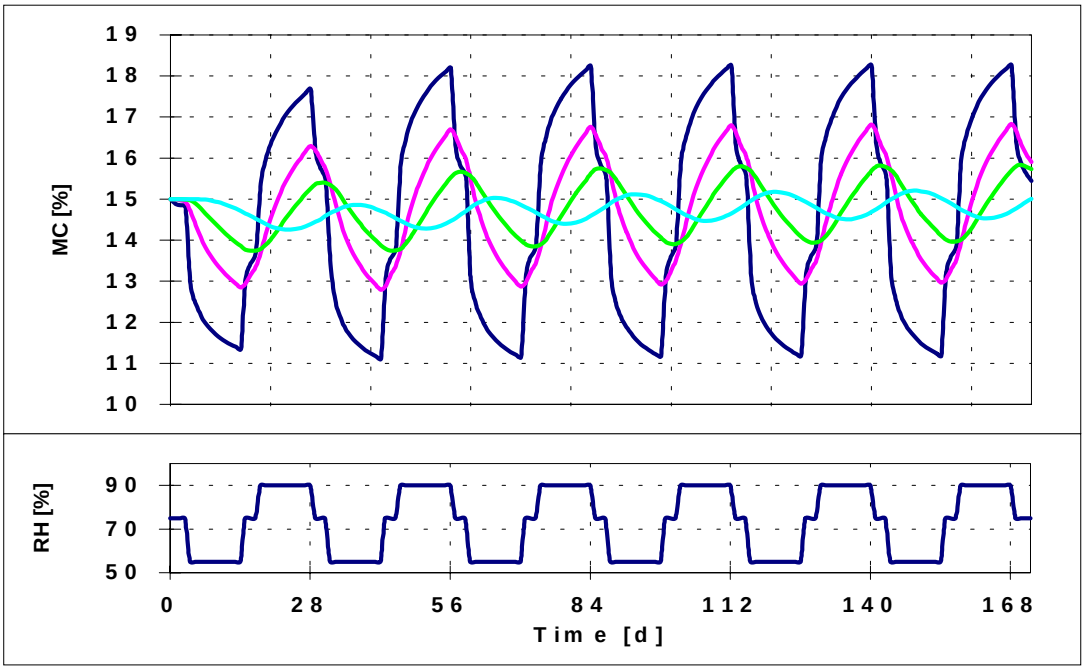

Figure 61. Calculated moisture history in experiments of S2 series in different depths from surface (0, 10, 20 and 45 mm).

Figure 62 shows the calculated stresses simulating tests in LT-C2-S6 series, which had wider (140 mm) beams in cyclic humidity. The same loads (mean stresses) result now in higher stresses in the middle of beam than was the case with thinner beam. Weibull stress caused by the average of short term strength (0.57 MPa) is 2.84 (for p = 47 mm), which is reached in cyclic climate at the end of load level 0.4 MPa. At that time 7 of 8 beams were broken.

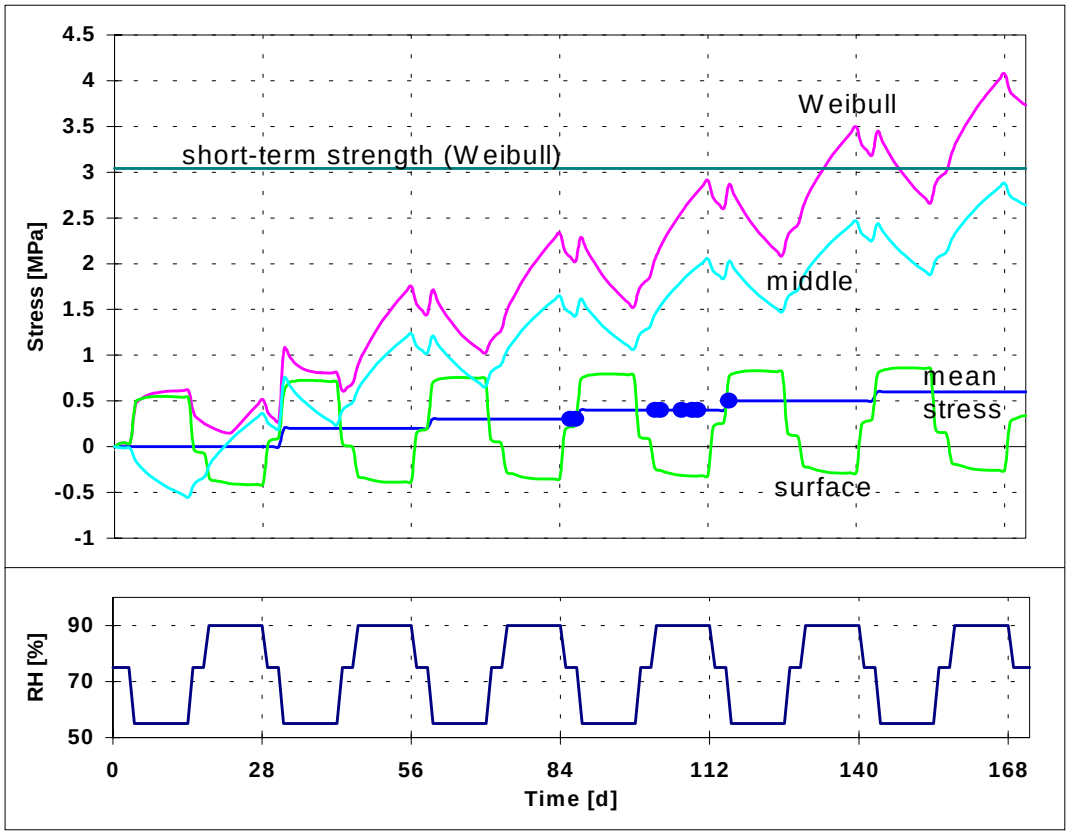

Figure 62. Calculated vertical stresses in the middle and at surface of beam simulating tests in LT-C2-S6 series. Weibull stress σ_W (eqn. (6)) is calculated with V_{ref} = 0.01m^3, V =0.14x0.6x4 m^3 and k = 5, p = d+t/2 = 47 mm. Weibull stress level corresponding to the average short term strength (p = 47 mm) is also given. Dots on mean stress curve denote the time of failures in test.

6.4.3 Summary of simulations

Calculated results are collected in Table 18 where duration of load factors are analysed. The table includes also the data of our earlier experiments of curved beams (Ranta-Maunus and Gowda, 1994). Weibull stresses are calculated for two pith distances representing normal lower and higher values observed in the specimens corresponding to median short term and long term strength (f_W). The ratio of long-term and short term f_W-values is considered as true DoL-ratio, denoted by k_t in eqn.(1). The rest of DoL-effect is assumed to be caused by redistribution of stresses, which appears to be important for cyclic environment. For constant humidity and painted beams a small stress redistribution effect is obtained because some moisture changes took place also in those experiments. Moisture cycling obviously increases effective Weibull stresses.

Figure 63 Shows the comparison of strength values between short term reference strength and long term ultimate tensile stress for all the test series. Figure 64 also shows similar results between long term and short term strengths. The average short term strength in terms of Weibull stress σ_w for the two pith values of 32 and 47 mm are plotted by superimposing their stress values together. Similarly, the maximum values of Weibull stresses for the same pith distances for long term loading are superimposed. Both short term and long term results for each group is shown together for comparison.

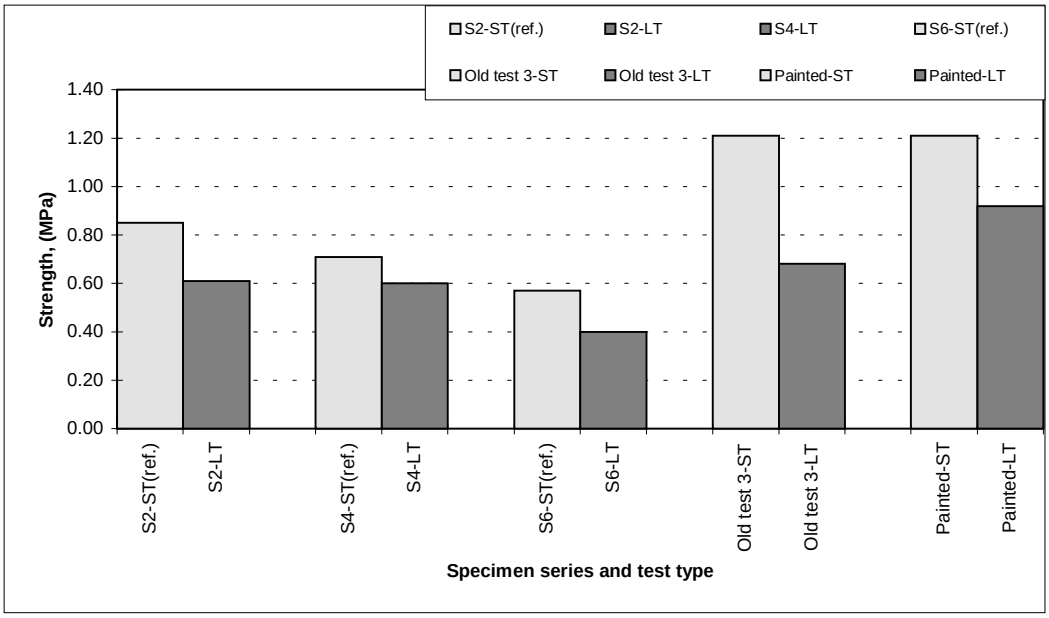

Figure 63. Comparison of short term reference strength and long term ultimate tensile stress for all series (experimental).

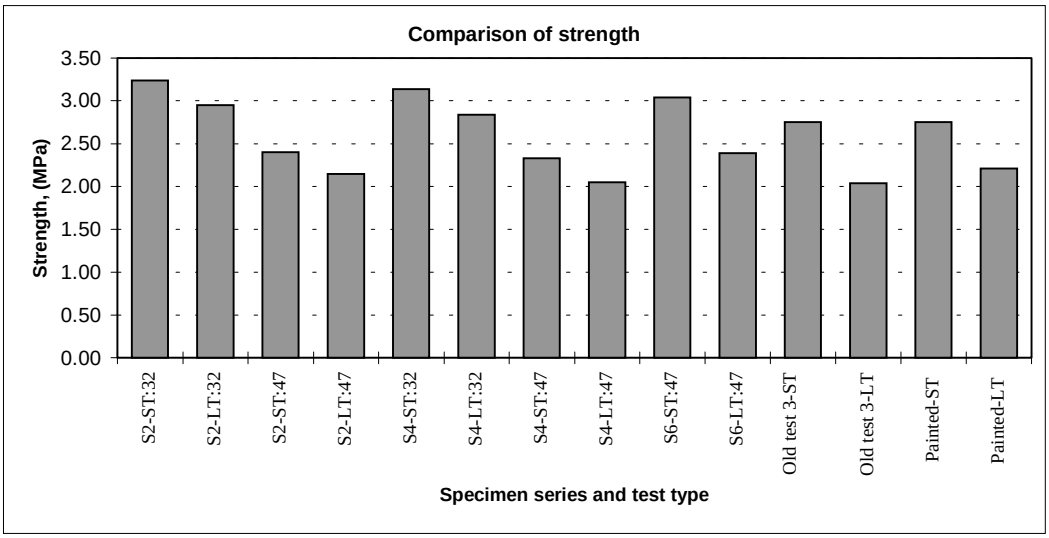

Figure 64 Comparison of average short term strength in terms of Weibull stress for the two pith values of 32 and 47 mm and the maximum Weibull stress under long term loading for the same pith values for all series.

6.4.4 Equivalent mechanical load

The effect of moisture cycles is compared to the effect of mechanical loading at constant humidity by computing the value of mechanical load which causes same Weibull stress as a combination of mechanical and moisture load. The results are given in Table 19.

It shows that the moisture cycle used without mechanical load corresponds to external load causing a mean stress in the range of 0.1 - 0.2 MPa. The combination of stepwise increasing load and cyclic humidity results in larger Weibull stresses than simply the addition of the effects of load and humidity cycle. This moisture load depends on pith distance but not so strongly as short term strength does. Consecutive cycles result in somewhat higher Weibull stress than a single change from equilibrium.

Test cycles and a single fast change from 76% to 85% RH have been analysed. Moisture load corresponds to an extra load of 0.14 to 0.25 MPa when acting simultaneously with mechanical load 0.2 MPa when the beam is not surface coated. A good surface coating (moisture barrier) will decrease the extra load to 0.06 MPa. The present test cycle seems to be more effective than the other cycles analysed. The effect of a single fast change is nearly the same. The conclusion is that fast changes of climate from dry weather to wet season with duration of several weeks are most harmful for curved structures loaded by tension stress perpendicular to grain.

Table 19. Equivalent mechanical (mean) stresses $\sigma_{t,90}$ for combinations of moisture cycling and load.

Thickness (mm)	RH cycle	Mean stress caused by external load (MPa)	Equi. external load (MPa) for combined effect	Pith distance in calculation (mm)
90	55%<->90% [1]	0	0.19	32 and 47
		0.2	0.45	
		0.5	0.81	
140	55%<->90% [1]	0	0.11	47
		0.2	0.36	
		0.5	0.73	
140	55%<->90% [1]	0	0.10	67
		0.2	0.34	
		0.5	0.68	
90	40%<->85% [2]	0	0.12	47
		0.2	0.35	
		0.5	0.71	
90	40%<->85% [2]	0	0.17	87
		0.2	0.41	
		0.5	0.79	
90	40%<->85% [2]	0	0.03	47
	painted	0.2	0.25	
		0.5	0.57	
90	40%<->85% [2]	0	0.06	87
	painted	0.2	0.26	
		0.5	0.59	
90	76%->85% [3]	0	0.11	32 and 47
		0.2	0.34	
90	76%->90%[3]	0	0.16	47
		0.2	0.40	
		0.5	0.73	
90	65%->90%[3]	0	0.27	47
		0.2	0.52	
		0.5	0.87	
140	76%->90%[3]	0	0.17	47
		0.2	0.41	
		0.5	0.75	
140	65%->90%[3]	0	0.29	47
		0.2	0.55	
		0.5	0.90	

1) Test cycle in this study. 2) Test cycle in old study (Ranta-Maunus and Gowda 1994).
3) Single fast change from equilibrium, lasting for 4 weeks.

7 CONCLUSIONS

Tensile stresses perpendicular to grain in curved beams, and in tension specimens, are found to be higher in the middle section, in the plane where pith is located, and much lower in the rest of the cross-section. The same is observed also during moisture cycling in long term loading. As a result, the failure will start when stresses in the middle exceed the strength. These are new scientific observations. In practical situations maximum stresses are obtained when a humid period is long. Tensile stresses at surface occur during dry periods, and they may become critical when drying is fast, width of beam is large or lamella includes the pith.

When the experimental values in cyclic and constant climate are compared (Table 20), we can conclude that when the beams are exposed to test cycle, at least 50% of the duration of load effect is caused by the change of stress distribution, and less than 50% by the weakening of the material. The effect of stress redistribution seems to depend on beam width. Under the same changing humidity conditions we obtained k_σ = 0.76 for beam width 90 mm, and 0.82 for beam width 140 mm. In this case, the smaller stress redistribution effect compensates at least partly the width effect observed in short term tests.

Table 20. Comparison of k- factors obtained in same cyclic moisture test.

	S2	S6
Beam width	90 mm	140 mm
Time to failure (days)	28 days	17 days
Estimated k_t	0.79	0.80
Observed total k_{DoL}	0.60	0.66
$k_\sigma = \frac{k_{DoL}}{k_t}$	0.76	0.82

The effect of moisture cycles is compared to the effect of mechanical loading at constant humidity by computing the value of mechanical load which causes same Weibull stress as a combination of mechanical and moisture load. Test cycles and a single fast change from 76% to 85% RH have been analysed. Moisture load corresponds to an extra load of 0.14 to 0.25 MPa when acting simultaneously with mechanical load 0.2 MPa, when the beam is not surface coated. A good surface coating (vapour barrier) will decrease the extra load to 0.06 MPa. The test cycle of AIR project seems to be more effective than the other cycles analysed. The effect of a single fast change from 75% to 85% is nearly the same and larger single changes are still more damaging. The conclusion is that fast changes of climate from dry weather to wet season with duration of several weeks are very harmful for curved structures loaded by tension stress perpendicular to grain.

Tensile stresses perpendicular to grain and the shape of stress distribution through width has been shown to be strongly dependent on two factors which have normally been neglected in strength considerations:

- the orientation of annual rings
- moisture gradients.

Both of these factors are obvious. However, it is surprising to notice how strong effect they have on the load bearing capacity. This factor was not fully recognised in the beginning of the project. Accordingly, some essential variables were not considered in the planning of the experiments. From scientific point of view the test material should have been so chosen that location of pith would have been the same or varied in a systematic way in all lamellae of test beams within a test series. This might have had more influence to the results than the strength grading of the material. The other factor, moisture gradients, appears to be still more important factor than was anticipated. Accordingly all changes in relative humidity, planned or unplanned, have great influence on the stress distribution and to the time to failure. Accordingly still more attention should have been given to the accuracy of humidity regulation to be sure that all moisture cycles are identical. In this project the imperfection of humidity regulation and variability of pith location increase the statistical deviation of the results and does not give so precise information on the duration of load effect as could have been in an ideal case.

While the annual ring orientation and moisture gradients have shown to be more important than was realised in advance, some other factors appeared to be less important than the two mentioned previously: creep after several moisture cycles seems not to change the level of stresses from that during the first cycle. Accordingly, for the analysis of the duration of load behaviour under tensile stress perpendicular to grain it is of great importance to consider the largest moisture cycle or change. All other duration of load effects are of much less importance, and can well be estimated on the basis of traditional stress ratio vs. log time to failure graph based on ideal constant humidity experiments.

Acknowledgements

This work is part of the project “Duration of load effect on different sized timber beams” (EC contract AIR2-CT94-1057). The work is also supported by VTT Building Technology, Academy of Finland, Technology Development Centre of Finland, Finnforest Oy and Late-Rakenteet Oy. The help of these organisations is gratefully acknowledged.

REFERENCES

Aicher, S. and Langer, D. 1995. Tension strength perpendicular to grain of supreme quality glulam conforming to CEN strength classes GL 32 and GL 36. Forschungs- und Materialprüfungsanstalt Baden-Württemberg (FMPA), Otto Graf Journal, Otto Graf Institute. Vol. 6. 15 p.

Dinwoodie, J. M. 1981. Timber, its nature and behaviour. Van Nostrand Reinhold Company, London. 190 p.

Fonselius, M. and Ranta-Maunus, A. 1996. Duration of load effect on LVL beams. Part 1. Short term reference tests. Espoo, Finland: VTT Research Notes 789. 23 p. + app. 17 p.

Gowda, S. S. and Ranta-Maunus, A. 1996. Duration of load effect on curved glulam beams. Part 1. Short term reference tests. Espoo, Finland: VTT Research Notes 1741. 66 p. + app. 11 p.

Gowda, S. S. and Ranta-Maunus, A. 1993. Curved and cambered glulam beams. Part 1. Short term load tests. VTT Research Notes 1500. Espoo, Finland: 96 p. + app. 39 p.

Hanhijärvi, A. 1995. Modelling of creep deformation mechanisms in wood. Espoo, Finland: VTT Publications 231. 143 p. + app. 3 p.

Hanhijärvi, A. and Ranta-Maunus, A. 1996. Computational analysis of the effect of transverse anisotropy and annual ring pattern in cross-sections of curved glulam beams on the size effect of strength. European Workshop on Application of Statistics and Probabilities in Wood Mechanics. Bordeaux. 12 p.

Hoffmeyer, P. 1996. Private consultation in project meeting.

Hukka, A. 1996. A simulation program for optimisation of medium temperature drying on an industrial scale. 5th Int. IUFRO Wood Drying Conference, Quebec City, Canada. 8 p.

Joyet, P. 1992. Comportement differe du materiau bois dans le plan transverse sous des conditions hydriques evolutives. L'Université Bordeaux I, Doctoral dissertation no. 812. (In French.).

Ranta-Maunus, A. 1990. Impact of mechano-sorptive creep to the long-term strength of timber. Holz als Roh- und Werkstoff 48, pp. 67 - 71.

Ranta-Maunus, A. and Gowda, S. S. 1994. Curved and cambered glulam beams. Part 2. Long term load tests under cyclically varying humidity. Espoo, Finland: VTT Publications 171. 36 p. + app. 18 p.

Welling, J. (editor 1994). European Drying Group Recommendation: Assessment of drying quality of timber. 28 p.

Appendix A

DENSITY AND MOISTURE CONTENT OF SAMPLES

Density and moisture content of samples for series LT-C2-S2

Sample number	Sample dimensions Hx W x L mm	Weight before ovendry (g)	Weight after ovendry (g)	Density **(D1)**before ovendry (kg/m3)	Density after ovendry (kg/m3)	Moisture content (%)	Laminate number from top
LT-C2-S2-1	29.28x81.94x81.65	99.27	87.40	506.75	446.16	13.58	1
	29.07x88.71x81.19	112.54	98.88	537.51	472.27	13.81	2
	26.85x88.63x72.76	88.42	78.09	510.66	451.00	13.23	3
	16.87x37.84x81.59	24.71	21.81	474.43	418.75	13.30	4
	15.17x88.65x81.88	46.40	40.95	421.38	371.89	13.31	5
	27.55x76.21x81.14	95.32	84.30	559.52	494.83	13.07	7
	25.59x88.50x79.41	91.56	80.74	509.12	448.95	13.40	8
	26.85x80.53x80.05	83.81	74.12	484.21	428.23	13.07	9
	19.36x54.12x81.50	44.39	39.28	519.83	459.99	13.01	10
	24.39x88.49x81.54	94.78	83.31	538.57	473.39	13.77	11
	22.09x70.52x81.00	79.52	70.16	630.21	556.03	13.34	12
	20.72x46.24x81.38	40.56	35.83	520.20	459.54	13.20	13
	25.75x56.57x81.63	60.19	53.10	506.19	446.56	13.35	14
	25.72x89.35x81.45	87.21	76.93	465.92	411.00	13.36	15
	13.96x75.34x81.24	40.09	43.18	574.53	505.36	13.69	16
	24.73x89.48x81.51	87.83	77.39	486.95	429.07	13.49	17
	23.83x89.56x81.40	83.64	73.87	481.45	425.21	13.23	18
LT-C2-S2-2	29.36x88.55x122.00	157.03	138.75	495.08	437.45	13.17	6 U
	15.40x80.65x121.68	73.12	64.80	483.83	428.78	12.84	7 C
	27.08x88.37x121.69	137.35	121.35	471.65	416.71	13.19	8 L
LT-C2-S2-3	27.50x89.32x121.33	160.50	141.21	538.55	473.82	13.66	9 U
	27.42x89.43x127.18	155.41	136.52	498.32	437.75	13.84	10 C
	30.80x89.37x126.45	165.09	145.33	474.31	417.54	13.60	11 L
LT-C2-S2-4	22.59x88.65x121.43	114.21	100.52	469.66	413.36	13.62	12 U
	22.83x88.67x121.77	130.07	114.68	527.66	465.23	13.42	13 L
LT-C2-S2-5	27.54x89.42x121.15	142.53	125.59	477.73	420.95	13.49	10 U
	21.17x72.67x70.87	57.04	50.56	523.17	463.73	12.82	11 C
	24.06x81.85x121.16	110.49	97.56	463.07	408.88	13.25	12 L
LT-C2-S2- 6	27.67x89.04x110.27	131.80	116.32	485.14	428.16	13.31	9 U
	28.07x31.33x123.26	60.71	53.65	560.06	494.93	13.16	10 C
	28.45x70.34x127.03	140.37	123.72	552.18	486.69	13.46	11 L
LT-C2-S2-7	27.94x90.05x121.15	170.45	150.05	559.21	492.27	13.60	10 U
	22.30x77.24x121.82	105.60	93.11	503.27	443.74	13.41	11 C
	27.08x90.01x86.20	113.68	100.25	541.09	477.13	13.40	12 L
LT-C2-S2-8	26.72x90.81x121.26	160.76	141.22	546.38	479.96	13.84	9 U
	20.48x78.17x121.17	101.90	89.43	526.39	461.02	13.94	10 C
	26.75x90.07x121.82	143.62	126.70	489.39	431.67	13.35	11 L

Note: Sample location from failure crack: U-upper; C-center; L-lower.

Appendix A2

Density and moisture content of samples for series LT-C2-S4.

Specimen	σ_b (MPa)	Time from start of cycle	Total loading time	Density (kg/m^3) $\rho_{\omega,\omega}$	Density (kg/m^3) $\rho_{0,\omega}$	ω %	Laminate
LT-C2-S4-1	0.61	3 d	87 d	490	441	11.0	2
				485	434	11.6	4
				572	511	11.9	7
				525	466	12.5	9
				499	449	11.2	10
LT-C2-S4-2	0.61	21 d	105 d	536	483	11.0	8
				515	462	11.5	9
LT-C2-S4-3	0.51	1 d	57 d	463	417	11.1	9
				510	457	11.6	10
LT-C2-S4-4	0.51	14 d	70 d	476	430	10.6	2
				523	470	11.3	3
				531	475	11.7	9
				514	460	11.7	10
LT-C2-S4-5	0.61	9 d	93 d	490	441	11.0	5
				550	495	11.1	6
				446	404	10.4	8
				439	398	10.2	11
LT-C2-S4-6				436	391	11.6	11
LT-C2-S4-7	0.61	14 d	98 d	501	453	10.7	8
				497	448	11.0	9
LT-C2-S4-8	0.61	4 d	88 d	439	400	10.0	2
				452	408	10.6	6
				471	425	10.8	11

Appendix A3

Density and moisture content of samples for series LT-C2-S6.

Sample Identification	Sample dimensions Hx W x L mm	Weight before ovendry (g)	Weight after ovendry (g)	Density before ovendry (kg/m3)	Density after ovendry (kg/m3)	Moisture content (%)	Laminate number from top*
LT-C2-S6-1	14.41x41.58x119.50	30.49	27.16	425.83	379.33	12.26	9
	18.64x41.34x117.58	38.49	34.38	424.81	379.45	11.95	10
LT-C2-S6-2	14.99x41.38x137.99	40.16	35.71	469.20	417.21	12.46	8
	17.62x42.10x126.39	45.23	40.17	482.42	428.45	12.60	9
	15.85x42.14x137.76	45.51	40.29	494.61	437.88	12.95	17
LT-C2-S6-3	20.33x40.06x137.67	58.79	47.90	479.75	427.22	12.80	9
	23.85x40.52x117.98	59.85	53.15	524.93	466.16	12.61	10
LT-C2-S6-4	15.06x40.42x137.28	40.14	35.60	480.34	426.01	12.75	7
	25.44x39.99x137.22	72.98	64.93	522.78	465.11	12.40	12
	26.39x40.58x136.76	66.87	59.55	456.58	406.60	12.29	13
LT-C2-S6-5	22.98x40.41x126.05	53.25	47.19	454.92	403.15	12.84	8
	24.08x40.11x136.71	61.97	54.91	469.32	415.86	12.86	9
LT-C2-S6-6	18.48x40.69x130.94	46.26	41.05	469.83	416.92	12.69	11
	25.05x40.25x137.50	69.68	61.79	502.61	445.70	12.77	12
LT-C2-S6-7	20.30x41.10x92.71	33.07	29.52	427.53	381.64	12.03	7
	17.17x40.90x90.91	27.79	24.80	435.29	388.46	12.06	9
	23.09x40.37x114.96	46.35	41.40	432.53	386.34	11.96	11
	16.68x35.56x137.25	41.42	36.88	508.79	453.02	12.31	13
LT-C2-S6-8	18.83x39.75x136.92	49.25	43.88	480.56	428.17	12.24	9
	16.09x39.92x138.72	45.49	40.45	510.54	453.98	12.46	10
	14.62x40.12x139.54	47.98	42.54	586.21	519.75	12.79	11
	24.29x40.11x139.23	73.72	65.46	543.47	482.57	12.62	12
	24.14x38.51x135.10	58.62	52.14	466.74	415.15	12.43	13

Note: * Laminate number where failure crack appeared.

Values of density and moisture content for series ST-C2-S5b.

Beam	Laminate	Height (mm)	Width (mm)	Length (mm)	Weight before ovendry	Weight after ovendry	Density before ovendry	Density after ovendry	Moisture content
					(kg/mm3)	(kg/mm3)	ρ_u	ρ_0	u (%)
ST-C2-S5b-1	8	18.59	39.87	136.21	46.49	41.23	461	408	12.8
ST-C2-S5b-1	9	24.57	40.05	136.46	64.83	57.19	483	426	13.4
ST-C2-S5b-2	6	18.32	41.89	139.29	50.38	44.37	471	415	13.6
ST-C2-S5b-2	7	25.86	41.69	139.87	72.83	64.05	483	425	13.7
ST-C2-S5b-3	10	23.77	40.62	138.67	66.08	58.35	494	436	13.3
ST-C2-S5b-3	11	18.05	39.29	138.41	45.30	39.94	462	407	13.4
ST-C2-S5b-4	7	18.68	42.19	137.35	53.49	47.51	494	439	12.6
ST-C2-S5b-4	8	19.00	41.76	110.43	45.31	40.09	517	458	13.0
Mean							**483**	**427**	**13.2**

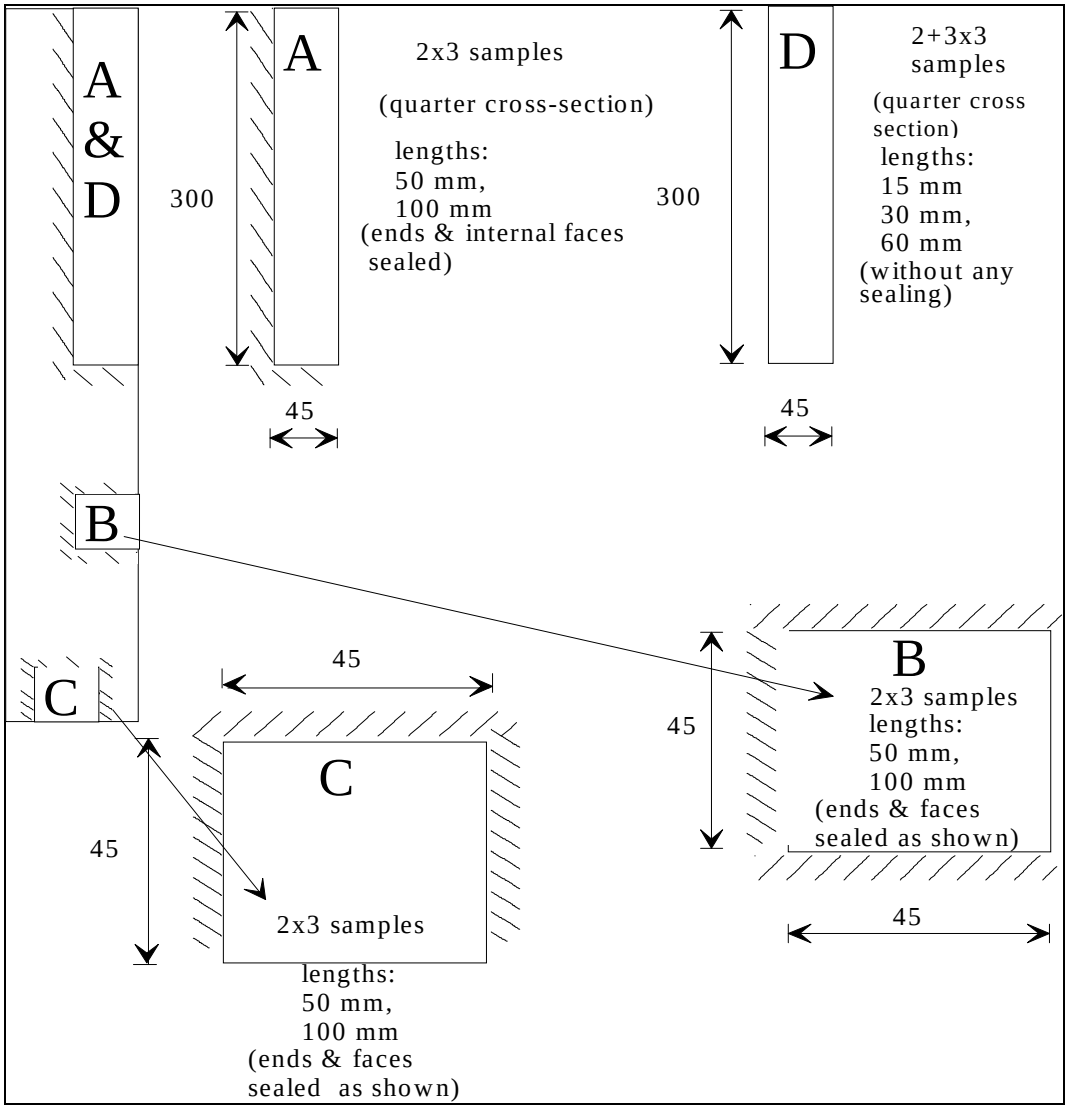

Glulam moisture samples

Tensile tests

Tensile tests were made perpendicular to grain in different depths from the top surface of a 140 mm thick beam. Test specimen corresponds to ASTM standard except that the thickness of specimen is 10 mm instead of 2 inches (see Figure). The results are shown in Table. Specimens with glue line in the middle show lower values and less variability depending on the position. Values at surface (about 45° angle between radial and tangential direction) are about 10 % higher than in the middle. The difference may be influenced by a higher density of wood closer to surface, which will result also in higher E-modulus and higher stresses in loading. Because the difference in strength values at different depths from surface is small, the main conclusion from these tests is that curved glulam can carry about the same vertical stress perpendicular to grain when the angle between radial direction and stress does not exceed 45°.

Table: Experimental results of tensile strength perpendicular to grain in different positions in 140 mm thick glulam.

	Location		
	Middle	¼ of width	Surface
Angle to radial direction, average [°]	0	30	45
Strength at glueline:mean [N/mm^2]/COV[%]	2,56 / 32	2,82 / 24	2,84/ 20
Strength in the middle of lamella: mean [N/mm^2]/COV[%]	2,53 / 26	3,29 / 18	2,77/ 25
sample size	20	10	20

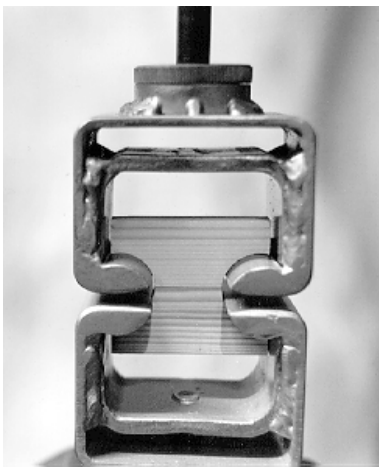

Figure. Test specimen and test grips for perpendicular to grain testing.

Material data

Term tangential	τ(h)	τ(-)	$J_t(10^{-10}\ Pa^{-1})$
0			12
ve1	0.001		8
ve2	0.01		8.02
ve3	0.1		8.96
ve4	1		18.94
ve5	10		69.44
ve6	100		242.4
ms1		0.01	30
ms2		0.1	31
ms3		1	94
ms4		10	759

$J_{i,r} = 0.5\ J_{i,t}$; $J_{i,rt} = 12.5\ J_{i,t}$; $\varepsilon_0 = J_0\sigma$; $d\varepsilon_{ve} = \sum_i \frac{\sigma - \varepsilon_i^{ve} / J_i^{ve}}{\tau_i^{ve} / J_i^{ve}} d\xi$;

$$d\xi = 10^a\, dt$$

$$a = 20(u - FSP) + 0.05(T - 30^\circ C)$$

$$d\varepsilon_{ms} = \sum \sum_i \frac{\sigma - \varepsilon_i^{ms} / J_i^{ms}}{\tau_i^{ms} / J_i^{ms}} |du|$$

Measurement of support reactions: S6 series

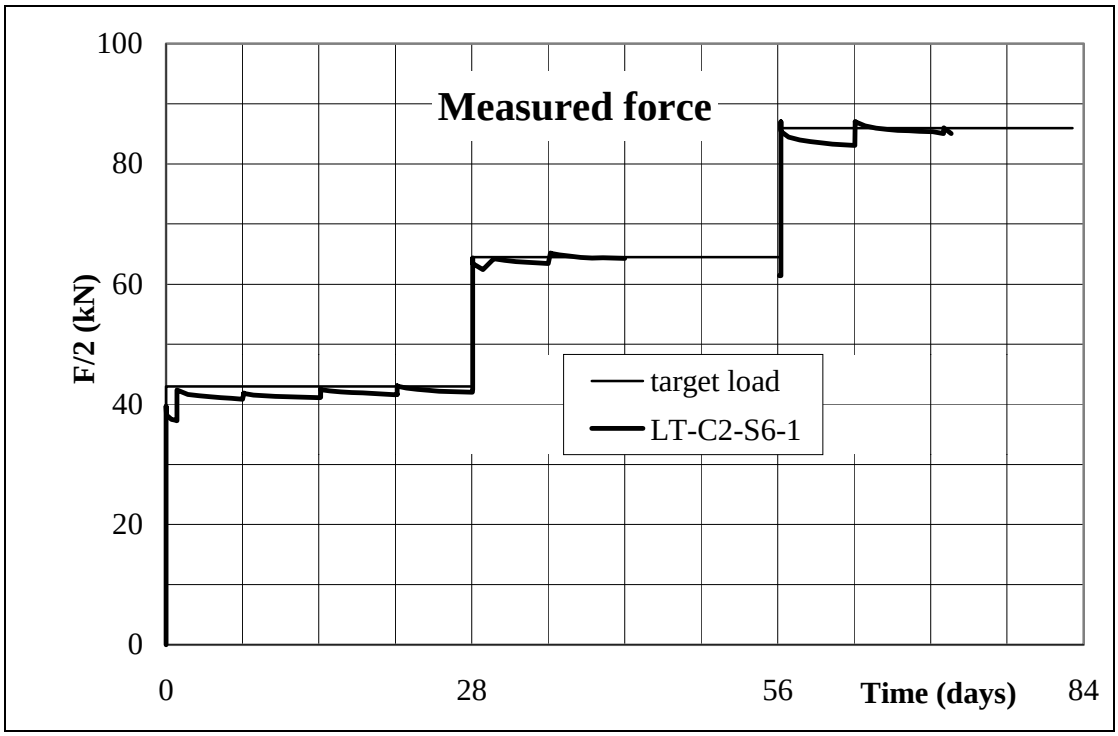

Measured support reaction and target load levels for beam LT-C2-S6-1.

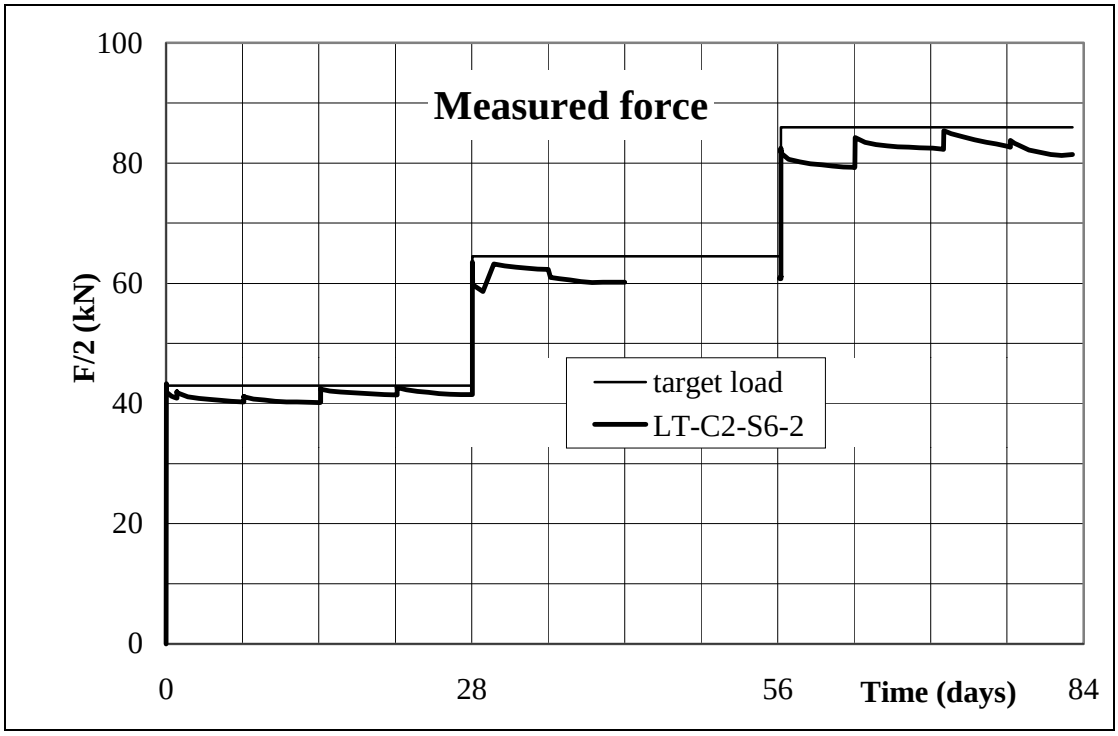

Measured support reaction and target load levels for beam LT-C2-S6-2.

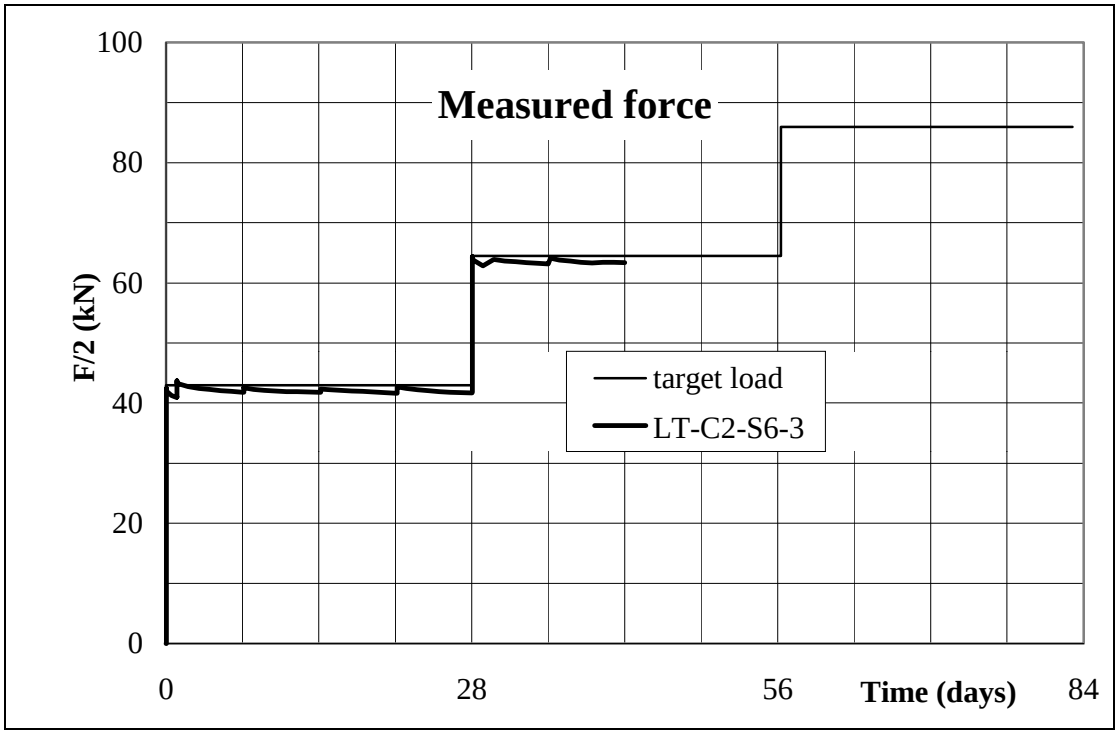

Measured support reaction and target load levels for beam LT-C2-S6-3.

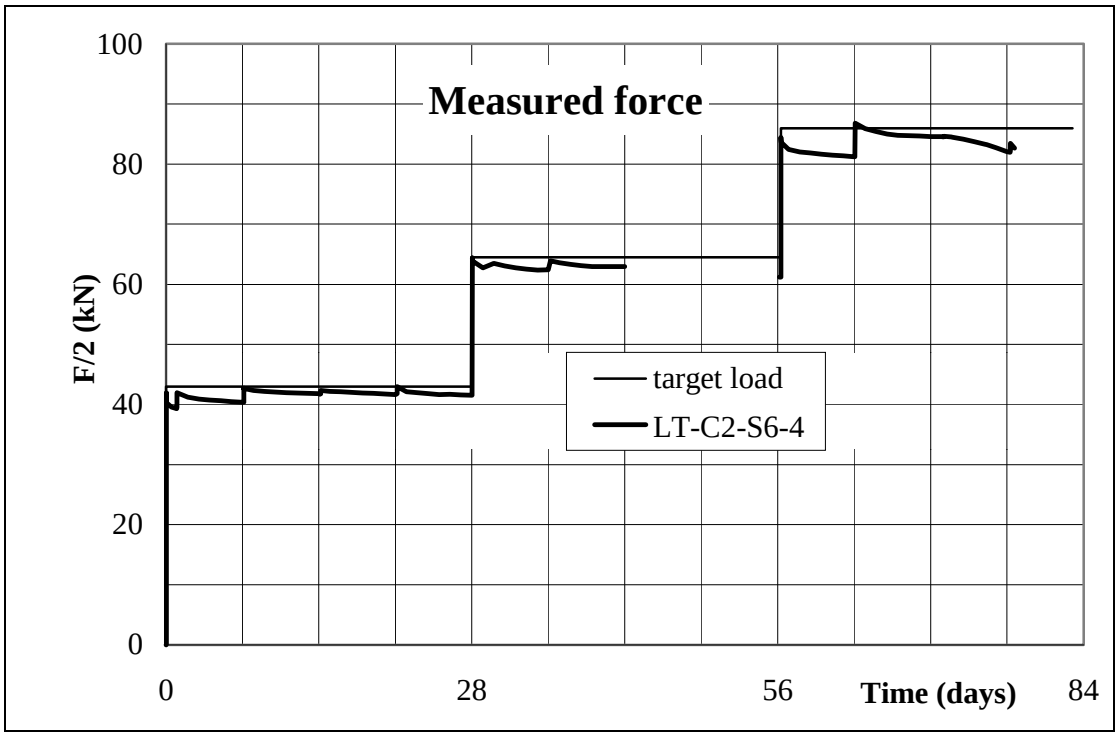

Measured support reaction and target load levels for beam LT-C2-S6-4.

Creep deformation of specimen: LT-C2-S2 Series

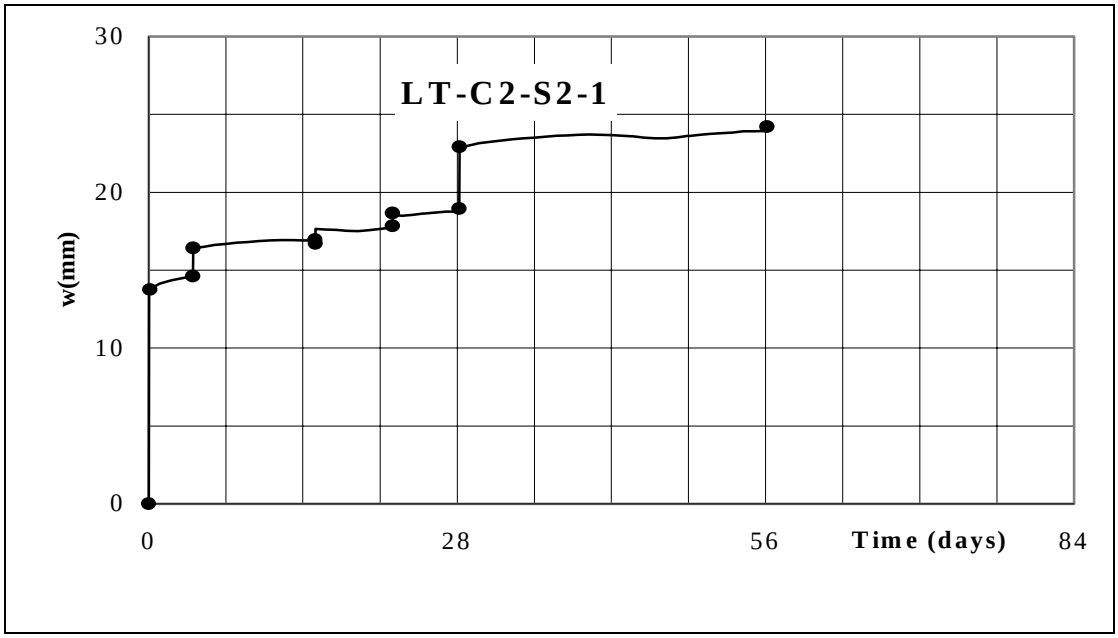

Creep deformation of specimen LT-C2-S2-1.

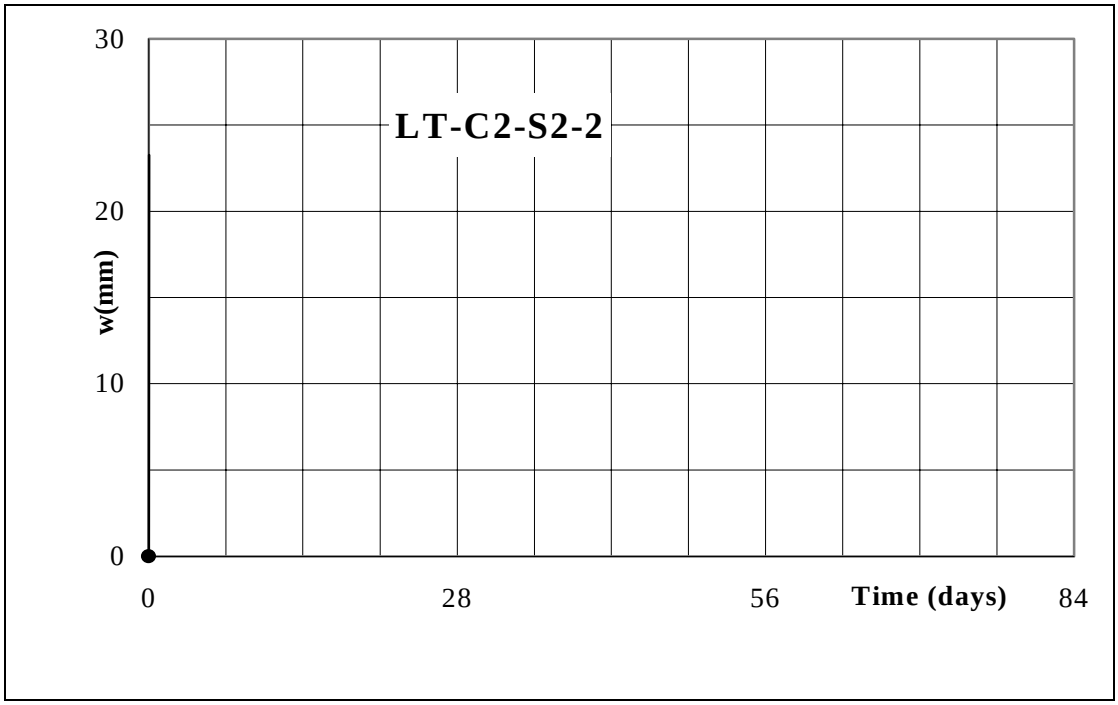

Creep deformation of specimen LT-C2-S2-2.

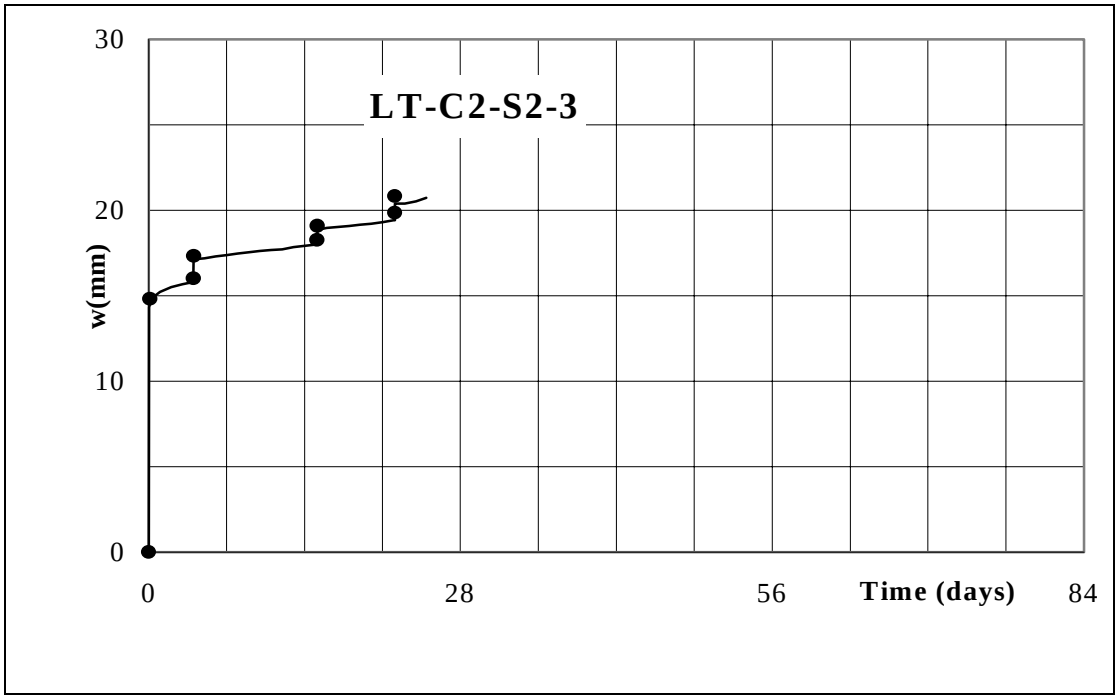

Creep deformation of specimen LT-C2-S2-3.

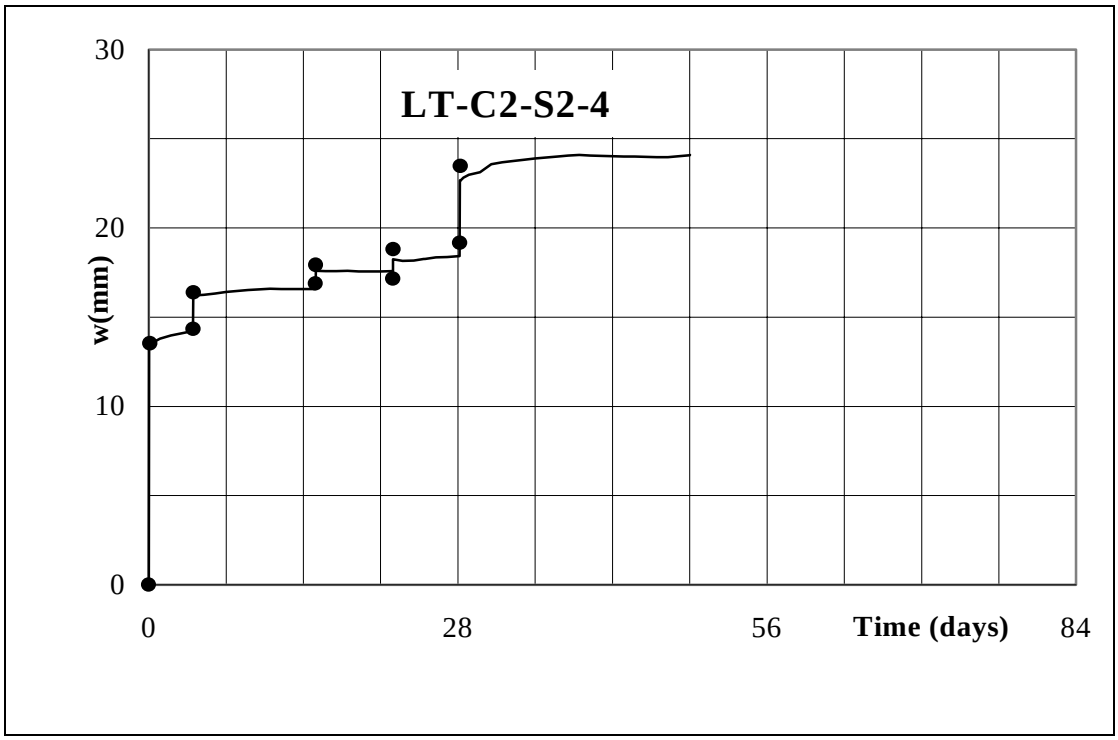

Creep deformation of specimen LT-C2-S2-4.

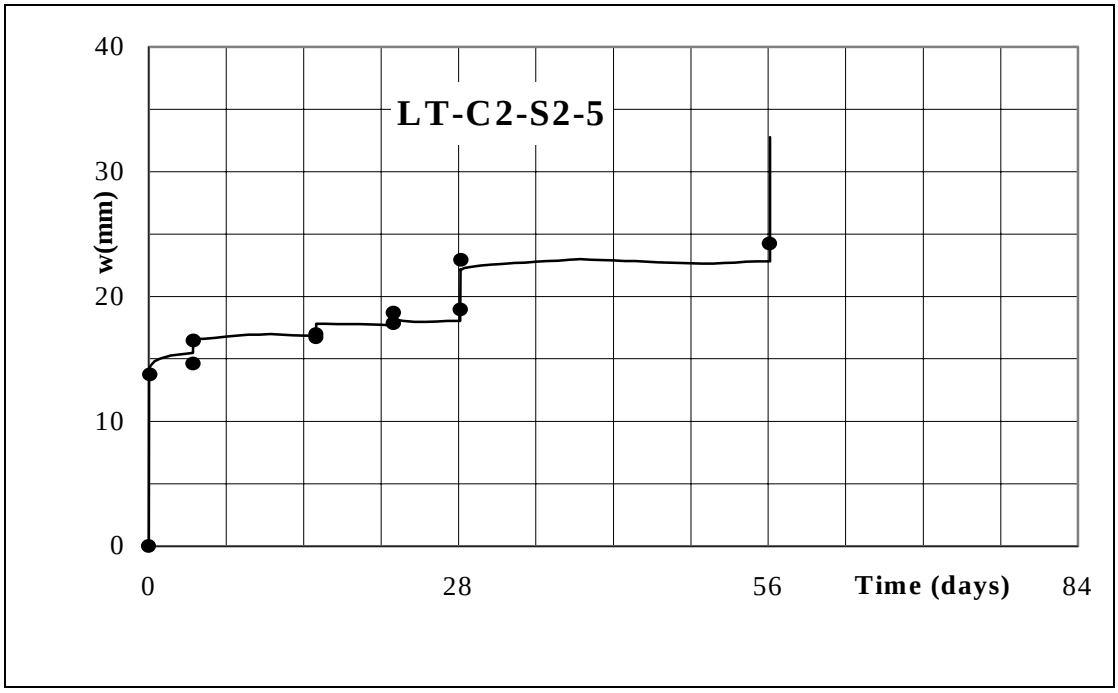

Creep deformation of specimen LT-C2-S2-5.

.

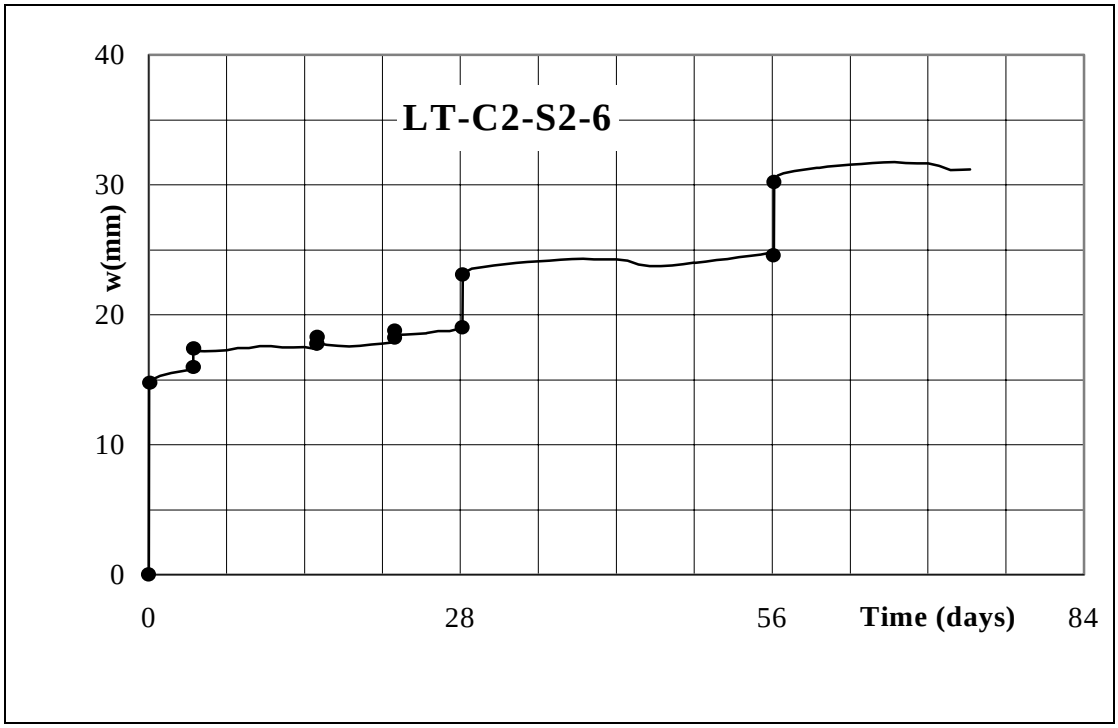

Creep deformation of specimen LT-C2-S2-6.

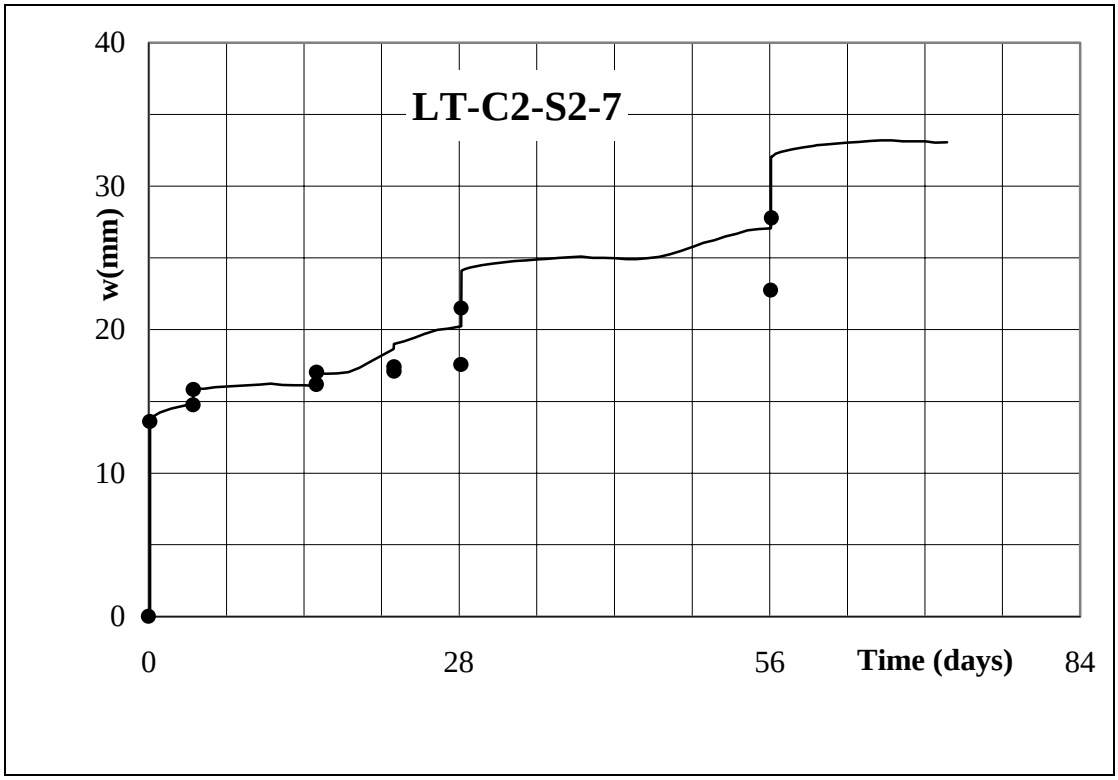

Creep deformation of specimen LT-C2-S2-7.

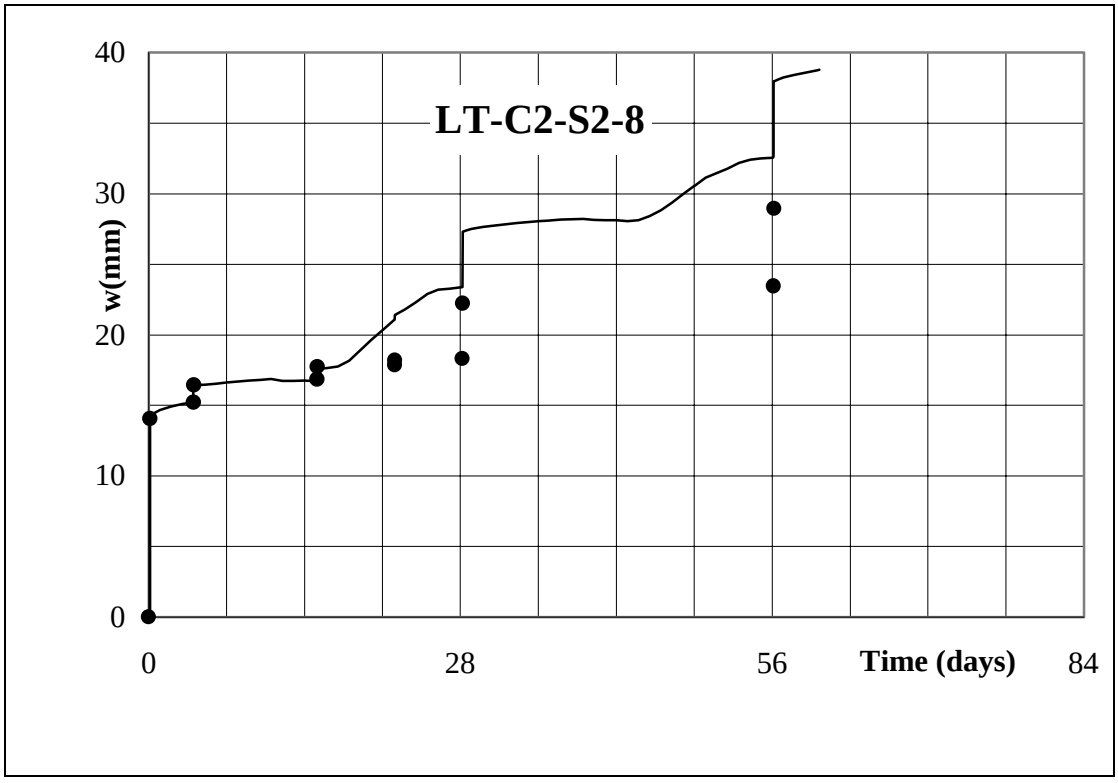

Creep deformation of specimen LT-C2-S2-8.

Creep deformation of specimens: LT-C2-S6 Series

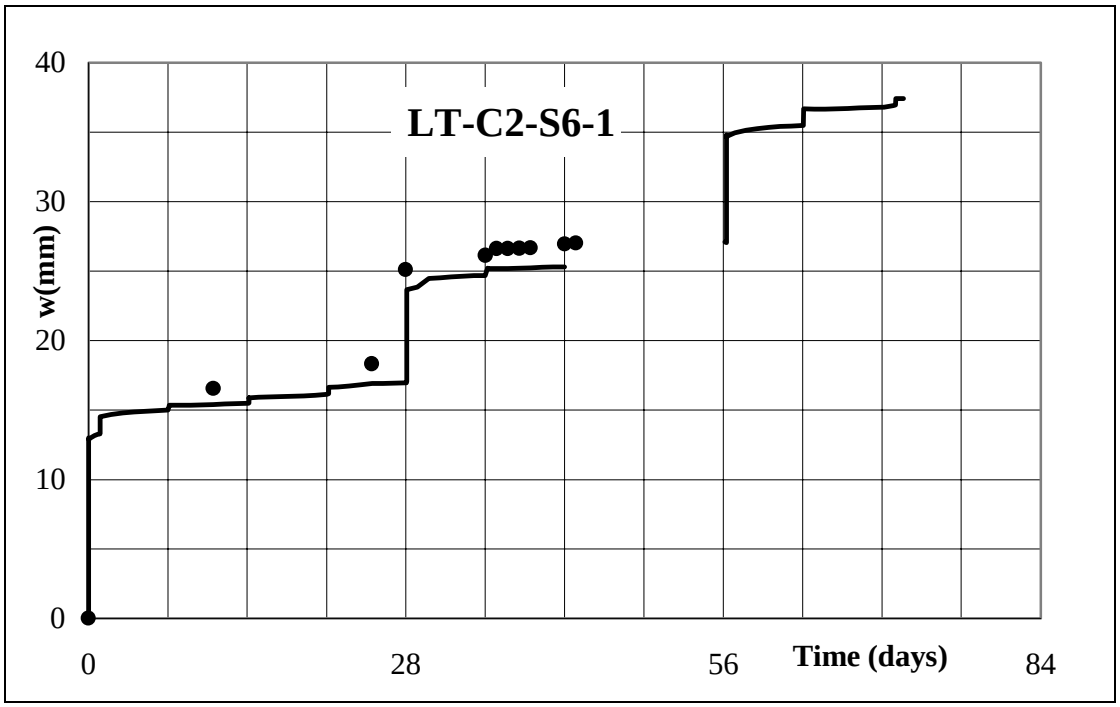

Creep deformation of specimen LT-C2-S6-1.

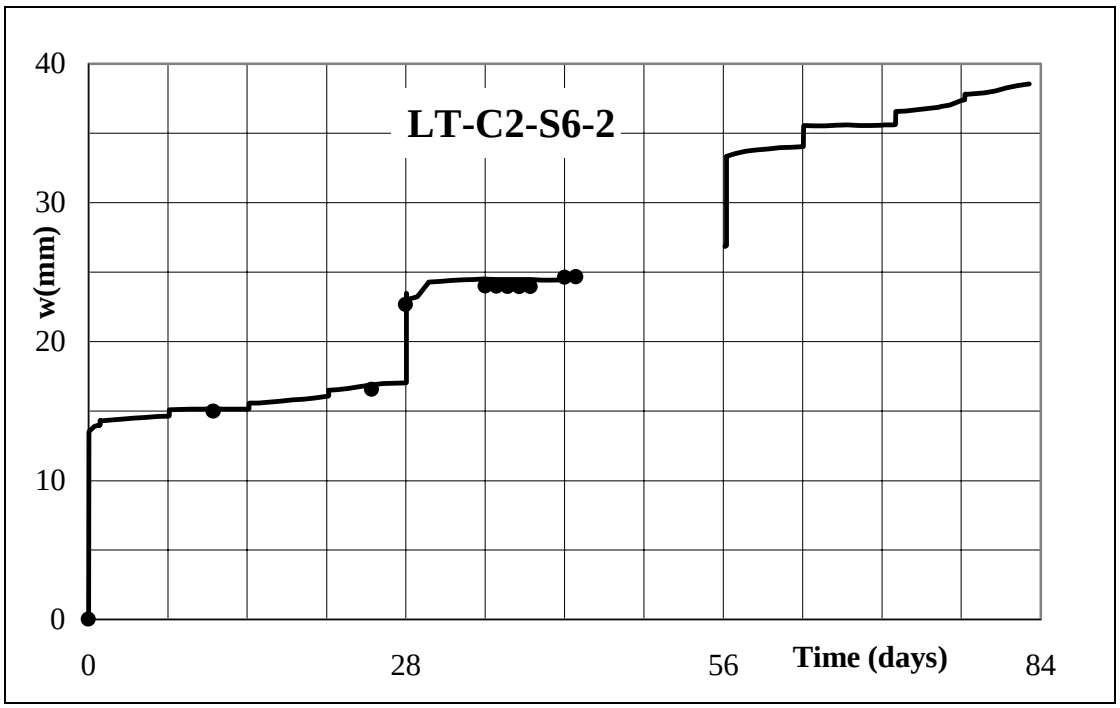

Creep deformation of specimen LT-C2-S6-2.

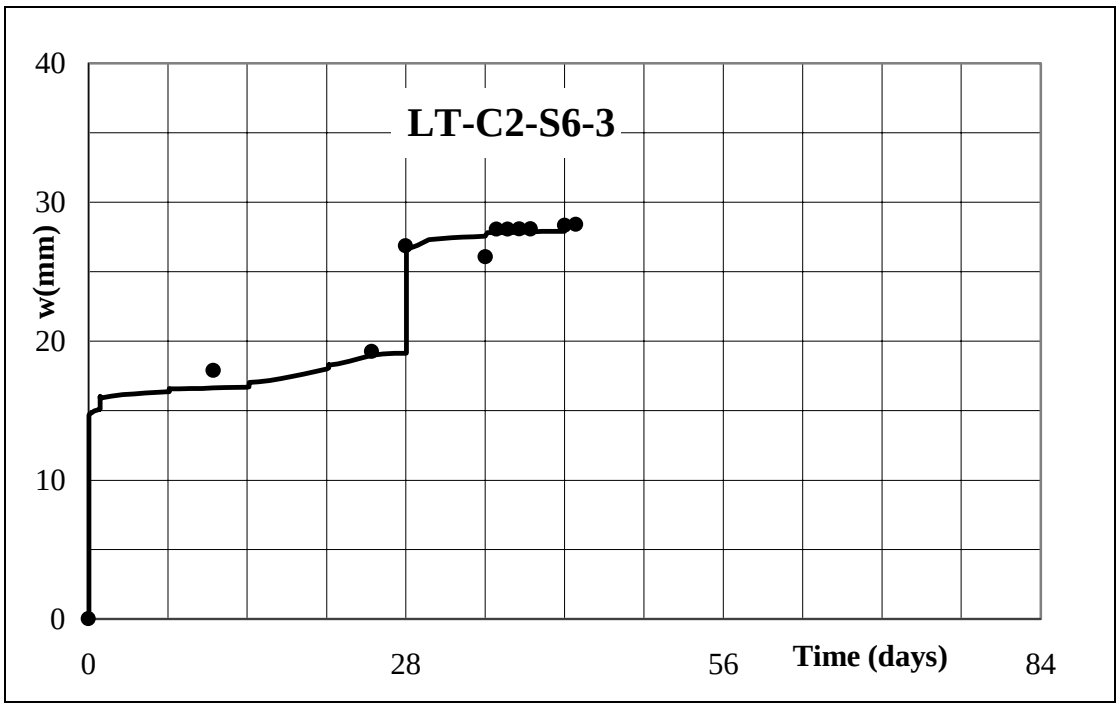

Creep deformation of specimen LT-C2-S6-3.

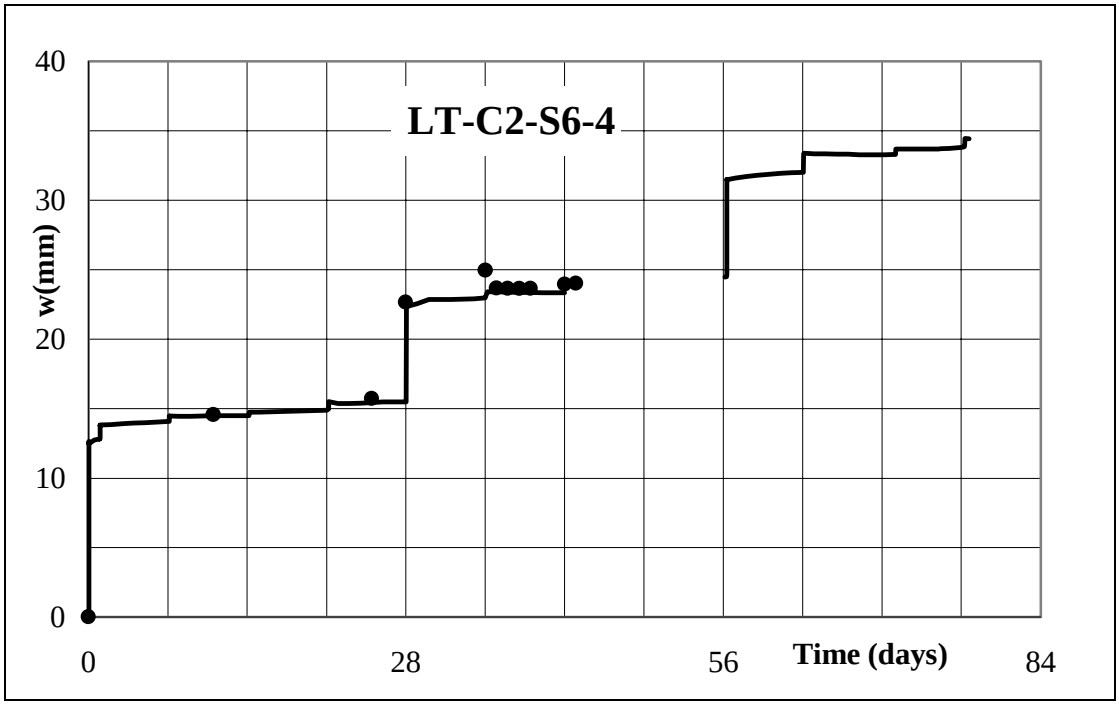

Creep deformation of specimen LT-C2-S6-4.

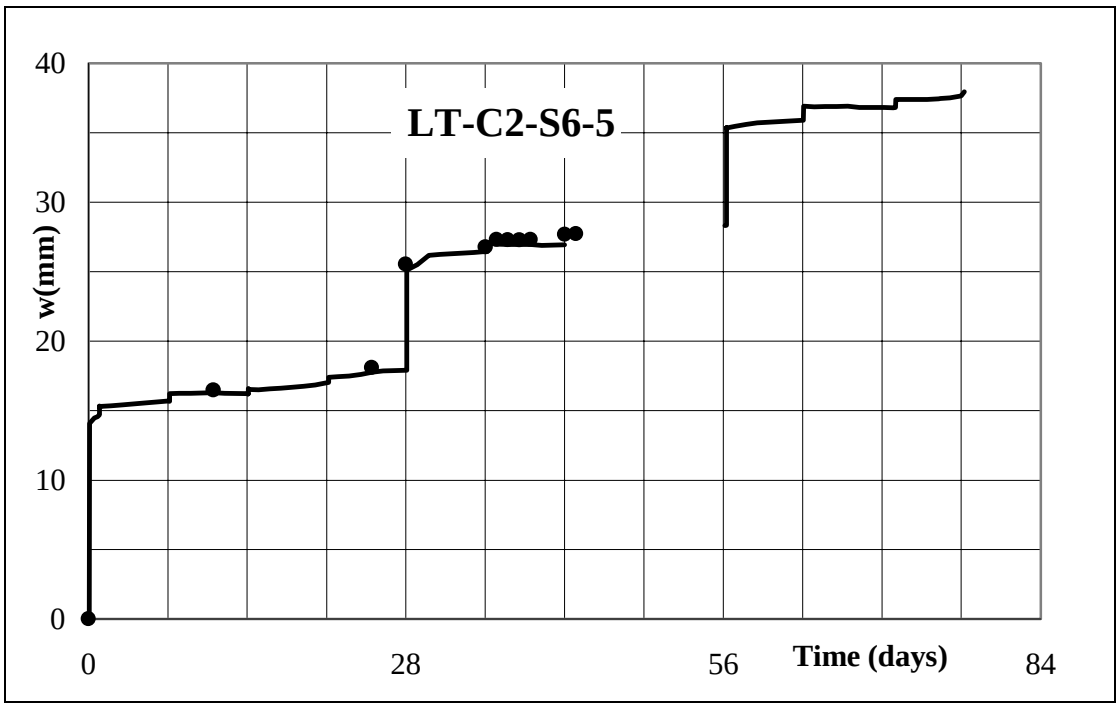

Creep deformation of specimen LT-C2-S6-5.

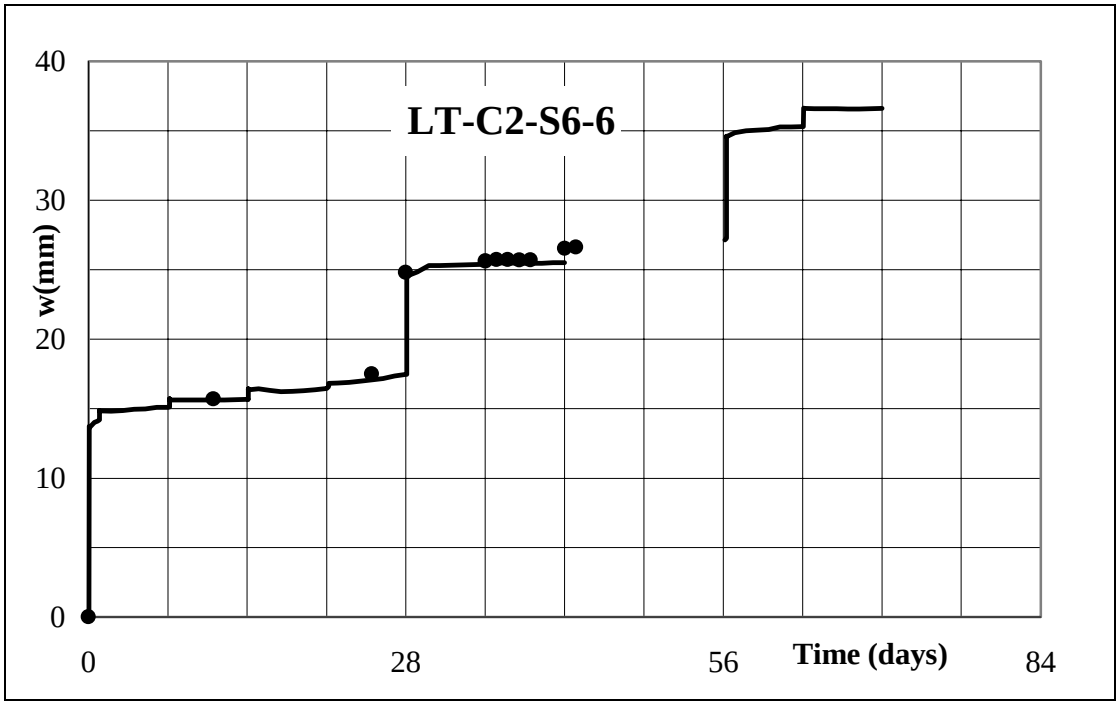

Creep deformation of specimen LT-C2-S6-6.

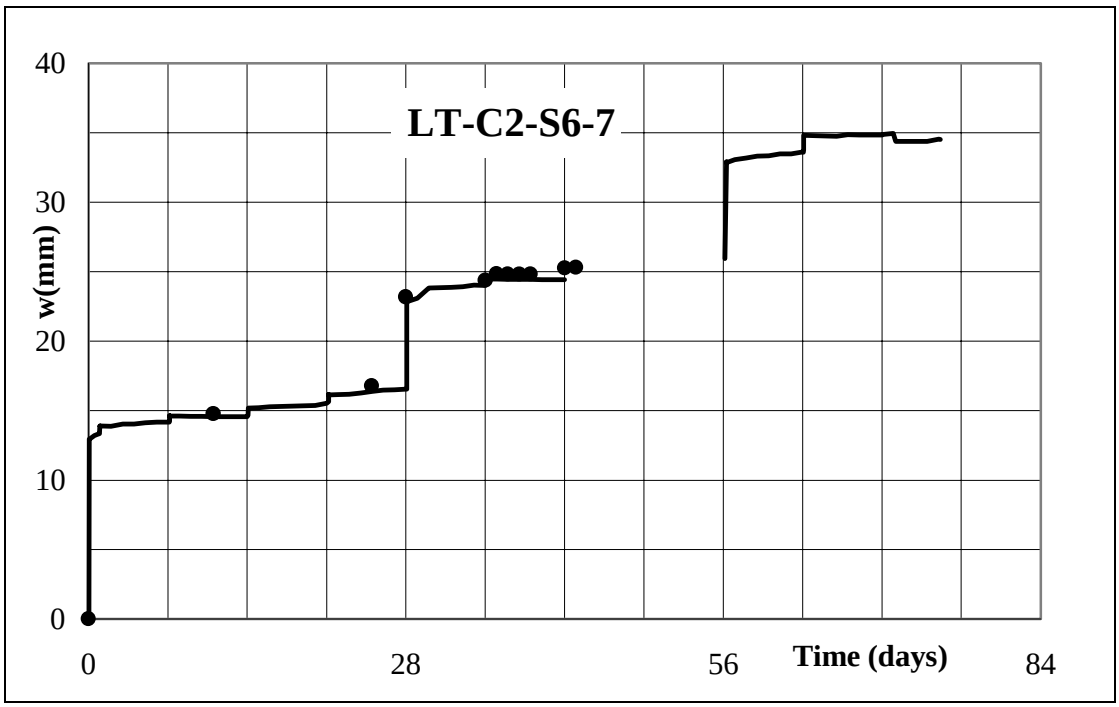

Creep deformation of specimen LT-C2-S6-7.

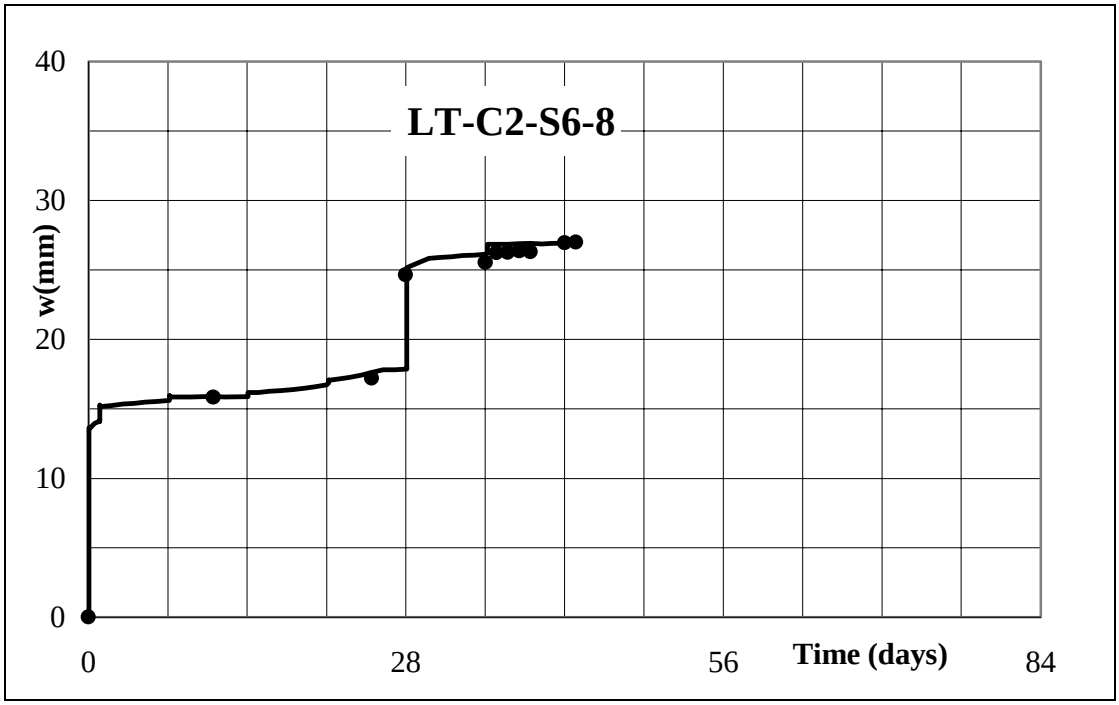

Creep deformation of specimen LT-C2-S6-8.

Appendix E

Failure behaviour of specimens: Short term tests

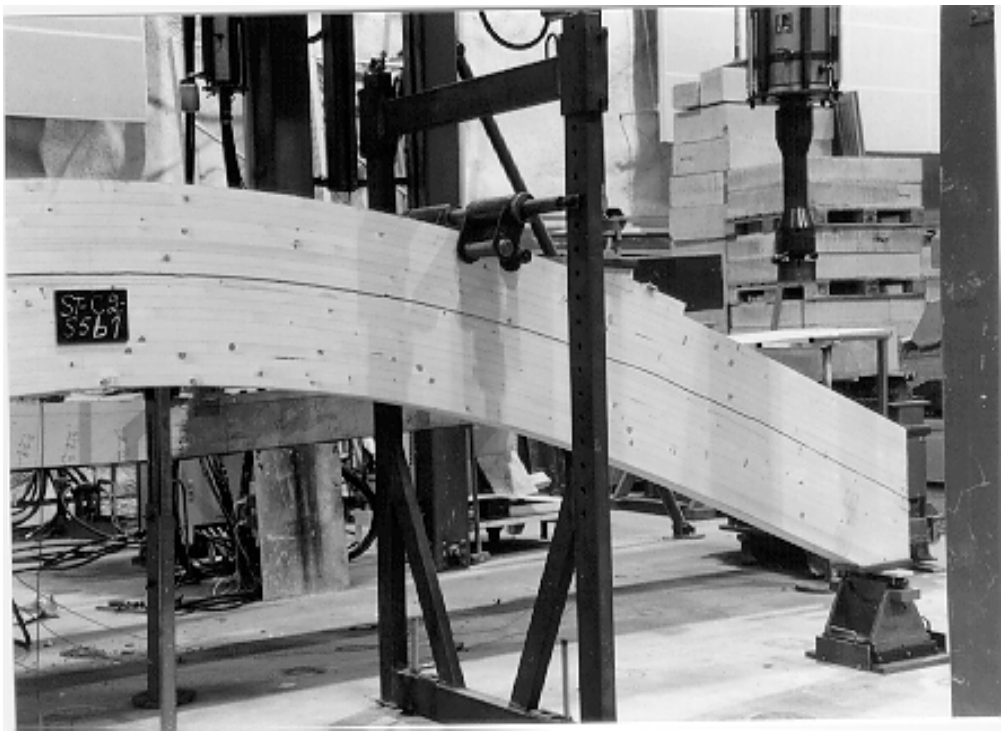

Failure behaviour of Specimen ST-C2-S5b-1.

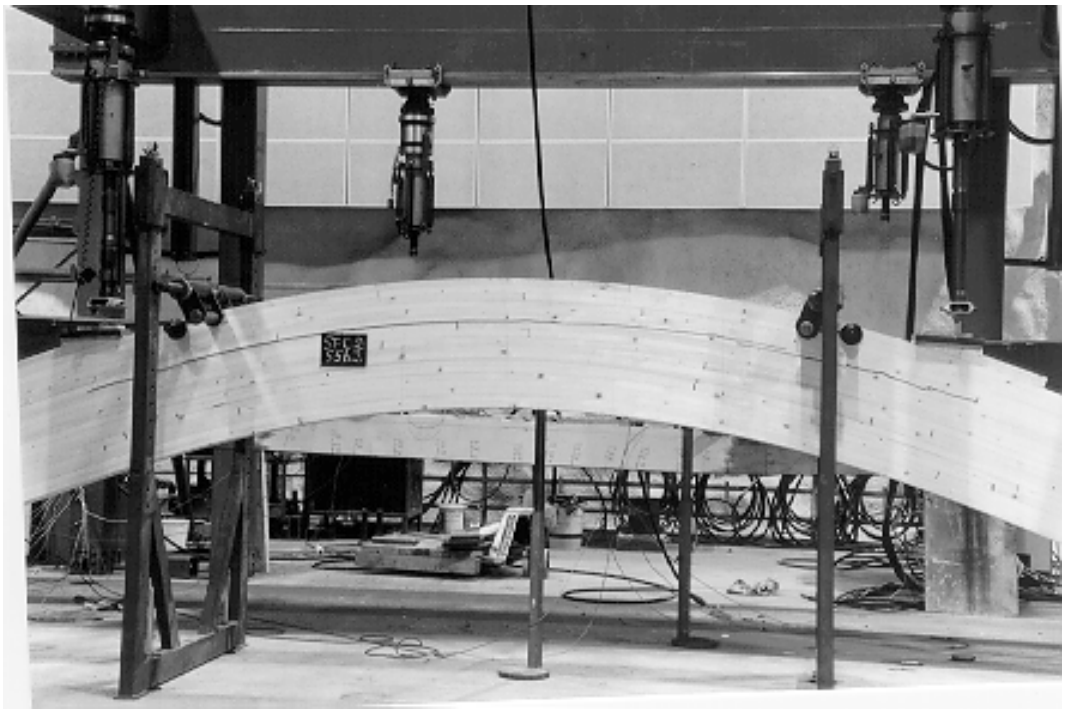

Failure behaviour of Specimen ST-C2-S5b-2.

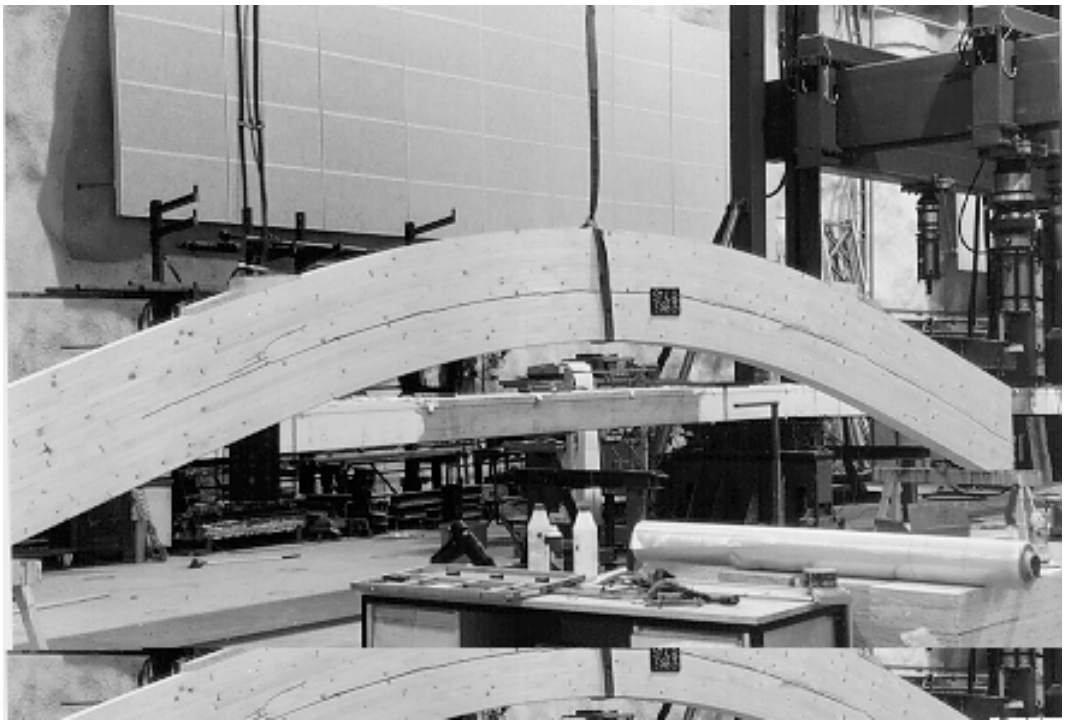

Failure behaviour of Specimen ST-C2-S5b-3.

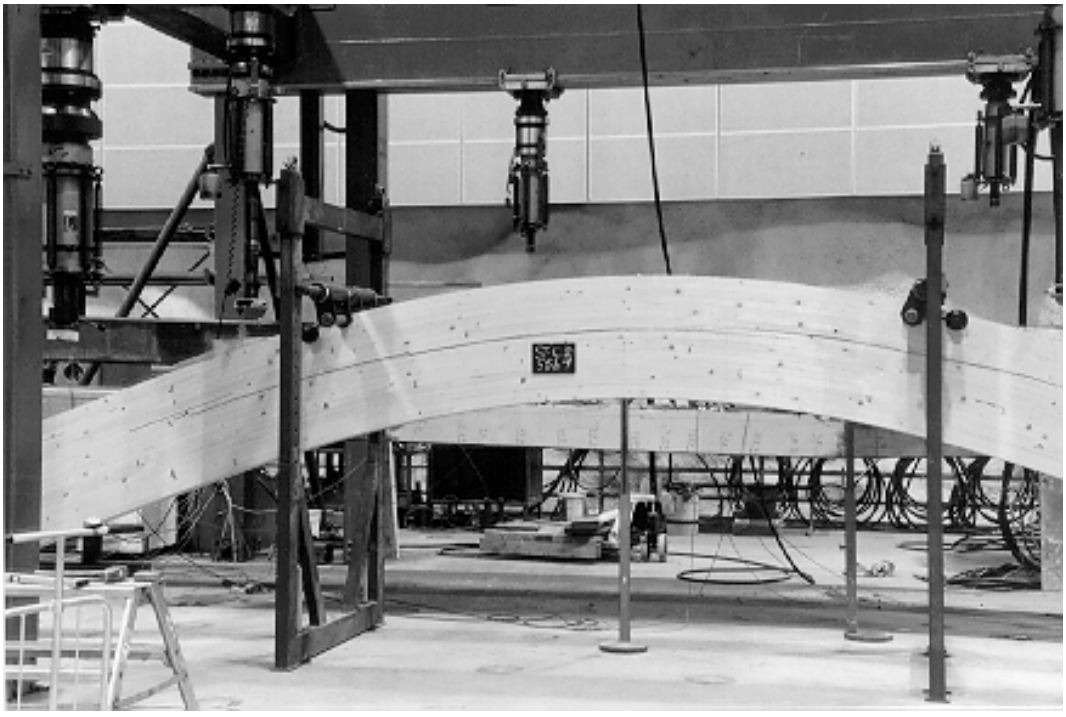

Failure behaviour of Specimen ST-C2-S5b-4.

Failure behaviour of specimens

Long term tests: Series LT-C2-S2

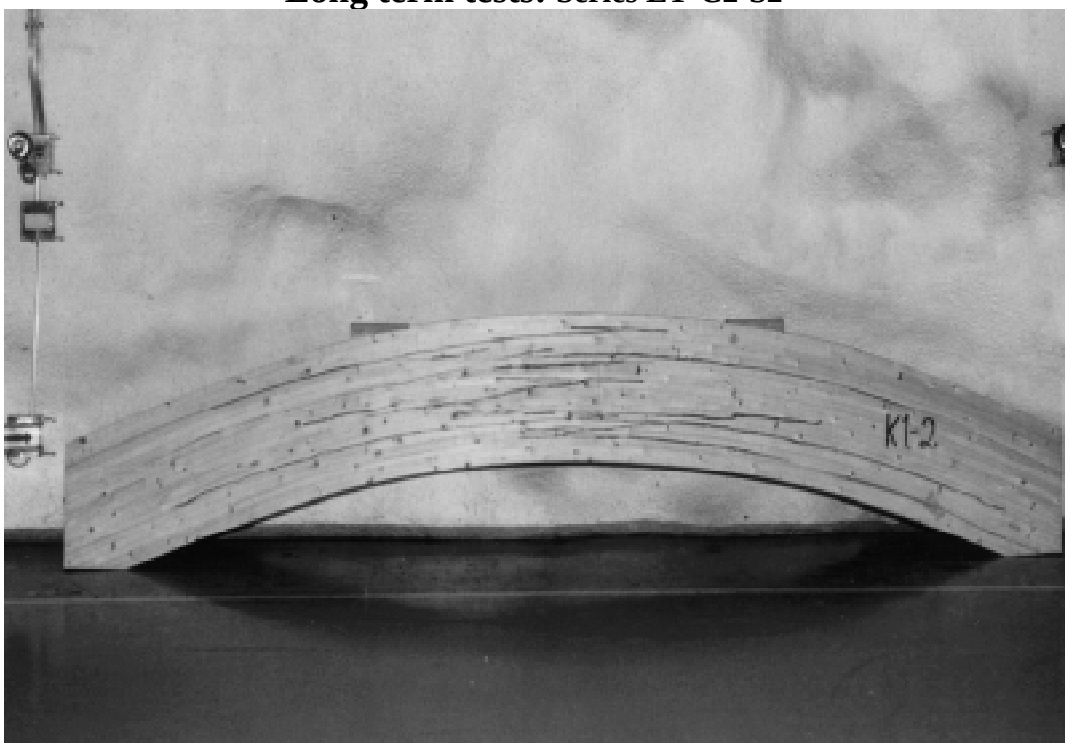

Failure behaviour of specimen LT-C2-S2-1.

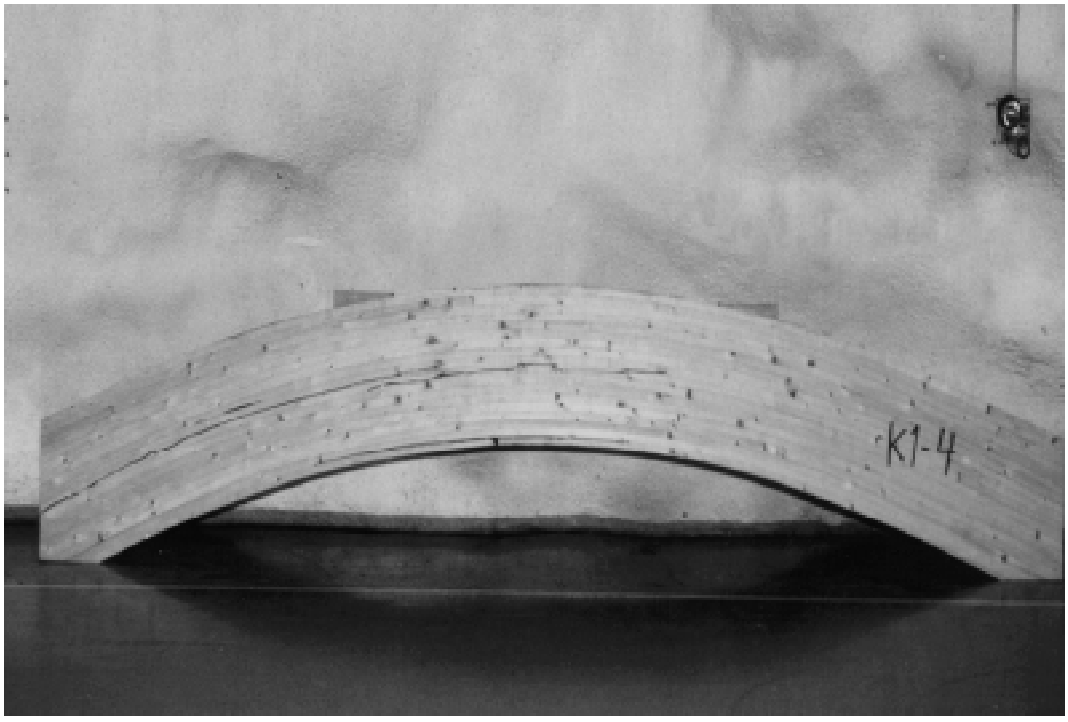

Failure behaviour of specimen LT-C2-S2-2

.

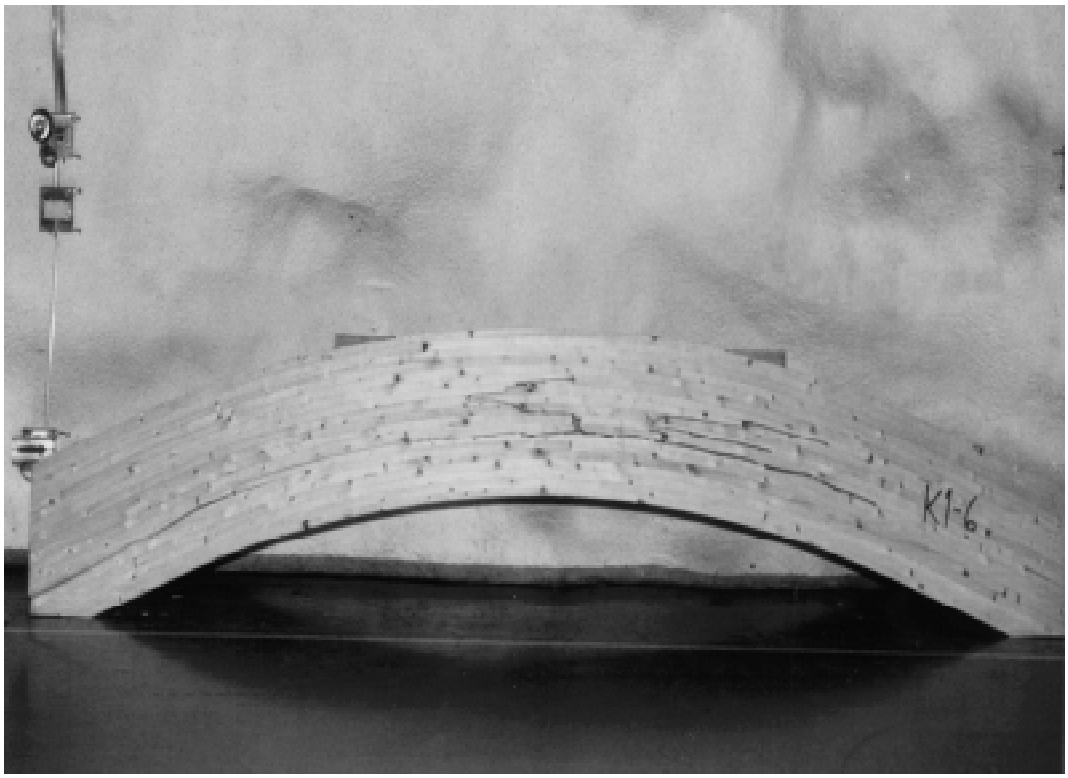

Failure behaviour of specimen LT-C2-S2-3.

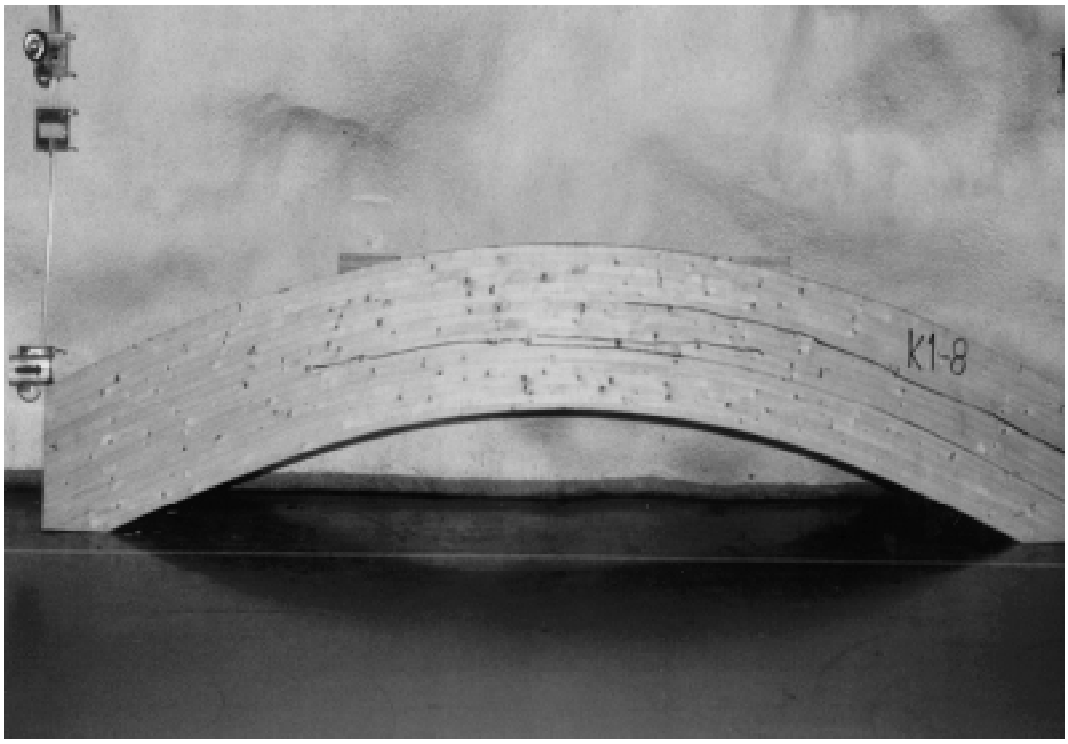

Failure behaviour of specimen LT-C2-S2-4.

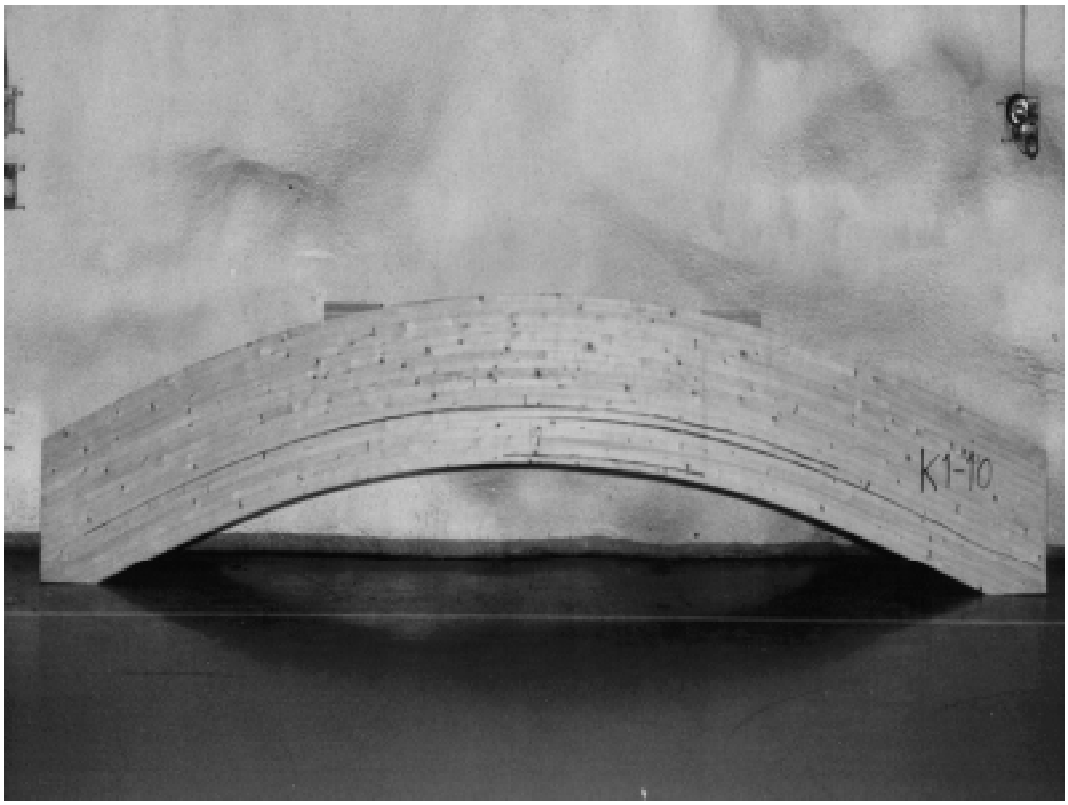

Failure behaviour of specimen LT-C2-S2-5.

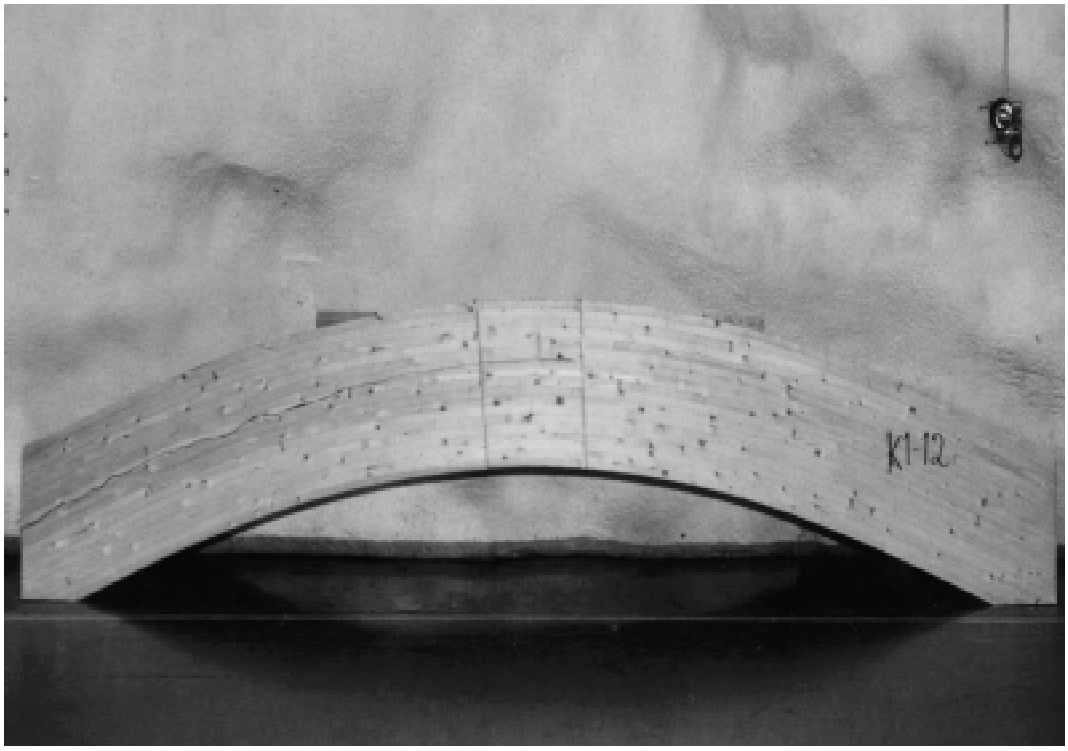

Failure behaviour of specimen LT-C2-S2-6.

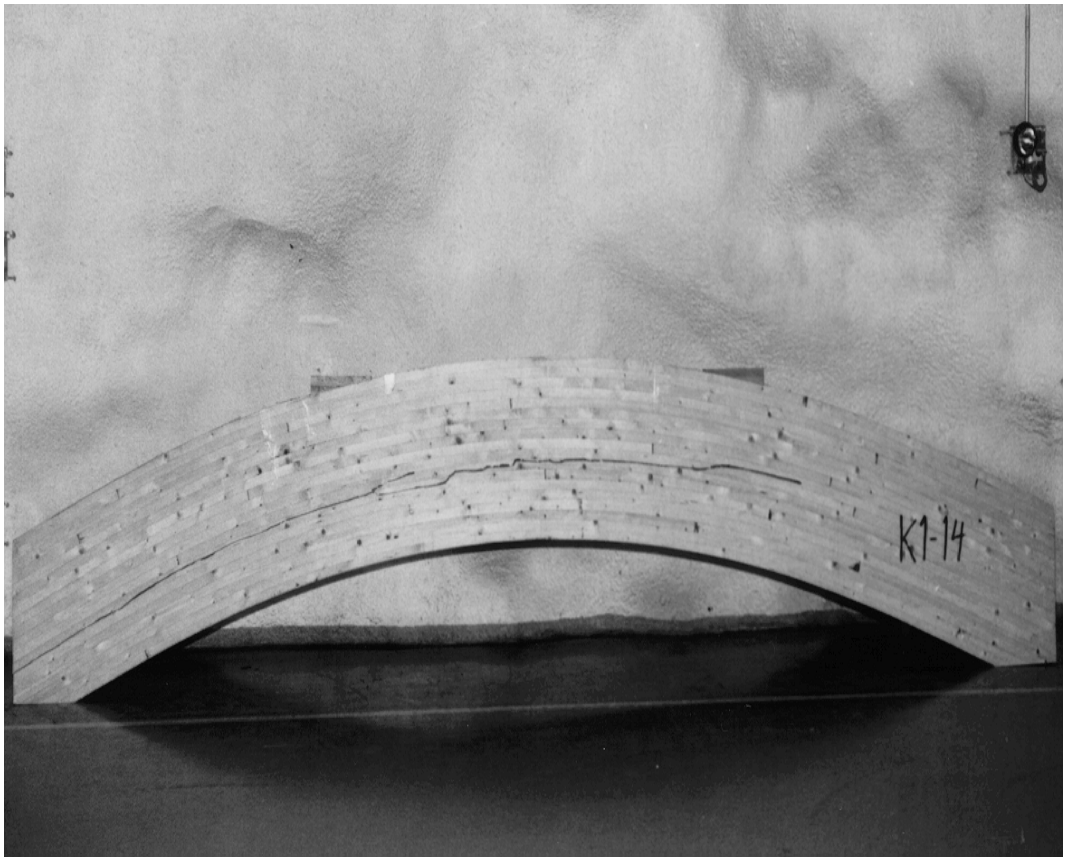

Failure behaviour of specimen LT-C2-S2-7.

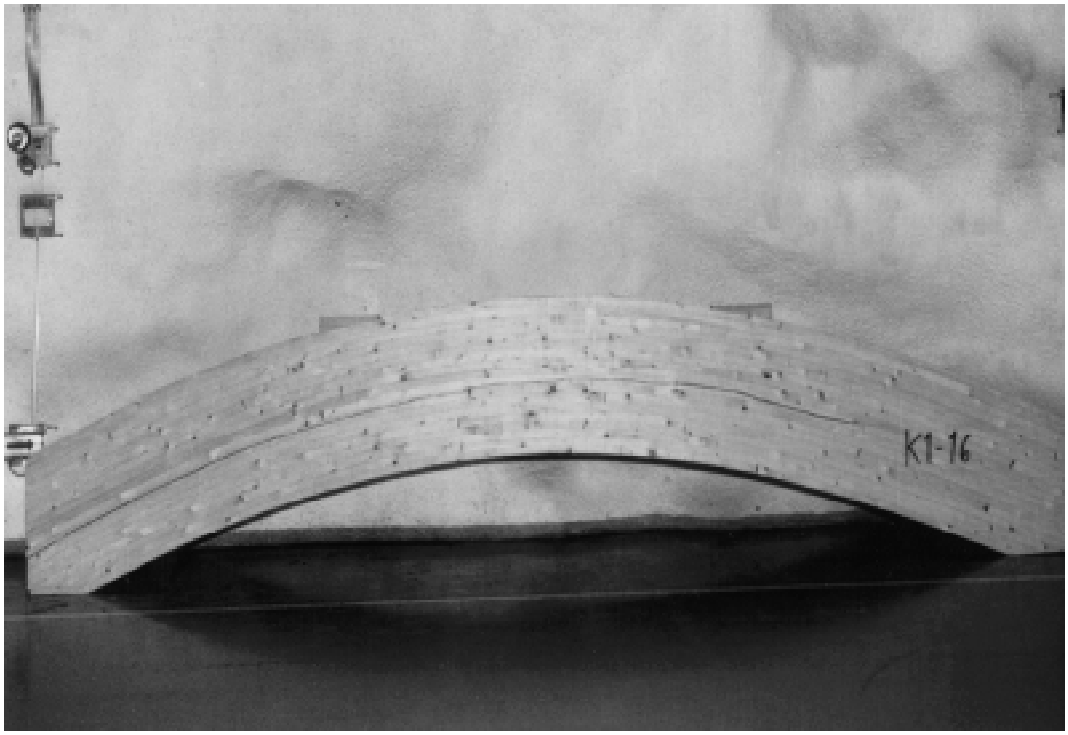

Failure behaviour of specimen LT-C2-S2-8.

Failure behaviour of Specimen LT-C2-S4-1 (AIR LT3 No.1).

Failure behaviour of Specimen LT-C2-S4-2 (AIR LT3 No.2).

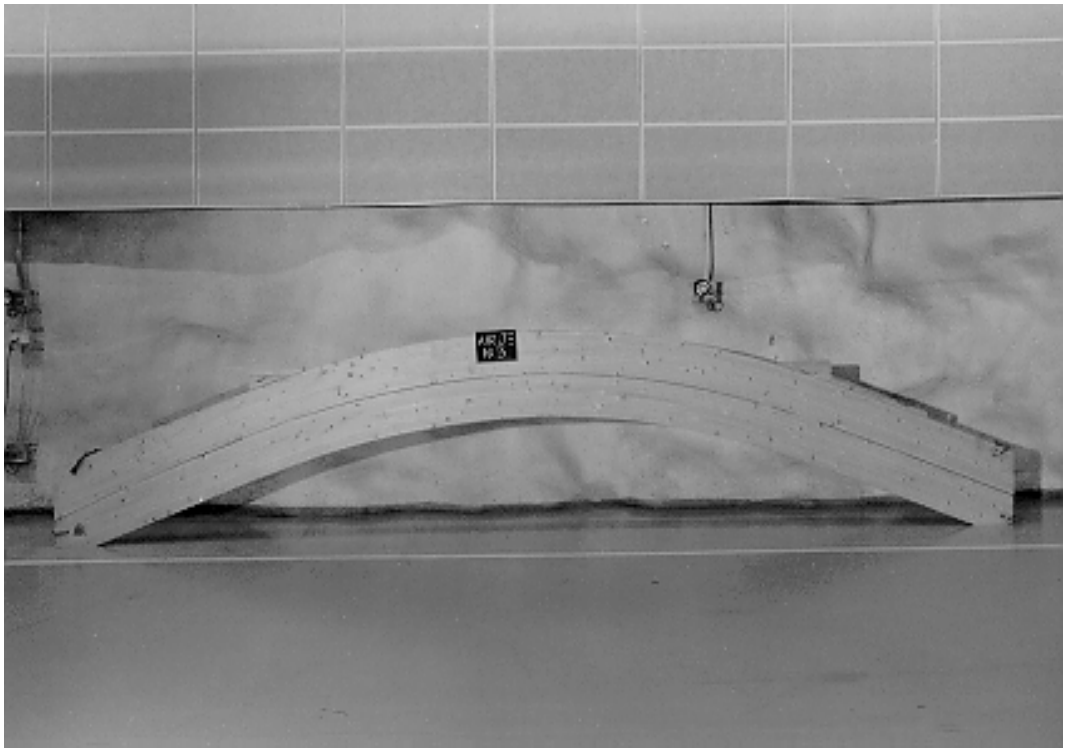

Failure behaviour of Specimen LT-C2-S4-3 (AIR LT3 No.3).

Failure behaviour of Specimen LT-C2-S4-4 (AIR LT3 No.4).

Failure behaviour of Specimen LT-C2-S4-5 (AIR LT3 No.5).

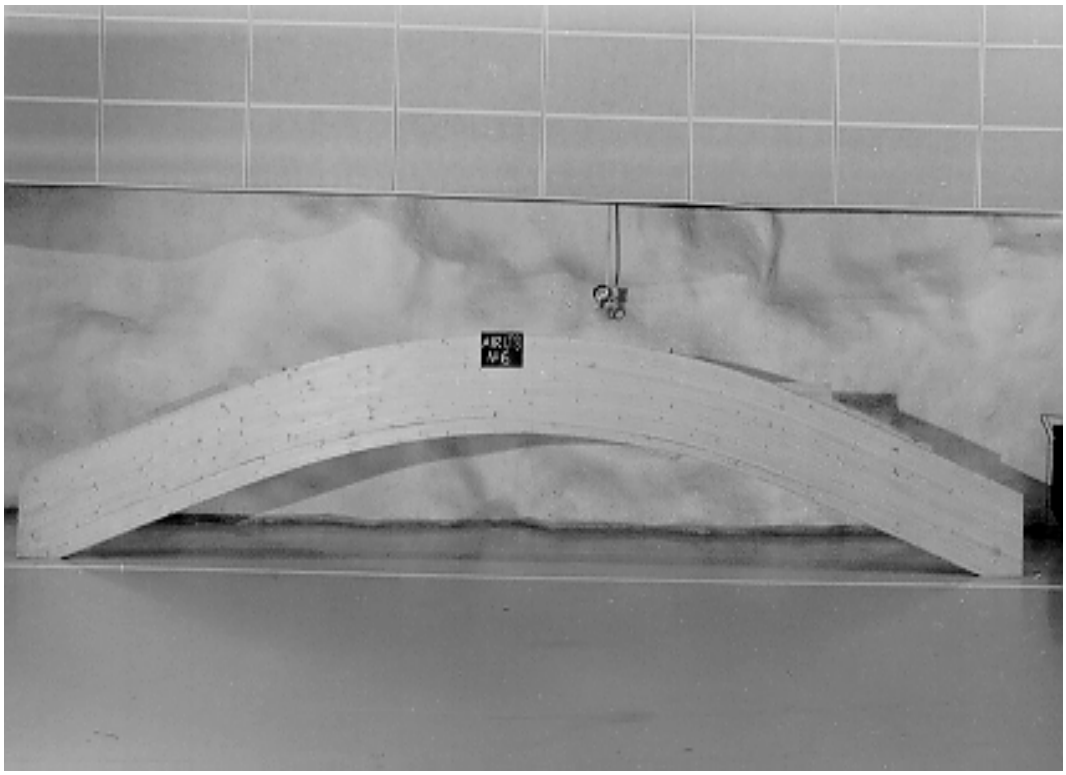

Failure behaviour of Specimen LT-C2-S4-6 (AIR LT3 No.6).

Failure behaviour of Specimen LT-C2-S4-7 (AIR LT3 No.7).

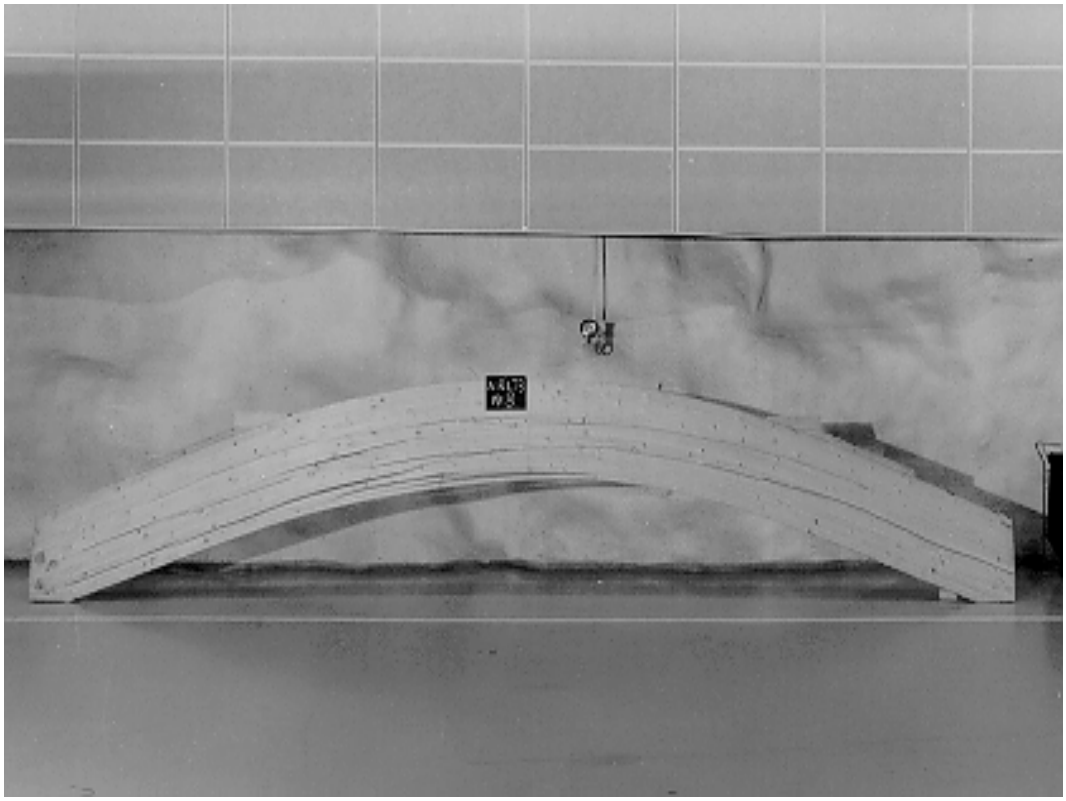

Failure behaviour of Specimen LT-C2-S4-8 (AIR LT3 No.8).

Long term tests: Series LT-C2-S8

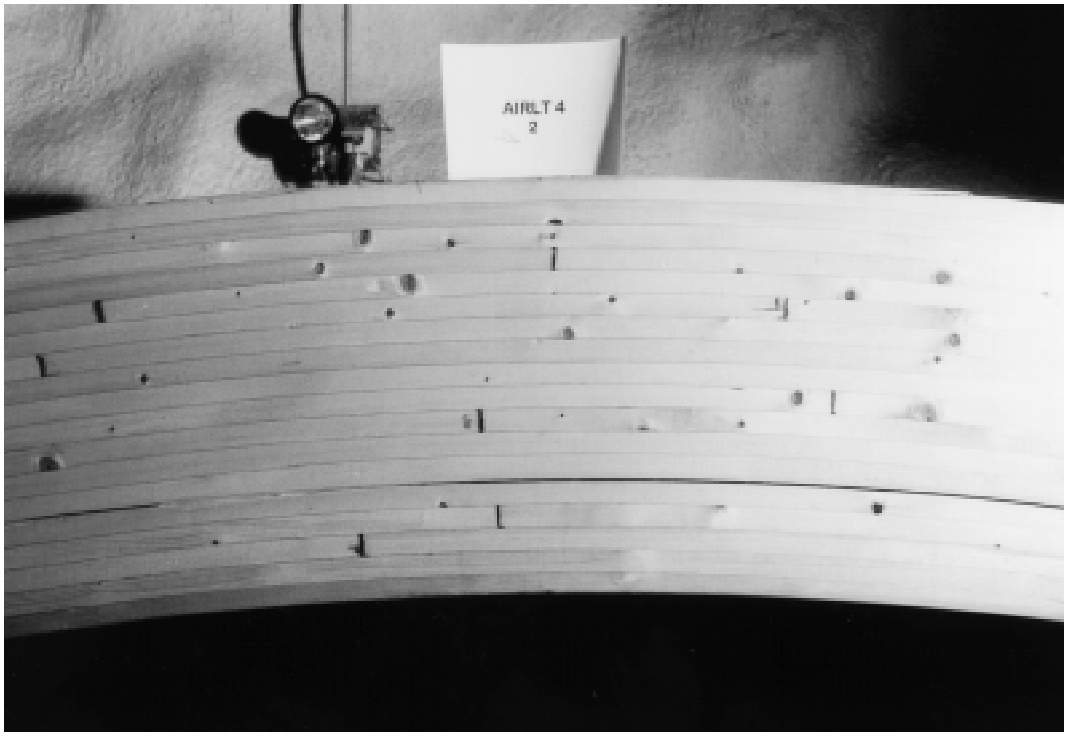

Failure behaviour of specimen LT-C2-S8-2.

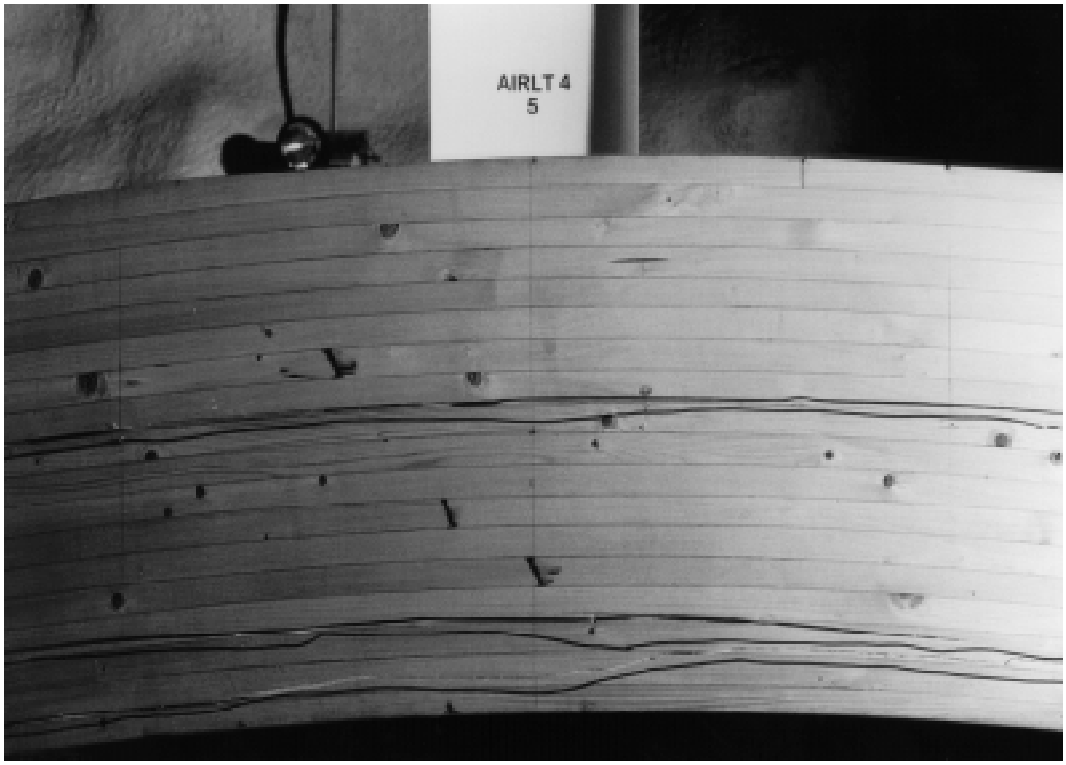

Failure behaviour of specimen LT-C2-S8-5.

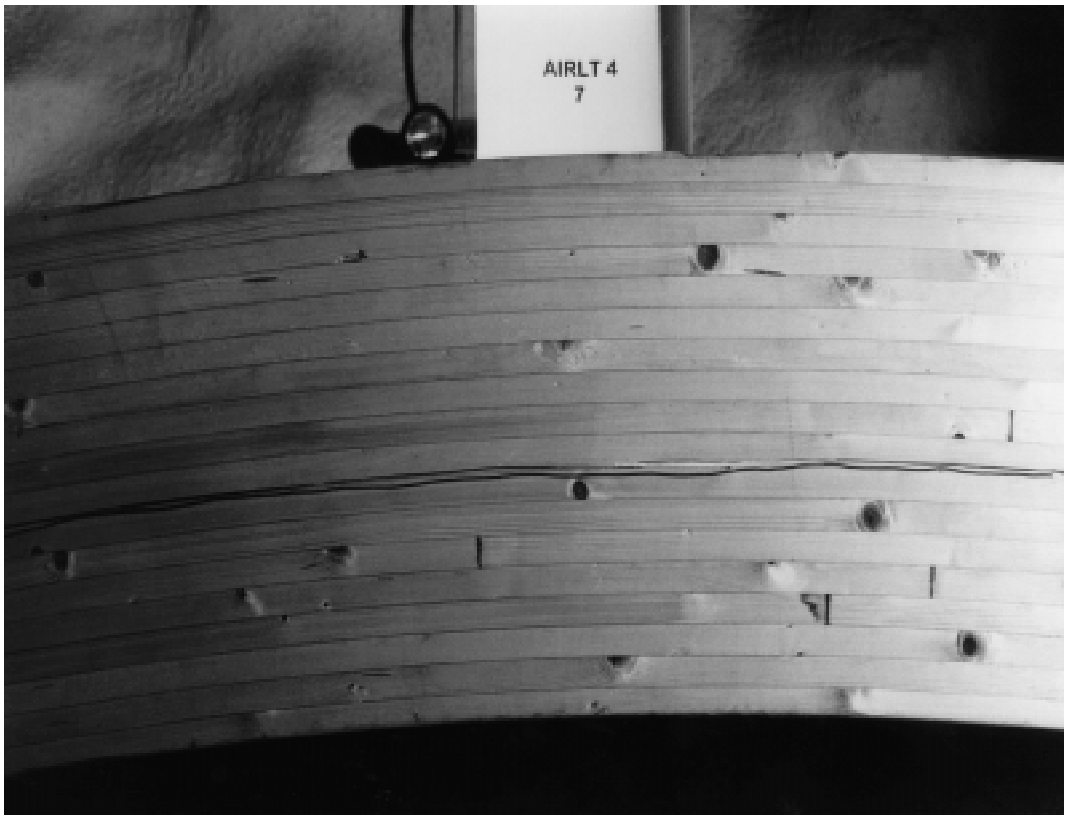

Failure behaviour of specimen LT-C2-S8-7.

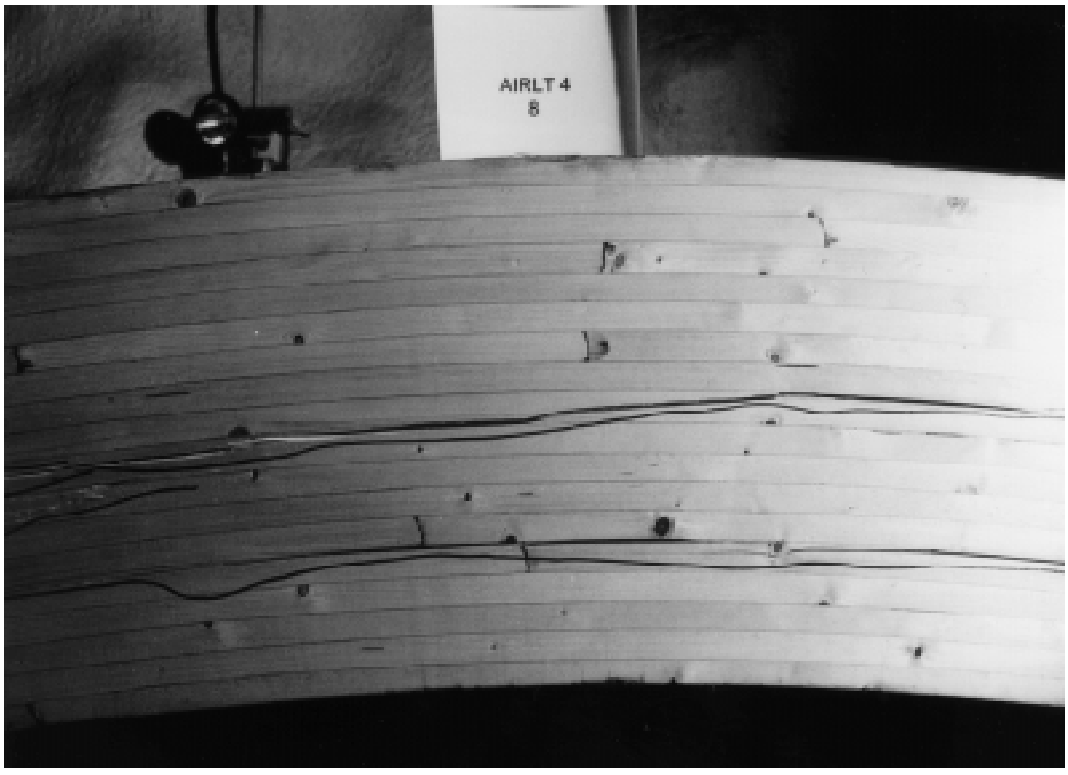

Failure behaviour of specimen LT-C2-S8-8.